arXiv:1510.01416v1 [math.DS] 6 Oct 2015

The structure of mode-locking regions of piecewise-linear continuous maps

D.J.W. Simpson

Institute of Fundamental Sciences
Massey University
Palmerston North
New Zealand

October 7, 2015

Abstract

The mode-locking regions of a dynamical system are the subsets of the parameter space of the system within which there exists an attracting periodic solution. For piecewise-linear continuous maps, these regions have a curious chain structure with points of zero width called shrinking points. In this paper we perform a local analysis about an arbitrary shrinking point. This is achieved by studying the symbolic itineraries of periodic solutions in nearby mode-locking regions and performing an asymptotic analysis on one-dimensional slow manifolds in order to build a comprehensive theoretical framework for the local dynamics. We obtain leading-order quantitative descriptions for the shape of nearby mode-locking regions, the location of nearby shrinking points, and the key properties of these shrinking points. We apply the results to the three-dimensional border-collision normal form, non-smooth Neimark-Sacker-like bifurcations, and grazing-sliding bifurcations in a model of a dry friction oscillator.

1 Introduction

This paper concerns piecewise-linear continuous maps of the form

$$x_{i+1} = f(x_i;\mu,\xi) := \begin{cases} A_L(\xi)x_i + B(\xi)\mu\ , & s_i \leq 0 \\ A_R(\xi)x_i + B(\xi)\mu\ , & s_i \geq 0 \end{cases}\ , \tag{1.1}$$

where $x_i \in \mathbb{R}^N$ ($N \geq 2$) and s_i denotes the first component of x_i, i.e.,

$$s_i := e_1^{\mathsf{T}} x_i\ . \tag{1.2}$$

In (1.1), A_L and A_R are real-valued $N \times N$ matrices and $B \in \mathbb{R}^N$. A_L, A_R and B are C^K functions of a parameter $\xi \in \mathbb{R}^M$, and $\mu \in \mathbb{R}$ is another parameter.

The assumption that (1.1) is continuous on the switching manifold $s = 0$ implies that A_L and A_R differ in only their first columns, i.e.,

$$A_R = A_L + Ce_1^{\mathsf{T}} , \tag{1.3}$$

for some $C \in \mathbb{R}^N$. Furthermore, (1.1) satisfies the linear scaling property

$$f(\gamma x; \gamma\mu, \xi) \equiv \gamma f(x; \mu, \xi) , \tag{1.4}$$

for any $\gamma > 0$. For this reason, the structure of the dynamics of (1.1) is independent of the magnitude of μ, and the size of any bounded invariant set of (1.1) is proportional to $|\mu|$.

Maps of the form (1.1) arise in diverse contexts. The tent map and the Lozi map, one and two-dimensional examples of (1.1), are instructive prototypical maps exhibiting chaos [1, 2]. Maps that can be put in the form (1.1) through a change of variables have been used to model phenomena involving a switch or abrupt event, particularly in social sciences [3]. Most importantly, maps of the form (1.1) describe the dynamics near border-collision bifurcations.

A border-collision bifurcation occurs when a fixed point of a piecewise-smooth map collides with a switching manifold under certain regularity conditions [4, 5, 6]. Except in special cases, (1.1) has a border-collision bifurcation at $\mu = 0$. The dynamics of (1.1) for $\mu < 0$ and $\mu > 0$ represent the dynamics on either side of the bifurcation. In this context, μ is the primary bifurcation parameter. By varying ξ in a continuous fashion, we can investigate how the dynamics created in the border-collision bifurcation changes with respect to other parameters.

This paper concerns mode-locking regions of (1.1). A mode-locking region of a map is a region of parameter space within which the map has an attracting periodic solution of a given period. We consider two-dimensional cross-sections of parameter space as these are simple to visualise and informative. For (1.1) we always consider cross-sections with fixed $\mu \neq 0$, so that we avoid the border-collision bifurcation at $\mu = 0$ and degeneracies due to the scaling property (1.4).

Fig. 1 shows an example using

$$A_L = \begin{bmatrix} \tau_L & 1 & 0 \\ -\sigma_L & 0 & 1 \\ \delta_L & 0 & 0 \end{bmatrix} , \qquad A_R = \begin{bmatrix} \tau_R & 1 & 0 \\ -\sigma_R & 0 & 1 \\ \delta_R & 0 & 0 \end{bmatrix} , \qquad B = \begin{bmatrix} 1 \\ 0 \\ 0 \end{bmatrix} , \tag{1.5}$$

where $\tau_L, \sigma_L, \delta_L, \tau_R, \sigma_R, \delta_R \in \mathbb{R}$. The map (1.1) with (1.5) is the border-collision normal form in three dimensions [5, 6]. Here parameter space (not including μ) is six-dimensional (we could write $\xi = (\tau_L, \sigma_L, \delta_L, \tau_R, \sigma_R, \delta_R)$). The two-dimensional cross-section of parameter space used in Fig. 1 is defined by the restriction

$$\tau_L = 0 , \qquad \sigma_L = -1 , \qquad \sigma_R = 0 , \qquad \delta_R = 2 . \tag{1.6}$$

The mode-locking regions are coloured by the period, n, of the corresponding stable periodic solution. Only mode-locking regions up to $n = 50$ are shown. The periodic solutions are "rotational", in a symbolic sense defined in §3.1, and can be assigned a rotation number, $\frac{m}{n}$. As we move from left to right across Fig. 1, the rotation number decreases roughly monotonically. For the parameters of Fig. 1 there also exist mode-locking regions corresponding to non-rotational periodic solutions, but these regions are small, relative to the rotational ones, and not shown in Fig. 1 or studied in this paper.

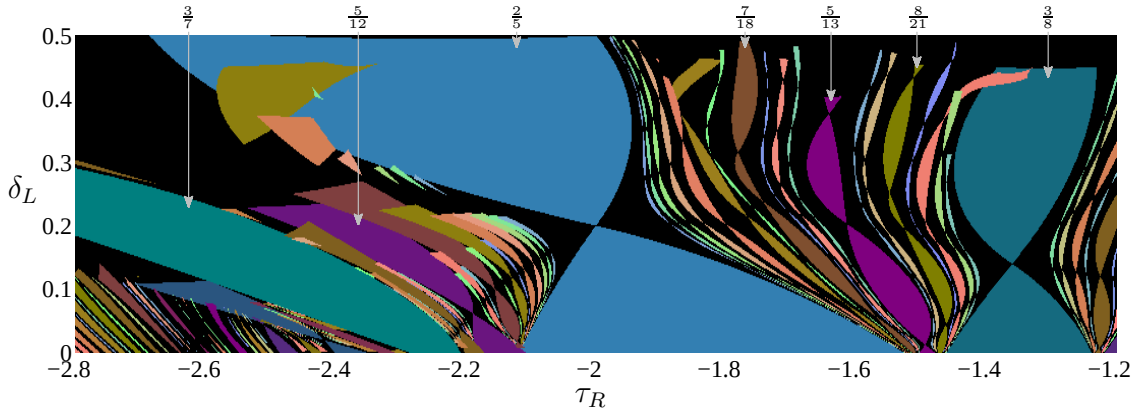

Figure 1: Mode-locking regions of (1.1) with (1.5)-(1.6) and $\mu > 0$ corresponding to rotational periodic solutions (defined in §2.1) of period $n \leq 50$. Selected mode-locking regions are labelled by their rotation number, $\frac{m}{n}$. This figure was computed by numerically checking the admissibility and stability of rotational periodic solutions on a 1024×256 grid of τ_R and δ_L values. At grid points where multiple stable periodic solutions exist, the periodic solution with the highest period (less than 50) is indicated.

The majority of the boundaries of the mode-locking regions shown in Fig. 1 are where one point of the corresponding periodic solution lies on the switching manifold ($s = 0$). These boundaries may be viewed as curves of border-collision bifurcations for the n^{th}-iterate of (1.1) [6]. The boundaries intersect at so-called shrinking points where (1.1) has a periodic solution with two points on the switching manifold.

Many of the mode-locking regions of Fig. 1 have several shrinking points and an overall structure that loosely resembles a string of sausages. This structure was first identified in piecewise-linear circle maps [7, 8], and subsequently described in piecewise-smooth models of a DC-DC power converter [9] and a trade cycle [10]. The structure has also been identified in an integrate-and-fire neuron model [11], a model of an oscillator subject to dry friction [12], and a model of the synchronisation of breathing to heart rate [13].

A rigorous study of shrinking points of (1.1) was performed in [14]. Here it was shown that the four curves of border-collision bifurcations that bound the mode-locking region near a shrinking point correspond to where four different points of a periodic solution lie on the switching manifold. These four points admit a simple characterisation in terms of the symbolic itinerary of the periodic solution. Furthermore, a local analysis reveals that as the boundaries emanate from the shrinking point, they curve in a manner that favours the boundaries reintersecting at other shrinking points.

However, the results of [14] do not provide us with any information about the dynamics of (1.1) outside the associated mode-locking region. In any neighbourhood of a typical shrinking point there are infinitely many mode-locking regions corresponding to higher periods. These are not readily apparent in Fig. 1, as only periods up to 50 are shown, but about shrinking points corresponding to relatively low periods, we can see the beginnings of sequences of mode-locking regions converging to the shrinking points.

The purpose of this paper is to describe nearby mode-locking regions and their associated

shrinking points. This is achieved by combining Farey addition, used to identify the symbolic itineraries of periodic solutions in nearby mode-locking regions, with calculations on one-dimensional slow manifolds in order to develop a comprehensive theoretical framework that explains the dynamics. To benefit the reader we begin in §2 by stating the main results. This requires introducing some notation and definitions. This is done as quickly as possible, skipping over derivations and explanations which are provided in later sections. In §2 we also demonstrate the scope of the results with a variety of examples.

In the subsequent three sections we provide an array of small mathematical results, many of which are new, that can be viewed as building blocks used to obtain the main results. Section 3 concerns the symbolic itineraries. Each shrinking point is associated with a rotational symbol sequence. By partitioning this sequence into blocks, and repeating the blocks appropriately, we can construct the symbol sequences of periodic solutions in nearby mode-locking regions. These sequences are also obtained via Farey addition. In §4 we combine symbolic representations with matrix algebra in order to compute periodic solutions. In §5 we describe fundamental properties of shrinking points and review the basic unfolding of shrinking points that was derived in [14].

In §6 we identify the locations of nearby shrinking points, and in §7 determine properties of these shrinking points. The key geometric tool used to obtain the results is that of a slow manifold. At a shrinking point, periodic dynamics are associated with $N-1$ stable directions and one neutral direction (corresponding to a unit eigenvalue). Near a shrinking point there are consequently one-dimensional slow manifolds (each point of the periodic solution has an associated slow manifold). By working on these slow manifolds our calculations reduce from N dimensions to one dimension.

Finally, in §8 we provide concluding comments. Some proofs are given in Appendix A.

2 Main results

In this section we present the main results. We begin in §2.1 by briefly introducing the essential symbolic concepts, notation used for shrinking points, and the shrinking point unfolding theorem of [14]. In §2.2 we state the main results as four theorems, and in §2.3 we illustrate the theorems with a variety of examples.

2.1 Basic definitions and properties of shrinking points

Let

$$f^L(x;\mu,\xi) := A_L(\xi)x + B(\xi)\mu\,, \qquad f^R(x;\mu,\xi) := A_R(\xi)x + B(\xi)\mu\,, \tag{2.1}$$

denote the two affine half-maps of (1.1). As in [6, 15, 16], we work with symbol sequences, $\mathcal{S} : \mathbb{Z} \to \{L, R\}$, and match periodic solutions of (1.1) to periodic symbol sequences. This is made precise by the following definition. (In this definition, and throughout this paper, $\mathcal{S}_i$ denotes the i^{th} element of $\mathcal{S}$.)

Definition 2.1. Let $\mathcal{S}$ be a periodic symbol sequence of period n. We refer to an n-tuple, $\{x_i^{\mathcal{S}}\}_{i=0}^{n-1}$, satisfying $x^{\mathcal{S}}_{(i+1) \bmod n} = f^{\mathcal{S}_i}\left(x_i^{\mathcal{S}}\right)$, for all $i = 0, \ldots, n-1$, as an $\mathcal{S}$-*cycle*.

As explained in §4.2, if each $x_i^{\mathcal{S}}$ lies on the "correct" side of the switching manifold (or on the switching manifold), then the $\mathcal{S}$-cycle is a periodic solution of (1.1) and said to be admissible.

Given a periodic symbol sequence $\mathcal{S}$ of period n, let

$$f^{\mathcal{S}} := f^{\mathcal{S}_{n-1}} \circ \cdots \circ f^{\mathcal{S}_0} \ . \tag{2.2}$$

A straight-forward expansion leads to

$$f^{\mathcal{S}}(x) = M_{\mathcal{S}} x + P_{\mathcal{S}} B\mu \ , \tag{2.3}$$

where

$$M_{\mathcal{S}} := A_{\mathcal{S}_{n-1}} \cdots A_{\mathcal{S}_0} \ , \tag{2.4}$$

$$P_{\mathcal{S}} := I + A_{\mathcal{S}_{n-1}} + A_{\mathcal{S}_{n-1}} A_{\mathcal{S}_{n-2}} + \cdots + A_{\mathcal{S}_{n-1}} \cdots A_{\mathcal{S}_1} \ . \tag{2.5}$$

Each $x_i^{\mathcal{S}}$ is a fixed point of $f^{\mathcal{S}^{(i)}}$, where we use $\mathcal{S}^{(i)}$ to denote the i^{th} left shift permutation of $\mathcal{S}$. If $\det(I - M_{\mathcal{S}}) \neq 0$, then the $\mathcal{S}$-cycle is unique and

$$s_i^{\mathcal{S}} = \frac{\det(P_{\mathcal{S}^{(i)}})\, \varrho^{\mathsf{T}} B\mu}{\det(I - M_{\mathcal{S}})} \ , \tag{2.6}$$

where $\varrho^{\mathsf{T}} := e_1^{\mathsf{T}} \mathrm{adj}\,(I - A_L)$. In view of (2.6), it is useful to treat a mode-locking region boundary on which $s_i^{\mathcal{S}} = 0$ as a curve on which $\det(P_{\mathcal{S}^{(i)}}) = 0$ [6, 15].

Definition 2.2. Given $\ell, m, n \in \mathbb{Z}^+$, with $\ell < n$, $m < n$ and $\gcd(m, n) = 1$, we define a symbol sequence $\mathcal{F}[\ell, m, n] : \mathbb{Z} \to \{L, R\}$ by

$$\mathcal{F}[\ell, m, n]_i := \begin{cases} L \ , & im \bmod n < \ell \\ R \ , & im \bmod n \geq \ell \end{cases} \ . \tag{2.7}$$

We say that $\mathcal{F}[\ell, m, n]$, and any shift permutation of $\mathcal{F}[\ell, m, n]$, is *rotational*.

We refer to $\frac{m}{n}$ as the rotation number of $\mathcal{F}[\ell, m, n]$. The requirement $\gcd(m, n) = 1$ ensures that $\frac{m}{n}$ is an irreducible fraction and that each $\mathcal{F}[\ell, m, n]$ is of period n [15]. Throughout this paper we let $d \in \{1, \ldots, n-1\}$ denote the multiplicative inverse of m modulo n (i.e. $md \bmod n = 1$). For brevity we omit "mod n" in subscripts where it is clear that modulo arithmetic is being used.

Next we provide a definition of a shrinking point of (1.1). Each shrinking point corresponds to a particular rotational symbol sequence, $\mathcal{S} = \mathcal{F}[\ell, m, n]$, and is referred to as an $\mathcal{S}$-shrinking point. As explained in §5.2, at an $\mathcal{S}$-shrinking point there are infinitely many $\mathcal{S}$-cycles. For this reason our definition of an $\mathcal{S}$-shrinking point refers to an $\mathcal{S}^{\overline{0}}$-cycle (which is unique), where we use $\mathcal{S}^{\overline{i}}$ to denote the symbol sequence that differs from $\mathcal{S}$ in only the indices $i + jn$, for all $j \in \mathbb{Z}$. It is important to note that $\mathcal{S}^{\overline{0}}$ is a shift permutation of $\mathcal{F}[\ell - 1, m, n]$, and $\mathcal{S}^{\overline{\ell d}} = \mathcal{F}[\ell + 1, m, n]$, see §3.1.

Definition 2.3. Consider (1.1) for some $\xi \in \mathbb{R}^M$ and $\mu \neq 0$, and suppose $\varrho^{\mathsf{T}} B \neq 0$. Let $\mathcal{S} = \mathcal{F}[\ell, m, n]$ be a rotational symbol sequence with $2 \leq \ell \leq n - 2$. Suppose $\det(I - M_{\mathcal{S}^{\overline{0}}}) \neq 0$ and $\det\left(I - M_{\mathcal{S}^{\overline{\ell d}}}\right) \neq 0$. If the $\mathcal{S}^{\overline{0}}$-cycle is admissible, and $s_i^{\mathcal{S}^{\overline{0}}} = 0$ only for $i = 0$ and $i = \ell d$, then we say that ξ is an *$\mathcal{S}$-shrinking point*.

In Definition 2.3, $s_0^{\mathcal{S}^{\overline{0}}} = 0$ and $s_{\ell d}^{\mathcal{S}^{\overline{0}}} = 0$ are the two codimension-1 conditions that specify an $\mathcal{S}$-shrinking point. The remaining conditions of the definition ensure genericity. At an $\mathcal{S}$-shrinking point, we let

$$y_i := x_i^{\mathcal{S}^{\overline{0}}} , \qquad t_i := s_i^{\mathcal{S}^{\overline{0}}} , \tag{2.8}$$

$$a := \det\left(I - M_{\mathcal{S}^{\overline{0}}}\right) , \qquad b := \det\left(I - M_{\mathcal{S}^{\overline{\ell d}}}\right) . \tag{2.9}$$

As shown in §5.5, we always have $ab < 0$.

At an $\mathcal{S}$-shrinking point, $M_{\mathcal{S}}$ has a unit eigenvalue of algebraic multiplicity 1 (see §5.2). It follows that the same is true for each $M_{\mathcal{S}^{(i)}}$. For each of the four indices $j = 0$, $(\ell-1)d$, ℓd and $-d$ (taken modulo n), we let u_j^{T} and v_j denote the left and right eigenvectors of $M_{\mathcal{S}^{(j)}}$ corresponding to the unit eigenvalue and normalised by $u_j^{\mathsf{T}} v_j = 1$ and $e_1^{\mathsf{T}} v_j = 1$. The restriction to the four given indices ensures this normalisation can always be achieved (see §5.3). As shown in §5.5, the eigenvectors satisfy

$$\frac{u_0^{\mathsf{T}} v_{-d}}{a} + \frac{u_{\ell d}^{\mathsf{T}} v_{(\ell-1)d}}{b} = \frac{u_{(\ell-1)d}^{\mathsf{T}} v_{\ell d}}{a} + \frac{u_{-d}^{\mathsf{T}} v_0}{b} = \frac{1}{c} , \tag{2.10}$$

where c denotes the product of the nonzero eigenvalues of $I - M_{\mathcal{S}}$, that is

$$c := \prod_{i=2}^{N} \lambda_i , \tag{2.11}$$

where λ_i are the eigenvalues of $I - M_{\mathcal{S}}$, counting multiplicity, and $\lambda_1 = 0$.

We now consider the properties of (1.1) near an $\mathcal{S}$-shrinking point. For simplicity we assume $\xi \in \mathbb{R}^2$ and write $\xi = (\xi_1, \xi_2)$. Suppose that (1.1) has an $\mathcal{S}$-shrinking point at some $\xi = \xi^*$. It follows that there exists a neighbourhood of ξ^* within which the $\mathcal{S}^{\overline{0}}$-cycle exists and is unique. By Definition 2.3, $s_0^{\mathcal{S}^{\overline{0}}} = s_{\ell d}^{\mathcal{S}^{\overline{0}}} = 0$ at $\xi = \xi^*$. We let

$$\eta := s_0^{\mathcal{S}^{\overline{0}}}(\xi_1, \xi_2) , \qquad \nu := s_{\ell d}^{\mathcal{S}^{\overline{0}}}(\xi_1, \xi_2) , \tag{2.12}$$

and assume that the coordinate change $(\xi_1, \xi_2) \to (\eta, \nu)$ is locally invertible, i.e. $\det(J) \neq 0$, where

$$J := \left[\begin{array}{cc} \frac{\partial \eta}{\partial \xi_1} & \frac{\partial \eta}{\partial \xi_2} \\ \frac{\partial \nu}{\partial \xi_1} & \frac{\partial \nu}{\partial \xi_2} \end{array}\right]\Bigg|_{\xi=\xi^*} . \tag{2.13}$$

In (η, ν)-coordinates the $\mathcal{S}$-shrinking point $\xi = \xi^*$ is located at $(\eta, \nu) = (0, 0)$.

As shown in [14], four border-collision bifurcation curves emanate from $(\eta, \nu) = (0, 0)$. Each curve corresponds to the existence of an $\mathcal{S}$-cycle with $s_j^{\mathcal{S}} = 0$, for $j = 0$, $(\ell - 1)d$, ℓd and $-d$. The curves are orientated as in Fig. 2 and locally define two regions, Ψ_1 and Ψ_2. In Ψ_1 there exist unique $\mathcal{F}[\ell, m, n]$ and $\mathcal{F}[\ell - 1, m, n]$-cycles, and in Ψ_2 there exist unique $\mathcal{F}[\ell, m, n]$ and $\mathcal{F}[\ell + 1, m, n]$-cycles. If, in both Ψ_1 and Ψ_2, one of the two periodic solutions is stable, then (1.1) has a mode-locking region with zero width at $\xi = \xi^*$. In this case, the $\mathcal{F}[\ell, m, n]$-cycle is stable on exactly one side of the shrinking point, as determined by the sign of a, Table 1.

Finally let $\sigma \geq 0$ denote the maximum of the moduli of the eigenvalues of $M_{\mathcal{S}}$, excluding the unit eigenvalue, at the $\mathcal{S}$-shrinking point. That is,

$$\sigma := \max_{i=2,\ldots,N} |\rho_i| , \tag{2.14}$$

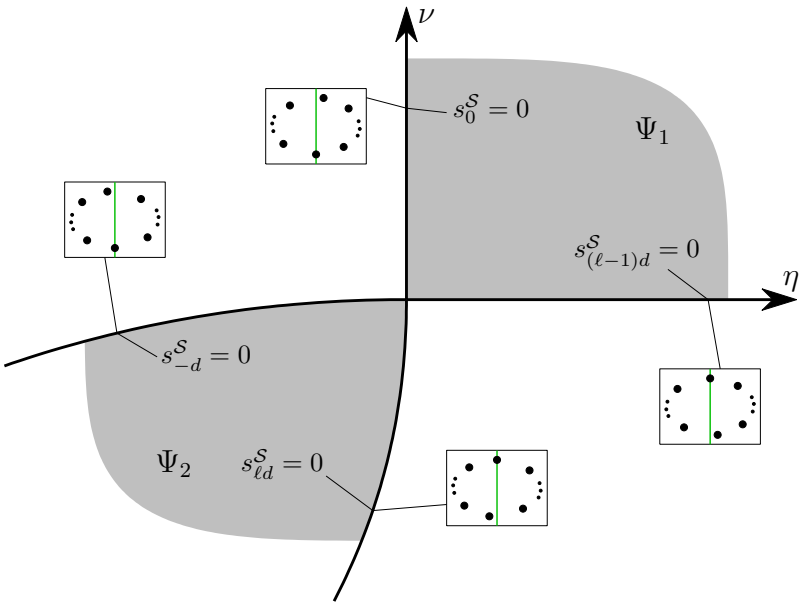

Figure 2: The basic unfolding of a generic $\mathcal{S}$-shrinking point of (1.1), as explained in the surrounding text and in more detail in §5.4. The (η, ν)-coordinates (2.12) provide a two-dimensional cross-section of parameter space for which two of the border-collision bifurcation curves coincide with the coordinate axes. The insets are schematic phase portraits indicating the location of the points of the $\mathcal{S}$-cycle relative to the switching manifold.

	$a < 0$	$a > 0$
$\mathcal{F}[\ell, m, n]$-cycle in Ψ_1	stable	unstable
$\mathcal{F}[\ell - 1, m, n]$-cycle in Ψ_1	unstable	stable
$\mathcal{F}[\ell, m, n]$-cycle in Ψ_2	unstable	stable
$\mathcal{F}[\ell + 1, m, n]$-cycle in Ψ_2	stable	unstable

Table 1: Cases for the stability of periodic solutions near an $\mathcal{S}$-shrinking point, where $\mathcal{S} = \mathcal{F}[\ell, m, n]$, in the scenario that stable periodic solutions exist on both sides of the shrinking point.

where ρ_i are the eigenvalues of $M_{\mathcal{S}}$, counting multiplicity, and $\rho_1 = 1$. In general the stability multipliers of an $\mathcal{S}$-cycle are the eigenvalues of $M_{\mathcal{S}}$, §4.2. Consequently we must have $\sigma < 1$ in order for there to exist a stable $\mathcal{S}$-cycle for some parameter values near the $\mathcal{S}$-shrinking point.

2.2 Theorems for nearby mode-locking regions

Each mode-locking region of Fig. 1 corresponds to stable $\mathcal{F}[\ell, m, n]$-cycles with fixed values of m and n, and values of ℓ that change by one each time we cross a shrinking point. Nearby mode-locking regions have rotation numbers close to $\frac{m}{n}$. This motivates the following definition.

Definition 2.4. Given $k \in \mathbb{Z}^+$, $\chi \in \mathbb{Z}$ with $|\chi| < k$, and a rotational symbol sequence $\mathcal{F}[\ell, m, n]$,

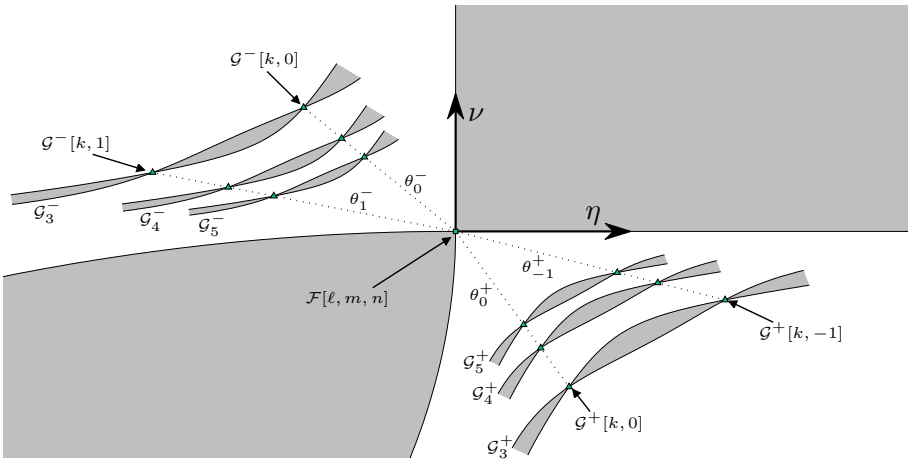

Figure 3: A sketch of typical $\mathcal{G}_k^{\pm}$-mode-locking regions (for $k = 3, 4, 5$) near an $\mathcal{F}[\ell, m, n]$-shrinking point in (η, ν)-coordinates in the case $a < 0$. Each shrinking point is labelled by its associated symbol sequence. Formulas for the angles, denoted $\theta_\chi^\pm$, about which sequences of $\mathcal{G}^\pm[k, \chi]$-shrinking points emanate from the $\mathcal{F}[\ell, m, n]$-shrinking point are given by (2.25)-(2.26). In the case $a > 0$, the relative location of the $\mathcal{G}_k^+$ and $\mathcal{G}_k^-$-mode-locking regions is reversed.

we let

$$\mathcal{G}^\pm[k,\chi] := \mathcal{F}\left[\ell_k^\pm + \chi, m_k^\pm, n_k^\pm\right] \ , \tag{2.15}$$

where

$$\ell_k^\pm := k\ell + \ell^\pm \ , \qquad m_k^\pm := km + m^\pm \ , \qquad n_k^\pm := kn + n^\pm \ , \tag{2.16}$$

and $\frac{m^-}{n^-}$ and $\frac{m^+}{n^+}$ are the left and right Farey roots of $\frac{m}{n}$, $\ell^+ := \left\lceil \frac{\ell n^+}{n} \right\rceil$, and $\ell^- := \left\lfloor \frac{\ell n^-}{n} \right\rfloor$. We also let $\tilde{\ell} := \ell_k^\pm + \chi$, and let $d_k^\pm$ denote the multiplicative inverse of $m_k^\pm$ modulo $n_k^\pm$.

Each $\mathcal{G}^\pm[k, \chi]$ is a rotational symbol sequence with rotation number $\frac{m_k^\pm}{n_k^\pm} = \frac{km+m^\pm}{kn+n^\pm}$. These rotation numbers limit to $\frac{m}{n}$, as $k \to \infty$, and are in the first level of complexity relative to $\frac{m}{n}$ [17]. Other rotational symbol sequences with rotation numbers near $\frac{m}{n}$ have rotation numbers of higher levels of complexity and are beyond the scope of this paper.

Near a typical shrinking point, there exist mode-locking regions corresponding to $\mathcal{G}^\pm[k, \chi]$-cycles for several consecutive values of χ, Fig. 3. We refer to these as $\mathcal{G}_k^\pm$-mode-locking regions.

For any $\chi_{\max} \in \mathbb{Z}^+$, we define the collection

$$\begin{aligned} \Xi_{\chi_{\max}} := &\left\{\mathcal{G}^+[k,\chi] \;\middle|\; k \in \mathbb{Z}^+, -\chi_{\max} \le \chi < \chi_{\max}, |\chi| < k\right\} \\ &\cup \left\{\mathcal{G}^-[k,\chi] \;\middle|\; k \in \mathbb{Z}^+, -\chi_{\max} < \chi \le \chi_{\max}, |\chi| < k\right\} \ . \end{aligned} \tag{2.17}$$

We define polar coordinates (r, θ) by

$$\eta = \left|\frac{ct_d}{a}\right| r\cos(\theta) \ , \qquad \nu = \left|\frac{ct_{(\ell-1)d}}{a}\right| r\sin(\theta) \ . \tag{2.18}$$

We also define a continuous function $\Gamma : \left(0, \frac{\pi}{2}\right) \to \mathbb{R}$ by

$$\Gamma(\theta) := \begin{cases} \frac{\ln(\cos(\theta)) - \ln(\sin(\theta))}{\cos(\theta) - \sin(\theta)} \,, & \theta \in \left(0, \frac{\pi}{2}\right) \setminus \left\{\frac{\pi}{4}\right\} \\ \sqrt{2} \,, & \theta = \frac{\pi}{4} \end{cases} \,, \tag{2.19}$$

and extend this definition to all non-integer multiples of $\frac{\pi}{2}$ in a periodic fashion:

$$\Gamma(\theta) := \Gamma\left(\theta \bmod \frac{\pi}{2}\right) \,, \quad \theta \neq \frac{j\pi}{2} \,, \quad j \in \mathbb{Z} \,. \tag{2.20}$$

The following theorem provides us with the location of the $\mathcal{G}_k^{\pm}$-mode-locking regions to leading order.

Theorem 2.1. *Suppose (1.1) with $K \geq 2$ has an $\mathcal{S}$-shrinking point satisfying $\sigma < 1$ and $\det(J) \neq 0$, and write $\mathcal{S} = \mathcal{F}[\ell, m, n]$. Then for all $\chi_{\max} \in \mathbb{Z}^+$, there exists $k_{\min} \in \mathbb{Z}^+$ and a neighbourhood $\mathcal{N}$ of $(\eta, \nu) = (0, 0)$, such that for all $\mathcal{T} = \mathcal{G}^{\pm}[k, \chi] \in \Xi_{\chi_{\max}}$ with $k \geq k_{\min}$, within $\mathcal{N}$ there exists a unique C^K curve on which $\det(P_{\mathcal{T}}) = 0$ and a unique C^K curve on which $\det\left(P_{\mathcal{T}^{\left((\tilde{\ell}-1)d_k^{\pm}\right)}}\right) = 0$, and both curves lie within $\mathcal{O}\left(\frac{1}{k^2}\right)$ of*

$$r = \frac{1}{k}\,\Gamma(\theta) \,, \tag{2.21}$$

where

$$\begin{gathered} \text{if } \mathcal{T} = \mathcal{G}^{+}[k, \chi] \text{ and } a < 0, \text{ or } \mathcal{T} = \mathcal{G}^{-}[k, \chi] \text{ and } a > 0, \text{ then } \theta \in \left(\tfrac{3\pi}{2}, 2\pi\right) , \\ \text{and if } \mathcal{T} = \mathcal{G}^{+}[k, \chi] \text{ and } a > 0, \text{ or } \mathcal{T} = \mathcal{G}^{-}[k, \chi] \text{ and } a < 0, \text{ then } \theta \in \left(\tfrac{\pi}{2}, \pi\right) . \end{gathered} \tag{2.22}$$

Theorem 2.1 tells us that if there exists a $\mathcal{G}_k^{\pm}$-mode-locking region, it has a width of at most $\mathcal{O}\left(\frac{1}{k^2}\right)$, lies approximately on the curve (2.21) (sketched in Fig. 4), and is located an $\mathcal{O}\left(\frac{1}{k}\right)$ distance from the $\mathcal{S}$-shrinking point. By (2.22), if $a < 0$ then the $\mathcal{G}_k^{+}$-mode-locking regions lie in the fourth quadrant of the (η, ν)-plane, and the $\mathcal{G}_k^{-}$-mode-locking regions lie in the second quadrant of the (η, ν)-plane (as in Fig. 3). If $a > 0$, then the opposite is true.

Next we investigate shrinking points on the $\mathcal{G}_k^{\pm}$-mode-locking regions. We find that $\mathcal{G}^{\pm}[k, \chi]$-shrinking points exist for arbitrarily large values of k only for certain values of χ, and that these

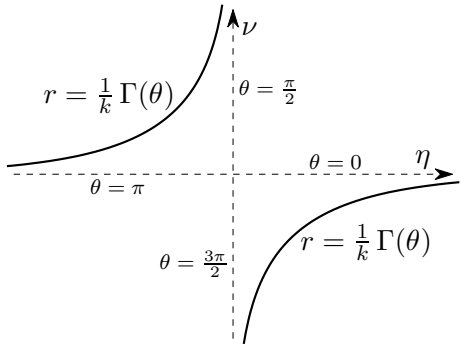

Figure 4: A sketch of (2.21).

$a<0$	$a>0$
$\theta_\chi^+ \in \left(\frac{3\pi}{2}, 2\pi\right)$ $\theta_\chi^- \in \left(\frac{\pi}{2}, \pi\right)$	$\theta_\chi^+ \in \left(\frac{\pi}{2}, \pi\right)$ $\theta_\chi^- \in \left(\frac{3\pi}{2}, 2\pi\right)$

Table 2: This table indicates the interval to which each θ_χ^+ (2.25) and θ_χ^- (2.26) belong, as determined by the sign of a.

values of χ depend on the given $\mathcal{S}$-shrinking point. To determine the appropriate values of χ, we define scalar quantities $\kappa_\chi^\pm$ by

$$\kappa_\chi^+ := \begin{cases} u_{\ell d}^\mathsf{T} M_{\mathcal{S}^{\overline{0}(\ell d)}}^{-\chi-1}\big|_{(\eta,\nu)=(0,0)} v_{(\ell-1)d} \,, & \chi \le -1 \\ u_0^\mathsf{T} M_{\mathcal{S}^{\overline{\ell d}}}^{\chi}\big|_{(\eta,\nu)=(0,0)} v_{-d} \,, & \chi \ge 0 \end{cases}, \tag{2.23}$$

$$\kappa_\chi^- := \begin{cases} u_{-d}^\mathsf{T} M_{\mathcal{S}^{\overline{0}}}^{-\chi}\big|_{(\eta,\nu)=(0,0)} v_0 \,, & \chi \le 0 \\ u_{(\ell-1)d}^\mathsf{T} M_{\mathcal{S}^{\overline{\ell d}(\ell d)}}^{\chi-1}\big|_{(\eta,\nu)=(0,0)} v_{\ell d} \,, & \chi \ge 1 \end{cases}. \tag{2.24}$$

To clarify these expressions, the matrix $M_{\mathcal{S}^{\overline{0}(\ell d)}}^{-\chi-1}$, for example, is the $(-\chi-1)^{\text{th}}$ power of $M_{\mathcal{S}^{\overline{0}(\ell d)}}$, where $M_{\mathcal{S}^{\overline{0}(\ell d)}}$ is given by (2.4) using $\mathcal{S}^{\overline{0}(\ell d)}$ – the $(\ell d)^{\text{th}}$ left shift permutation of $\mathcal{S}^{\overline{0}}$. In (2.23) this matrix is evaluated at the $\mathcal{S}$-shrinking point.

We also define

$$\theta_\chi^+ := \begin{cases} \tan^{-1}\left(\frac{t_{(\ell+1)d}}{t_{(\ell-1)d}\left|\kappa_\chi^+\right|}\right) \,, & \chi \le -1 \\ \tan^{-1}\left(\frac{t_d}{t_{-d}\left|\kappa_\chi^+\right|}\right) \,, & \chi \ge 0 \end{cases}, \tag{2.25}$$

$$\theta_\chi^- := \begin{cases} \tan^{-1}\left(\frac{t_d\left|\kappa_\chi^-\right|}{t_{-d}}\right) \,, & \chi \le 0 \\ \tan^{-1}\left(\frac{t_{(\ell+1)d}\left|\kappa_\chi^-\right|}{t_{(\ell-1)d}}\right) \,, & \chi \ge 1 \end{cases}, \tag{2.26}$$

assuming $\kappa_\chi^\pm \neq 0$, where the ambiguity of each $\tan^{-1}(\cdot)$ is resolved by Table 2.

Theorem 2.2. *Suppose (1.1) with $K \ge 2$ has an $\mathcal{S}$-shrinking point satisfying $\sigma < 1$ and $\det(J) \neq 0$, and write $\mathcal{S} = \mathcal{F}[\ell, m, n]$. Then for all $\chi_{\max} \in \mathbb{Z}^+$, there exists $k_{\min} \in \mathbb{Z}^+$, and a neighbourhood $\mathcal{N}$ of $(\eta, \nu) = (0, 0)$, such that for all $\mathcal{T} = \mathcal{G}^\pm[k, \chi] \in \Xi_{\chi_{\max}}$ with $k \ge k_{\min}$, if $\kappa_\chi^\pm \neq 0$, then within $\mathcal{N}$:*

i) there exists a unique point $(\eta_\mathcal{T}, \nu_\mathcal{T})$ at which $\det(I - M_\mathcal{T}) = \det(P_\mathcal{T}) = 0$ if and only if $\kappa_\chi^\pm > 0$, and $(\eta_\mathcal{T}, \nu_\mathcal{T})$ lies within $\mathcal{O}\left(\frac{1}{k^2}\right)$ of (2.21) with $\theta = \theta_\chi^\pm$;

ii) there exists a unique C^K curve on which (1.1) has a $\mathcal{T}$-cycle with an associated stability multiplier of -1 if and only if $\kappa_\chi^\pm < 0$, and this curve intersects $\det(P_\mathcal{T}) = 0$ at a point within $\mathcal{O}\left(\frac{1}{k^2}\right)$ of (2.21) with $\theta = \theta_\chi^\pm$.

By Theorem 2.2, each $\left(\eta_{\mathcal{G}^{\pm}[k,\chi]}, \nu_{\mathcal{G}^{\pm}[k,\chi]}\right)$ is a potential $\mathcal{G}^{\pm}[k,\chi]$-shrinking point and exists if $\kappa_{\chi}^{\pm} > 0$. If $\kappa_{\chi}^{\pm} < 0$, then no such points exist (for sufficiently large values of k). For a fixed value of χ, $\left(\eta_{\mathcal{G}^{+}[k,\chi]}, \nu_{\mathcal{G}^{+}[k,\chi]}\right)$ and $\left(\eta_{\mathcal{G}^{-}[k,\chi]}, \nu_{\mathcal{G}^{-}[k,\chi]}\right)$ are sequences of points that limit to the $\mathcal{S}$-shrinking point as $k \to \infty$. Each $\left(\eta_{\mathcal{G}^{\pm}[k,\chi]}, \nu_{\mathcal{G}^{\pm}[k,\chi]}\right)$ is a $\mathcal{G}^{\pm}[k,\chi]$-shrinking point if all the statements in Definition 2.3 (applied to $\mathcal{G}^{\pm}[k,\chi]$) are satisfied. Naturally we would like identify a practical set of testable conditions that ensure $\left(\eta_{\mathcal{G}^{\pm}[k,\chi]}, \nu_{\mathcal{G}^{\pm}[k,\chi]}\right)$ is a $\mathcal{G}^{\pm}[k,\chi]$-shrinking point. However, this is difficult (and not achieved in this paper) because in order to show that the $\mathcal{G}^{\pm}[k,\chi]^{\overline{0}}$-cycle is admissible we have to determine the sign of $s_i^{\mathcal{G}^{\pm}[k,\chi]^{\overline{0}}}$ for all $kn + n^{\pm}$ values of i. Numerical investigations reveal that the $\mathcal{G}^{\pm}[k,\chi]^{\overline{0}}$-cycle is often admissible when $\kappa_{\chi}^{\pm} > 0$, but this is not always the case.

Already the identity (2.10) provides some restrictions on the combinations of signs possible for the $\kappa_{\chi}^{\pm}$. The next result tells us that, for large k, if $\left(\eta_{\mathcal{G}^{\pm}[k,\chi]}, \nu_{\mathcal{G}^{\pm}[k,\chi]}\right)$ is a $\mathcal{G}^{\pm}[k,\chi]$-shrinking point (this requires $\kappa_{\chi}^{\pm} > 0$), then either $\kappa_{\chi-1}^{\pm} > 0$ or $\kappa_{\chi+1}^{\pm} > 0$ (as determined by the sign of a). Essentially this says that the existence of a $\mathcal{G}^{\pm}[k,\chi]$-shrinking point implies the existence of a neighbouring shrinking point in the $\mathcal{G}_k^{\pm}$-mode-locking region, if admissibility is satisfied.

Theorem 2.3. *Suppose (1.1) with $K \geq 2$ has an $\mathcal{S}$-shrinking point satisfying $\sigma < 1$ and $\det(J) \neq 0$, and write $\mathcal{S} = \mathcal{F}[\ell, m, n]$. For any $\chi \in \mathbb{Z}$, if $\kappa_{\chi}^{\pm} > 0$ and the point $\left(\eta_{\mathcal{G}^{+}[k,\chi]}, \nu_{\mathcal{G}^{+}[k,\chi]}\right)$ (as specified by Theorem 2.2) is a $\mathcal{G}^{+}[k,\chi]$-shrinking point for arbitrarily large values of k, then,*

$$\begin{aligned} &\text{if } a < 0, \text{ then } \kappa_{\chi-1}^{\pm} > 0\,, \\ &\text{and if } a > 0, \text{ then } \kappa_{\chi+1}^{\pm} > 0\,. \end{aligned} \tag{2.27}$$

Finally we provide some properties of nearby $\mathcal{G}^{\pm}[k,\chi]$-shrinking points. Here we use tildes to denote quantities of a $\mathcal{G}^{\pm}[k,\chi]$-shrinking point. For any $\mathcal{T} \in \Xi_{\chi_{\max}}$ with $\kappa_{\chi}^{\pm} > 0$, we let $\tilde{a} = \det\left(I - M_{\mathcal{T}^{\overline{0}}}\right)$ and $\tilde{b} = \det\left(I - M_{\mathcal{T}^{\overline{\ell d_k}}}\right)$, evaluated at $(\eta_{\mathcal{T}}, \nu_{\mathcal{T}})$. We denote the $\mathcal{T}^{\overline{0}}$-cycle by $\{\tilde{y}_i\}$ and let $\tilde{t}_i = e_1^{\mathsf{T}}\tilde{y}_i$. We also let $\tilde{\eta} = s_0^{\mathcal{T}^{\overline{0}}}$, $\tilde{\nu} = s_{\ell d_k^{\pm}}^{\mathcal{T}^{\overline{0}}}$, and

$$\tilde{J} := \left.\begin{bmatrix} \frac{\partial\tilde{\eta}}{\partial\eta} & \frac{\partial\tilde{\eta}}{\partial\nu} \\ \frac{\partial\tilde{\nu}}{\partial\eta} & \frac{\partial\tilde{\nu}}{\partial\nu} \end{bmatrix}\right|_{(\eta_{\mathcal{T}},\nu_{\mathcal{T}})}. \tag{2.28}$$

Theorem 2.4. *Suppose (1.1) with $K \geq 2$ has an $\mathcal{S}$-shrinking point satisfying $\sigma < 1$ and $\det(J) \neq 0$, and write $\mathcal{S} = \mathcal{F}[\ell, m, n]$. Then for all $\chi_{\max} \in \mathbb{Z}^{+}$, there exists $k_{\min} \in \mathbb{Z}^{+}$, such that for all $\mathcal{T} \in \Xi_{\chi_{\max}}$ with $k \geq k_{\min}$, if $\kappa_{\chi}^{\pm} > 0$ and $(\eta_{\mathcal{T}}, \nu_{\mathcal{T}})$ is a $\mathcal{T}$-shrinking point, then*

i) $\operatorname{sgn}(\tilde{a}) = \operatorname{sgn}(a)$ *and* $\det\left(\tilde{J}\right) > 0$,

ii) at $(\eta_{\mathcal{T}}, \nu_{\mathcal{T}})$, all eigenvalues of $M_{\mathcal{T}}$, excluding the unit eigenvalue, have modulus $\mathcal{O}\left(\sigma^k\right)$.

By part (i) of Theorem 2.4, $\mathcal{G}^{\pm}[k,\chi]$-shrinking points exhibit the unfolding depicted in Fig. 2, and have the same orientation as the $\mathcal{S}$-shrinking point. By part (ii) of Theorem 2.4, it follows that there exists a stable $\mathcal{G}^{\pm}[k,\chi]$-cycle on one side of the $\mathcal{G}^{\pm}[k,\chi]$-shrinking point.

2.3 Examples illustrating the main results

The three-dimensional border-collision normal form

The map (1.1) with (1.5) has an $\mathcal{F}[2,2,5]$-shrinking point at

$$\begin{aligned} \tau_L &= 0\,, \qquad \sigma_L = -1\,, \qquad \delta_L = 0.2\,, \\ \tau_R &= -2\,, \qquad \sigma_R = 0\,, \qquad \delta_R = 2\,, \end{aligned} \tag{2.29}$$

and $\mu > 0$. This point is located in the middle of Fig. 1. The corresponding mode-locking region has a stable $\mathcal{F}[2,2,5]$-cycle in the lower section ($\delta_L < 0.2$), and a stable $\mathcal{F}[3,2,5]$-cycle in the upper section ($\delta_L > 0.2$). The parameters τ_R and δ_L unfold the shrinking point generically in the sense that $\det(J) \neq 0$, where J is given by (2.13) using $\xi_1 = \tau_R$ and $\xi_2 = \delta_L$. This implies that

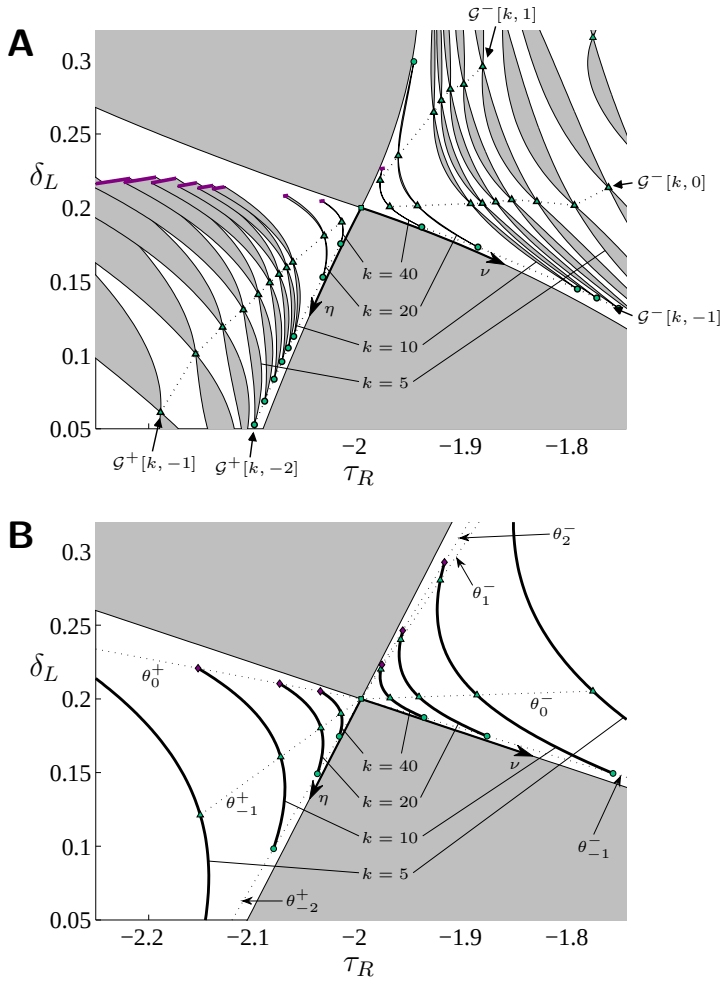

Figure 5: Panel A shows mode-locking regions of (1.1) with (1.5), $\mu > 0$, and with the remaining parameter values given by (2.29) (except τ_R and δ_L are variable). This figure is centred about the $\mathcal{F}[2,2,5]$-shrinking point shown in Fig. 1. The other mode-locking regions correspond to stable $\mathcal{G}^{\pm}[k,\chi]$-cycles. Panel B illustrates the predictions of Theorems 2.1 and 2.2, as discussed in the text.

under the smooth transformation to (η, ν)-coordinates (2.12), the mode-locking region conforms to Fig. 2 locally.

Fig. 5-A shows a magnified area of Fig. 2 and indicates the η and ν axes. Parts of $\mathcal{G}_k^{\pm}$-mode-locking regions are also shown. These were computed by numerically continuing the bifurcation boundaries. The regions are shown for all $k \leq 10$ in order to illustrate the proximity of the regions to one another (indeed they overlap slightly) and also for $k = 20$ and $k = 40$ in order to illustrate the location and shape of the regions for relatively large values of k without cluttering the figure. Triangles indicate $\mathcal{T}$-shrinking points for $\mathcal{T} \in \Xi_1$. Circles indicate $\mathcal{T}$-shrinking points for $\mathcal{T} \in \Xi_2 \setminus \Xi_1$. For clarity the mode-locking regions are not shown beyond these shrinking points. The additional (purple) curves are boundaries at which stable periodic solutions lose stability via an associated stability multiplier attaining the value -1.

The results of §2.2 explain how the $\mathcal{G}_k^{\pm}$-mode-locking regions behave in the limit $k \to \infty$ based on various key quantities of the $\mathcal{F}[2,2,5]$-shrinking point. To begin with, (2.21) provides an approximation to the location and shape of the mode-locking regions. Fig. 5-B illustrates this approximation for $k = 5, 10, 20, 40$. For simplicity we used a linear approximation to the coordinate change $(\tau_R, \delta_L) \to (\eta, \nu)$ to produce Fig. 5-B.

Theorem 2.2 provides approximations to the locations of nearby shrinking points and stability loss bifurcation boundaries based on the scalar quantities $\kappa_\chi^{\pm}$ (2.23)-(2.24) and $\theta_\chi^{\pm}$ (2.25)-(2.26). For the shrinking point (2.29) we have

$$\begin{aligned} \kappa_{-2}^{+} &= \frac{236}{33}\,, & \kappa_{-1}^{-} &= \frac{494}{55}\,, \\ \kappa_{-1}^{+} &= \frac{38}{55}\,, & \kappa_{0}^{-} &= \frac{43}{55}\,, \\ \kappa_{0}^{+} &= -\frac{5}{11}\,, & \kappa_{1}^{-} &= \frac{10}{33}\,, \\ \kappa_{1}^{+} &= \frac{26}{33}\,, & \kappa_{2}^{-} &= -\frac{32}{165}\,. \end{aligned} \tag{2.30}$$

We have used these values to generate Fig. 5-B. Recall, Theorem 2.2 tells us that $\kappa_\chi^{\pm} > 0$ implies there may exist $\mathcal{G}^{+}[k,\chi]$-shrinking points, whereas $\kappa_\chi^{\pm} < 0$ implies stability loss curves (corresponding to a stability multiplier of -1). In both cases these are located within $\mathcal{O}\left(\frac{1}{k^2}\right)$ of the curve (2.21) at $\theta = \theta_\chi^{\pm}$. Only θ_1^{+} is not shown in Fig. 5-B because at each $\left(\eta_{\mathcal{G}^{+}[k,1]}, \nu_{\mathcal{G}^{+}[k,1]}\right)$ the $\mathcal{G}^{+}[k,1]^{\overline{0}}$-cycle is virtual.

In summary, Fig. 5-B illustrates Theorems 2.1 and 2.2 with $\chi_{\max} = 2$. We see that Fig. 5-B provides a good approximation to the mode-locking regions shown in Fig. 5-A, including the shrinking points and stability loss boundaries, and the accuracy of the approximation increases with k. If we double the value of k, for example, then to leading order the distance of the mode-locking region to the $\mathcal{F}[2,2,5]$-shrinking point is halved.

Alternate cross-sections of parameter space

The signs of the $\kappa_\chi^{\pm}$ determine which $\mathcal{G}^{+}[k,\chi]$ have shrinking points and which $\mathcal{G}^{+}[k,\chi]$ have stability loss boundaries. The values of $\theta_\chi^{\pm}$ determine the relative location and spacing of these features on the curves (2.21). Yet each $\kappa_\chi^{\pm}$ and $\theta_\chi^{\pm}$ is a property of the $\mathcal{S}$-shrinking point, and so is independent to the parameters used to unfold the $\mathcal{S}$-shrinking point. Therefore with any

non-degenerate two-dimensional slice of parameter space through the $\mathcal{F}[2,2,5]$-shrinking point (2.29), the nearby mode-locking regions will appear as some smooth transformation of Fig. 5-B.

To illustrate this, Fig. 6 shows the nearby mode-locking regions for two different cross-sections. These indeed appear as distortions of Fig. 5-B. For example, in both panels of Fig. 6, there are $\mathcal{G}^+[k,-1]$-shrinking points and short curves along which a $\mathcal{G}^+[k,0]$-cycle has a stability multiplier of -1, and k these features are relatively far apart.

Changes in the properties of an $\mathcal{S}$-shrinking point

A shrinking point is a codimension-two phenomenon, therefore within three-dimensional regions of parameter space there exist curves of shrinking points. As we follow a curve of $\mathcal{S}$-shrinking points in a continuous manner, the values of $\kappa_\chi^\pm$ and $\theta_\chi^\pm$ change continuously. Therefore the structure of nearby mode-locking regions varies along the curve, and there may be critical points at which the structure changes in a fundamental way (e.g. at a point where one of the $\kappa_\chi^\pm$ changes

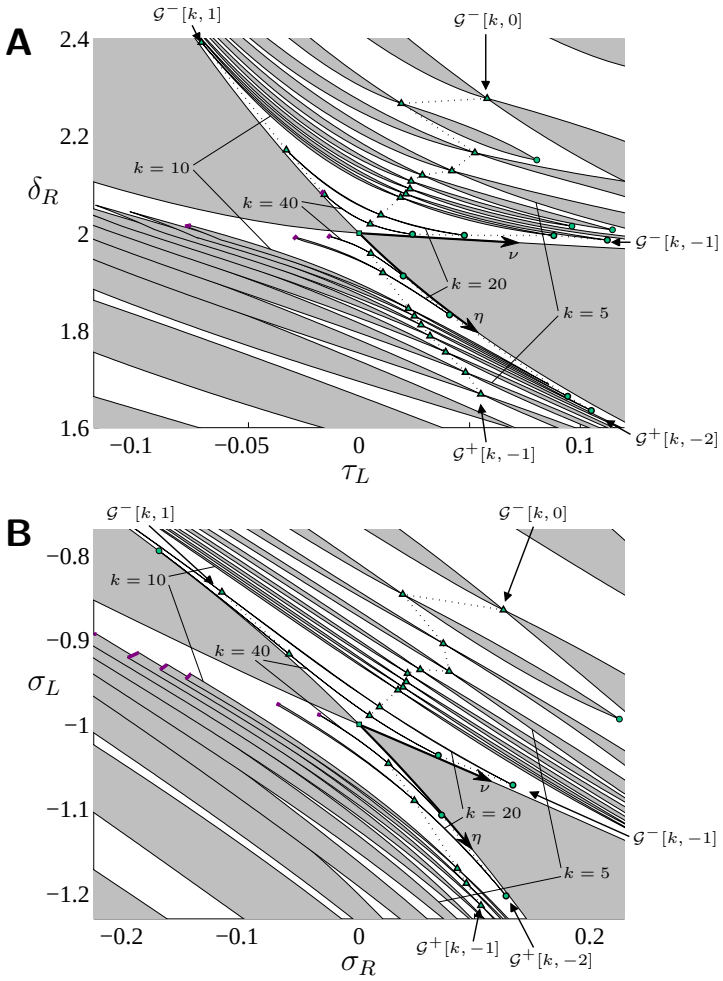

Figure 6: Panel A shows mode-locking regions of (1.1) with (1.5) with $(\sigma_L, \delta_L, \tau_R, \sigma_R) = (-1, 0.2, -2, 0)$ and $\mu > 0$. Panel B shows mode-locking regions of (1.1) with (1.5) with $(\tau_L, \delta_L, \tau_R, \delta_R) = (0, 0.2, -2, 2)$ and $\mu > 0$.

sign). Here we show an example.

For all $\delta_R > 0.5865$, approximately, the map (1.1) with (1.5) has an $\mathcal{F}[2,2,5]$-shrinking point at

$$\tau_L = 0\ , \qquad \sigma_L = -1\ , \qquad \delta_L = \frac{\delta_R + 2}{\delta_R\,(\delta_R^2 + 2\delta_R + 2)}\ ,$$
$$\tau_R = -\frac{\delta_R^2 + \delta_R + 2}{\delta_R + 2}\ , \qquad \sigma_R = 0\ , \tag{2.31}$$

and $\mu > 0$, see [6]. The $\mathcal{F}[2,2,5]$-shrinking point (2.29), considered above, is given by (2.31) with $\delta_R = 2$.

As we decrease the value of δ_R from $\delta_R = 2$ (at which the $\kappa_\chi^\pm$ are given by (2.30)) to $\delta_R = 1$, the sign of κ_2^- changes from negative to positive (at $\delta_R \approx 1.4597$), whereas the signs of the other seven values of $\kappa_\chi^\pm$ remains unchanged. With $\delta_R = 1$ the nearby mode-locking regions, as shown in Fig. 7-A, have the same structure as those in Fig. 5-A except that $\mathcal{G}^-[k,2]$-shrinking points exist for arbitrarily large values of k.

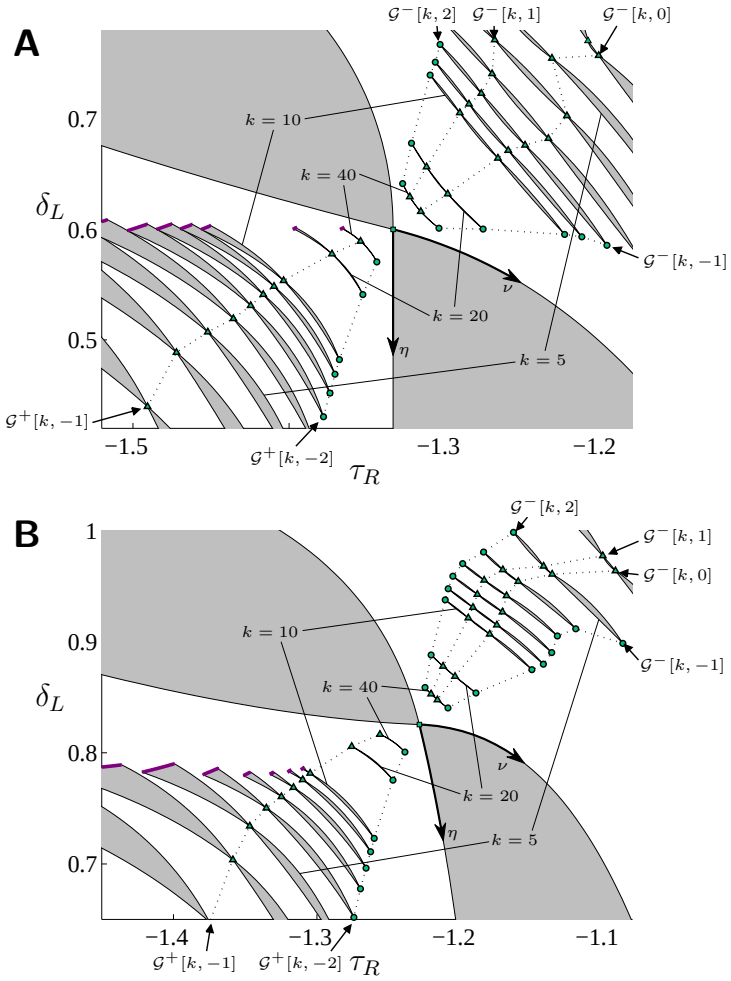

Figure 7: Mode-locking regions of (1.1) with (1.5) about the $\mathcal{F}[2,2,5]$-shrinking point (2.31) (i.e. $\tau_L = 0$, $\sigma_L = -1$, $\sigma_R = 0$ and $\mu > 0$). In panel A, $\delta_R = 1$; in panel B, $\delta_R = 0.8$. These regions are shown for $\delta_R = 2$ in Fig. 5-A.

Upon a further decrease in the value of δ_R, we have $\theta_0^+ = \theta_{-1}^+$ at $\delta_R \approx 0.8665$. Fig. 7-B shows nearby mode-locking regions using $\delta_R = 0.8$. At this value of δ_R the mode-locking regions do not extend beyond the $\mathcal{G}^+[k,-1]$ shrinking points, for sufficiently large values of k. This is because $\theta_0^+ > \theta_{-1}^+$ and so the bifurcation boundaries on which an $\mathcal{G}^+[k,0]$-cycle has a stability multiplier of -1 have become virtual.

Nonsmooth Neimark-Sacker-like bifurcations

As another example, consider (1.1) with

$$A_L = \begin{bmatrix} 2r_L\cos(2\pi\omega_L) & 1 \\ -r_L^2 & 0 \end{bmatrix}, \qquad A_R = \begin{bmatrix} \frac{2}{s_R}\cos(2\pi\omega_R) & 1 \\ -\frac{1}{s_R^2} & 0 \end{bmatrix}, \qquad B = \begin{bmatrix} 1 \\ 0 \end{bmatrix}, \tag{2.32}$$

where $r_L, s_R, \omega_L, \omega_R \in \mathbb{R}$ are parameters. The map (1.1) with (2.32) was studied in [18] in order to investigate nonsmooth Neimark-Sacker-like bifurcations.

Fig. 8 shows mode-locking regions of (1.1) with (2.32). This figure can be interpreted as showing the mode-locking dynamics created in the border-collision bifurcation at $\mu = 0$, where this bifurcation is akin to a Neimark-Sacker bifurcation in that an invariant circle is usually created as the values of μ passes through 0. In Fig. 8 there is a dominant curve of shrinking points running diagonally from the bottom-left of the figure to the top-right. Numerical computations of Lyapunov exponents reveal that this curve appears to be a boundary for chaotic dynamics [18]. The geometric mechanism responsible for this boundary of chaos is not fully understood.

The shrinking point in the large mode-locking region in the top-right of Fig. 8 corresponds to $\mathcal{S} = \mathcal{F}[2,1,4]$. Fig. 9-A shows a magnification of Fig. 8 about this shrinking point, and Fig. 9-B illustrates the predictions of Theorems 2.1 and 2.2. As expected, the leading-order approximations to the nearby mode-locking regions, and their shrinking points and stability loss boundaries, match well to their true locations with the degree of accuracy increasing with the value of k.

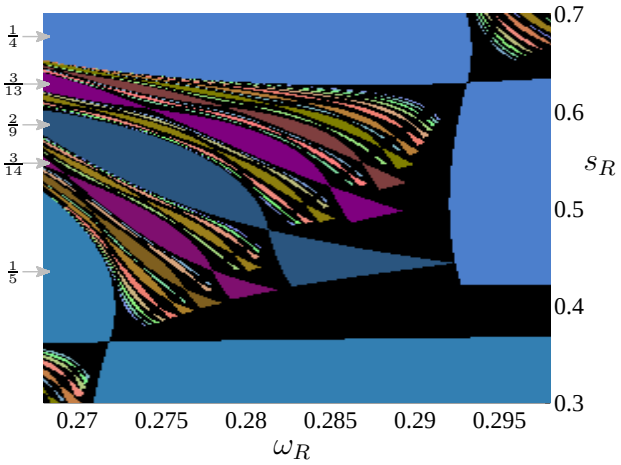

Figure 8: Mode-locking regions of (1.1) with (2.32), $r_L = 0.3$, $\omega_L = 0.09$ and $\mu > 0$. (as in Fig. 13 of [18]).

Application to grazing-sliding bifurcations

Dynamics near grazing-sliding bifurcations of $(N+1)$-dimensional piecewise-smooth systems of ordinary differential equations are captured by return maps of the form (1.1) for which either $\det(A_L) = 0$ or $\det(A_R) = 0$ [19, 20]. In [12], the authors investigate mode-locking regions near a grazing-sliding bifurcation in a model of a mechanical oscillator subject to dry friction. The return map that they analyse can, through an affine change of variables, be put in the form (1.1) with

$$A_L = \begin{bmatrix} 2e^{\xi_2}\cos(\xi_1) & 1 \\ -e^{2\xi_2} & 0 \end{bmatrix}, \qquad A_R = \begin{bmatrix} e^{\xi_2}\cos(\xi_1) & 1 \\ 0 & 0 \end{bmatrix}, \qquad B = \begin{bmatrix} 1 \\ 0 \end{bmatrix}, \tag{2.33}$$

where $\xi_1, \xi_2 \in \mathbb{R}$. Mode-locking regions of (1.1) with (2.33) are shown in Fig. 10.

Fig. 11-A shows a magnification of Fig. 10 about an $\mathcal{F}[8, 2, 13]$-shrinking point. It is interesting

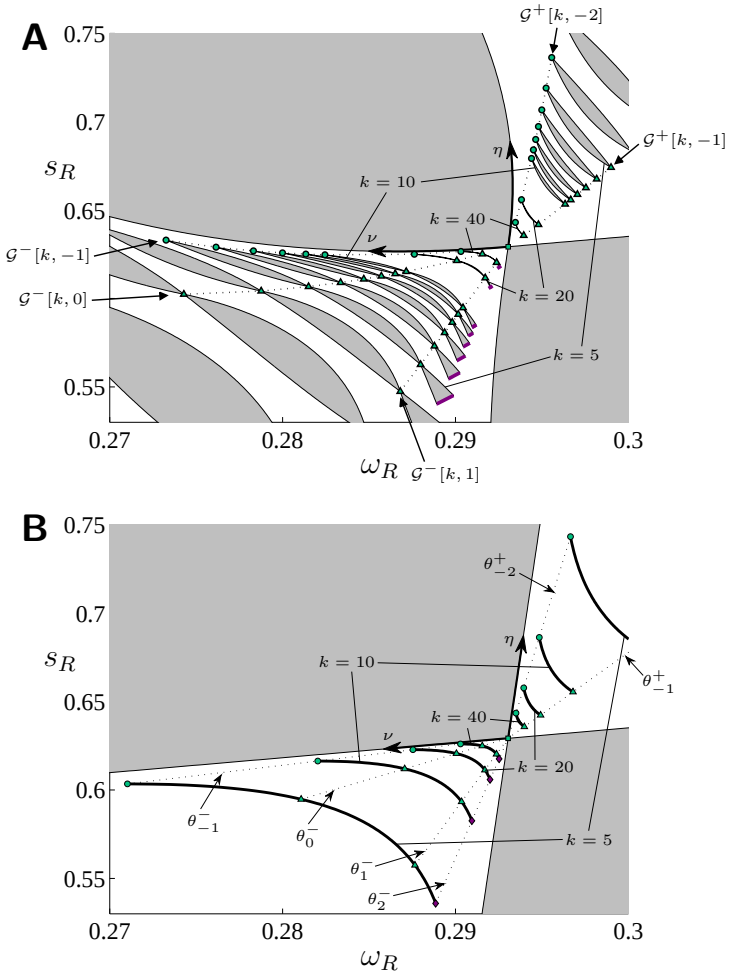

Figure 9: Panel A shows mode-locking regions of (1.1) with (2.32), $r_L = 0.3$, $\omega_L = 0.09$ and $\mu > 0$, obtained by numerically continuing bifurcation boundaries. Panel B shows the leading-order approximation to the mode-locking regions, as well as shrinking points and stability loss boundaries, as given by Theorems 2.1 and 2.2 (using a linear approximation to the coordinate change $(\omega_R, s_R) \leftrightarrow (\eta, \nu)$). For a further explanation refer to the discussion surrounding Fig. 5.

that since $\det(A_R) = 0$, curves of shrinking points admit simple analytic expressions [12]. For example the dashed curve in Fig. 11-A is given by

$$e^{5\xi_2}\sin(4\xi_1) - e^{4\xi_2}\sin(5\xi_1) + \sin(\xi_1) = 0\,. \tag{2.34}$$

As with the previous two examples, Fig. 11-B illustrates the predictions of Theorems 2.1 and 2.2. Here $a > 0$, so $\mathcal{G}_k^+$-mode-locking regions lie on the same side as the ν-axis (the previous examples have $a < 0$). Again, the leading order approximations of Fig. 11-B match well to the numerical computations of Fig. 11-A.

3 Symbolic representation

Here we develop symbolic notation on the alphabet $\{L, R\}$, following [6, 14, 15]. A *word* is a finite list of the symbols L and R, e.g. $\mathcal{S} = LRR$. We index the elements of a word from $i = 0$ to $i = n - 1$, where n is the length of the word. Thus for the previous example $n = 3$ and $\mathcal{S}_0 = L$, $\mathcal{S}_1 = R$, $\mathcal{S}_2 = R$.

Given two words $\mathcal{S}$ and $\mathcal{T}$, the concatenation $\mathcal{S}\mathcal{T}$ is a word that has a length equal to the sum of the lengths of $\mathcal{S}$ and $\mathcal{T}$. The power $\mathcal{S}^k$, where $k \in \mathbb{Z}^+$, is the concatenation of k instances of $\mathcal{S}$. A word is said to be primitive if it cannot be written as a power with $k > 1$.

Given a word $\mathcal{S}$, for any $j \in \mathbb{Z}$ we let $\mathcal{S}^{(j)}$ denote the j^{th} left cyclic permutation of $\mathcal{S}$. That is, $\mathcal{S}_i^{(j)} = \mathcal{S}_{(i+j) \bmod n}$ for all $i = 0, \ldots, n-1$. Also we let $\mathcal{S}^{\overline{j}}$ denote the word that differs from $\mathcal{S}$ in only the symbol $\mathcal{S}_{j \bmod n}$. For example, with $\mathcal{S} = LRR$,

$$\begin{aligned} \mathcal{S}^{(0)} &= \mathcal{S} = LRR\,, & \mathcal{S}^{\overline{0}} &= RRR\,, \\ \mathcal{S}^{(1)} &= RRL\,, & \mathcal{S}^{\overline{1}} &= LLR\,, \\ \mathcal{S}^{(2)} &= RLR\,, & \mathcal{S}^{\overline{2}} &= LRL\,. \end{aligned}$$

A *symbol sequence* $\mathcal{S}$ is a bi-infinite list of the symbols L and R. $\mathcal{S}$ is periodic with period $n \in \mathbb{Z}^+$, if $\mathcal{S}_{i+jn} = \mathcal{S}_i$, for all $i = 0, \ldots, n-1$ and $j \in \mathbb{Z}$. Given a periodic symbol sequence $\mathcal{S}$

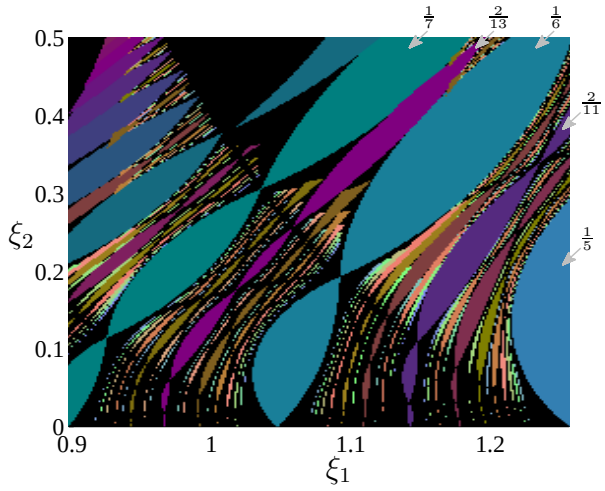

Figure 10: Mode-locking regions of (1.1) with (2.33) and $\mu < 0$ (as in Fig. 4 of [12]).

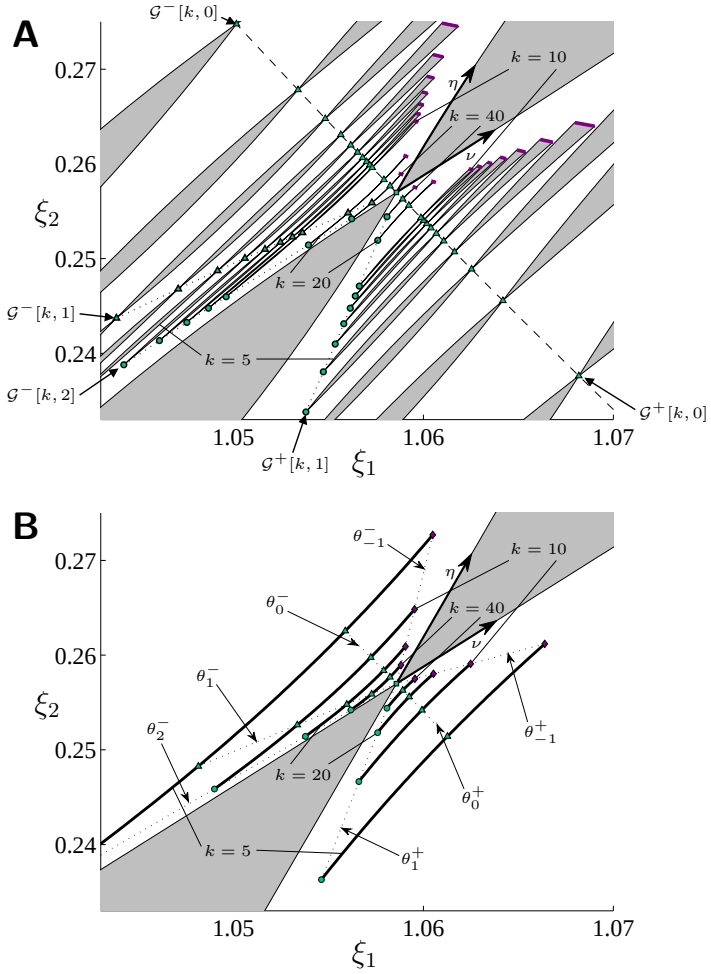

Figure 11: Panel A shows mode-locking regions of (1.1) with (2.33) and $\mu < 0$ obtained by numerically continuing bifurcation boundaries. Panel B shows the leading-order approximation to the mode-locking regions, as well as shrinking points and stability loss boundaries, as given by Theorems 2.1 and 2.2 (using a linear approximation to the coordinate change $(\xi_1, \xi_2) \leftrightarrow (\eta, \nu)$). For a further explanation refer to the discussion surrounding Fig. 5.

of minimal period n, the word $\mathcal{S}_0 \cdots \mathcal{S}_{n-1}$ is primitive and completely determines $\mathcal{S}$. Conversely, given a primitive word $\mathcal{S}$ of length n, the infinite repetition of this word generates a symbol sequence $\mathcal{S}$ of minimal period n. For these reasons, in order to minimise the complexity of our notation, we use periodic symbol sequences and primitive words interchangeably and denote them with the same symbol, e.g. $\mathcal{S}$.

3.1 Rotational symbol sequences

In this paper we use periodic symbol sequences to describe periodic solutions to (1.1). We restrict our attention to rotational symbol sequences $\mathcal{F}[\ell, m, n]$, defined in Definition 2.2, as these relate to shrinking points of (1.1), [14, 15, 16]. Rotational symbol sequences were originally studied independently of piecewise-linear maps by Slater in [21, 22].

Rotational symbol sequences can be interpreted as rigid rotation on a circle [14, 15]. To see this, we treat the values $im \bmod n$, that appear in the definition (2.7), as points on a circle. This is shown in Fig. 12 for $\mathcal{F}[3,5,7]$, which was constructed by applying the following steps.

1) Draw a circle intersecting a vertical line.
2) Draw n nodes on the circle, with ℓ of them to the left of the line.
3) Find the first node that lies to the left of the lower intersection point of the circle and the line, and call it 0.
4) For each $i = 1, \ldots, n-1$, step m nodes clockwise from node $i-1$, and call it node i.
5) Then $\mathcal{F}[\ell, m, n]_i$ is equal to L if node i is left of the line and equal to R otherwise.

As we label the n nodes in this fashion we revolve clockwise around the circle m times. For this reason we refer to $\frac{m}{n}$ as the rotation number of $\mathcal{F}[\ell, m, n]$.

It is a simple combinatorial exercise to show that (2.7) has the equivalent form,

$$\mathcal{F}[\ell, m, n]_{jd \bmod n} = \begin{cases} L\,, & j = 0, \ldots, \ell - 1 \\ R\,, & j = \ell, \ldots, n-1 \end{cases}\,, \tag{3.1}$$

where d is the multiplicative inverse of m modulo n. The next result is a simple consequence of (3.1) and we omit a proof.

Proposition 3.1. *For any $\mathcal{F}[\ell, m, n]$, if $\ell \neq 1$ then*

$$\mathcal{F}[\ell, m, n]^{\overline{(\ell-1)d}} = \mathcal{F}[\ell - 1, m, n]\,, \tag{3.2}$$

$$\mathcal{F}[\ell, m, n]^{\overline{0}} = \mathcal{F}[\ell - 1, m, n]^{(-d)}\,, \tag{3.3}$$

and if $\ell \neq n - 1$ then

$$\mathcal{F}[\ell, m, n]^{\overline{\ell d}} = \mathcal{F}[\ell + 1, m, n]\,, \tag{3.4}$$

$$\mathcal{F}[\ell, m, n]^{\overline{-d}} = \mathcal{F}[\ell + 1, m, n]^{(d)}\,. \tag{3.5}$$

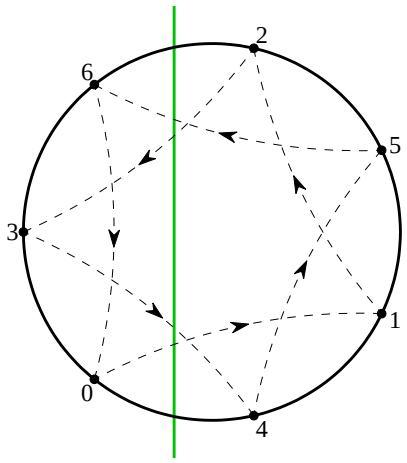

Figure 12: A pictorial interpretation of the rotational symbol sequence $\mathcal{F}[3,5,7] = LRRLRRL$.

By combining (3.3) and (3.4) we obtain the following identity which is central to our understanding of shrinking points.

Corollary 3.2. *For any* $\mathcal{F}[\ell, m, n]$,

$$\mathcal{F}[\ell, m, n]^{\overline{0}\,\overline{\ell d}(d)} = \mathcal{F}[\ell, m, n] \ . \tag{3.6}$$

Example 3.1. As an example, let us illustrate (3.5) with $(\ell, m, n) = (3, 5, 7)$. We have

i	0	1	2	3	4	5	6
$im \bmod n$	0	5	3	1	6	4	2

thus by (2.7), $\mathcal{F}[3, 5, 7] = LRRLRRL$ (see also Fig. 12). Moreover, $\mathcal{F}[4, 5, 7] = LRLLRRL$. Here $d = 3$, and so to evaluate the left hand-side of (3.5) we use $-d = 4$ (in modulo 7 arithmetic). Flipping the symbol $\mathcal{F}[3, 5, 7]_4$ produces $\mathcal{F}[3, 5, 7]^{\overline{-d}} = LRRLLRL$. Conversely, the right hand-side of (3.5) is given by the third left shift permutation of $\mathcal{F}[4, 5, 7]$, namely $\mathcal{F}[4, 5, 7]^{(3)} = LRRLLRL$, which we see is indeed the same as $\mathcal{F}[3, 5, 7]^{\overline{-d}}$.

3.2 Partitions of rotational symbol sequences

Definition 3.2. For any $\mathcal{S} = \mathcal{F}[\ell, m, n]$, let

$$\mathcal{X} = \mathcal{S}_0 \cdots \mathcal{S}_{(\ell d-1) \bmod n} \ , \qquad \mathcal{Y} = \mathcal{S}_{\ell d \bmod n} \cdots \mathcal{S}_{n-1} \ , \tag{3.7}$$

$$\hat{\mathcal{X}} = \mathcal{S}_0 \cdots \mathcal{S}_{(-d-1) \bmod n} \ , \qquad \hat{\mathcal{Y}} = \mathcal{S}_{-d \bmod n} \cdots \mathcal{S}_{n-1} \ , \tag{3.8}$$

$$\check{\mathcal{X}} = \mathcal{S}_{\ell d \bmod n} \cdots \mathcal{S}_{((\ell-1)d-1) \bmod n} \ , \qquad \check{\mathcal{Y}} = \mathcal{S}_{(\ell-1)d \bmod n} \cdots \mathcal{S}_{(\ell d-1) \bmod n} \ . \tag{3.9}$$

These six words are determined by the values of ℓ, m and n. We do not explicitly write them as functions of ℓ, m and n as it should always be clear which values of ℓ, m and n are being used.

The word $\mathcal{X}$, for instance, consists of the first $\ell d \bmod n$ symbols of $\mathcal{S}$, and $\mathcal{Y}$ consists of the remaining symbols of the word $\mathcal{S}$. We can therefore write $\mathcal{F}[\ell, m, n] = \mathcal{X}\mathcal{Y}$. Further partitions of $\mathcal{F}[\ell, m, n]$ are provided below in Proposition 3.3.

First let us resolve a minor ambiguity in the definitions of $\check{\mathcal{X}}$ and $\check{\mathcal{Y}}$. To be precise, $\check{\mathcal{X}}$ consists of the symbols of $\mathcal{S}$ in cyclical order starting from $\mathcal{S}_{\ell d \bmod n}$ and ending with $\mathcal{S}_{((\ell-1)d-1) \bmod n}$ (and similarly for $\check{\mathcal{Y}}$). For example, with $\mathcal{F}[3, 5, 7] = LRRLRRL$, we have $d = 3$, thus $\ell d \bmod n = 2$, and $((\ell - 1)d - 1) \bmod n = 5$. Thus $\check{\mathcal{X}} = RLRR$, and similarly $\check{\mathcal{Y}} = LLR$.

Fig. 13 illustrates the words (3.7)-(3.9) pictorially. For instance, the word $\mathcal{X}$ "follows" $\mathcal{S}$ from node 0 to node $\ell d \bmod n$, and the word $\check{\mathcal{X}}$ "follows" $\mathcal{S}$ from node $\ell d \bmod n$ to node $(\ell-1)d \bmod n$.

The words (3.7)-(3.9) can be used to partition $\mathcal{F}[\ell, m, n]$ in different ways and are useful to us for constructing the symbol sequences of periodic solutions in nearby mode-locking regions of (1.1). We omit a proof of Proposition 3.3 as it follows simply from (3.7)-(3.9) and Proposition 3.1.

Proposition 3.3. *For any* $\mathcal{F}[\ell, m, n]$,

$$\mathcal{F}[\ell,m,n] = \mathcal{X}\mathcal{Y}\,, \qquad \mathcal{F}[\ell,m,n] = \hat{\mathcal{X}}\hat{\mathcal{Y}}\,, \tag{3.10}$$

$$\mathcal{F}[\ell,m,n]^{(\ell d)} = \mathcal{Y}\mathcal{X}\,, \qquad \mathcal{F}[\ell,m,n]^{(\ell d)} = \check{\mathcal{X}}\check{\mathcal{Y}}\,, \tag{3.11}$$

$$\mathcal{F}[\ell,m,n]^{(-d)} = \mathcal{X}^{\overline{0}}\mathcal{Y}^{\overline{0}}\,, \qquad \mathcal{F}[\ell,m,n]^{(-d)} = \hat{\mathcal{Y}}\hat{\mathcal{X}}\,, \tag{3.12}$$

$$\mathcal{F}[\ell,m,n]^{((\ell-1)d)} = \mathcal{Y}^{\overline{0}}\mathcal{X}^{\overline{0}}\,, \qquad \mathcal{F}[\ell,m,n]^{((\ell-1)d)} = \check{\mathcal{Y}}\check{\mathcal{X}}\,. \tag{3.13}$$

The next result equates various concatenations of the words (3.7)-(3.9). These can be understood intuitively by following the arrows in Fig. 13. For instance, roughly speaking, both $\mathcal{X}\check{\mathcal{X}}$ and $\hat{\mathcal{X}}\mathcal{X}^{\overline{0}}$ take us from node 0 to node $(\ell-1)d \bmod n$ via an intermediary node.

Proposition 3.4. *For any* $\mathcal{F}[\ell, m, n]$,

$$\mathcal{X}\check{\mathcal{X}} = \hat{\mathcal{X}}\mathcal{X}^{\overline{0}}\,, \tag{3.14}$$

$$\mathcal{Y}\hat{\mathcal{X}} = \check{\mathcal{X}}\mathcal{Y}^{\overline{0}}\,, \tag{3.15}$$

$$\hat{\mathcal{Y}}\mathcal{X} = \mathcal{X}^{\overline{0}}\check{\mathcal{Y}}\,, \tag{3.16}$$

$$\check{\mathcal{Y}}\mathcal{Y} = \mathcal{Y}^{\overline{0}}\hat{\mathcal{Y}}\,. \tag{3.17}$$

Proof. Here we derive (3.14). The remaining identities can be derived similarly.

Let $\mathcal{S} = \mathcal{F}[\ell, m, n]$. By (3.7) and (3.9),

$$\mathcal{X}\check{\mathcal{X}} = \mathcal{S}_0 \cdots \mathcal{S}_{(\ell d-1) \bmod n}\mathcal{S}_{\ell d \bmod n} \cdots \mathcal{S}_{((\ell-1)d-1) \bmod n}\,. \tag{3.18}$$

Also $\mathcal{S}^{(-d)} = \mathcal{X}^{\overline{0}}\mathcal{Y}^{\overline{0}}$, (3.12). Therefore $\mathcal{X}^{\overline{0}}$ consists of the first ℓd symbols of $\mathcal{S}^{(-d)}$, i.e. $\mathcal{X}^{\overline{0}} = \mathcal{S}_{-d \bmod n} \cdots \mathcal{S}_{((\ell-1)d-1) \bmod n}$. Therefore

$$\hat{\mathcal{X}}\mathcal{X}^{\overline{0}} = \mathcal{S}_0 \cdots \mathcal{S}_{(-d-1) \bmod n}\mathcal{S}_{-d \bmod n} \cdots \mathcal{S}_{(\ell-1)d-1) \bmod n}\,, \tag{3.19}$$

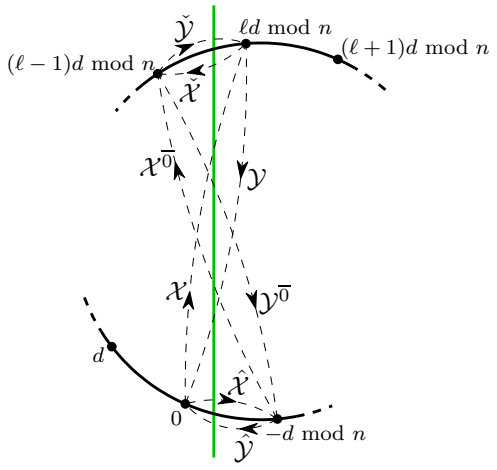

Figure 13: A pictorial interpretation of the words (3.7)-(3.9).

where we have substituted the definition of $\hat{\mathcal{X}}$ (3.8). Therefore $\mathcal{X}\check{\mathcal{X}}$ and $\hat{\mathcal{X}}\mathcal{X}^{\overline{0}}$ both consist of the symbols of $\mathcal{S}$ in cyclical order starting from $\mathcal{S}_0$ and ending with $\mathcal{S}_{(\ell-1)d-1 \bmod n}$. The words $\mathcal{X}$ and $\mathcal{X}^{\overline{0}}$ both have length $\ell d \bmod n$, and the words $\check{\mathcal{X}}$ and $\hat{\mathcal{X}}$ both have length $-d \bmod n$. Thus $\mathcal{X}\check{\mathcal{X}}$ and $\hat{\mathcal{X}}\mathcal{X}^{\overline{0}}$ consist of the same number of symbols, which verifies (3.14). □

3.3 Sequences of symbol sequences

We begin by reviewing Farey addition and the Farey tree, and then apply the results to the symbol sequences $\mathcal{G}^{\pm}[k,\chi]$ (2.15).

The Farey tree is a graph with the rational numbers in $[0,1]$ as its vertices [23, 24]. The Farey tree can be constructed by starting with the numbers $\frac{0}{1}$ and $\frac{1}{1}$ and supposing that there is an edge between them. Then all rational numbers between 0 and 1 are incorporated into the tree by repeatedly applying the following rule. Given any two fractions $\frac{m^-}{n^-}$ and $\frac{m^+}{n^+}$ that are connected by an edge, we create the new fraction $\frac{m}{n} = \frac{m^-+m^+}{n^-+n^+}$ (this is *Farey addition*), and say that this fraction is connected by an edge to both $\frac{m^-}{n^-}$ and $\frac{m^+}{n^+}$. Assuming $\frac{m^-}{n^-} < \frac{m^+}{n^+}$, we refer to $\frac{m^-}{n^-}$ and $\frac{m^+}{n^+}$ as the *left* and *right roots* of $\frac{m}{n}$, respectively.

For any $\frac{m}{n}$ in the Farey tree, $\frac{m}{n}$ is irreducible, i.e. $\gcd(m,n) = 1$, and its left and right roots satisfy $m^+n^- - m^-n^+ = 1$. As a consequence, $mn^- - m^-n = 1$, $m^+n - mn^+ = 1$, $d = n^-$, and $-d \bmod n = n^+$ (where again d is the multiplicative inverse of m modulo n). By applying these observations to the quantities in Definition 2.4 we immediately obtain the following result (illustrated in Fig. 14).

Lemma 3.5. *Write $m_0^{\pm} = m^{\pm}$ and $n_0^{\pm} = n^{\pm}$ (to accommodate the case $k = 1$). For all $k \in \mathbb{Z}^+$, the left and right roots of $\frac{m_k^+}{n_k^+}$ are $\frac{m}{n}$ and $\frac{m_{k-1}^+}{n_{k-1}^+}$, respectively, and the left and right roots of $\frac{m_k^-}{n_k^-}$ are $\frac{m_{k-1}^-}{n_{k-1}^-}$ and $\frac{m}{n}$, respectively. Moreover $d_k^+ = n$ and $-d_k^- \bmod n_k^- = n$.*

The next result concerns $\tilde{\ell}$ – the number of L's in $\mathcal{G}^{\pm}[k,\chi]$. This result is useful in later

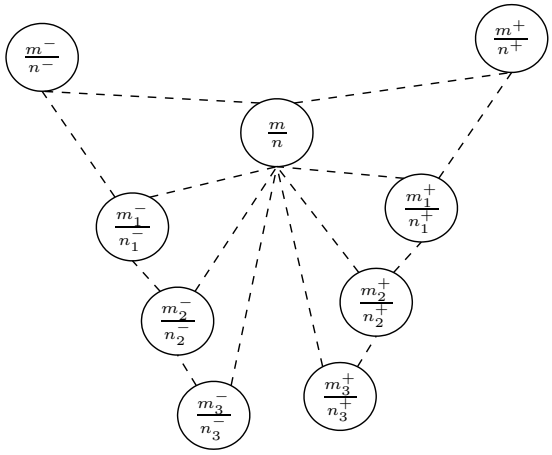

Figure 14: Part of the Farey tree centred about an arbitrary irreducible fraction $\frac{m}{n}$.

sections because $\tilde{\ell} d_k^{\pm} \bmod n_k^{\pm}$ is one of the four indices corresponding to a curve of border-collision bifurcations emanating from a $\mathcal{G}^{\pm}[k,\chi]$-shrinking point.

Lemma 3.6. *For any $k \in \mathbb{Z}^+$, $|\chi| < k$, and $\mathcal{F}[\ell,m,n]$,*

$$\tilde{\ell} d_k^{\pm} \bmod n_k^{\pm} = (\ell d \bmod n \pm \chi n) \bmod n_k^{\pm} , \tag{3.20}$$

Proof. By (2.16) and the definition of ℓ^+,

$$\ell_k^+ = k\ell + \left\lceil \frac{\ell n^+}{n} \right\rceil = k\ell + \frac{\ell n^+}{n} + \left(\frac{-\ell n^+}{n} \bmod 1 \right) = \frac{\ell n_k^+}{n} + \left(\frac{\ell d}{n} \bmod 1 \right) , \tag{3.21}$$

where in the last step we substituted $n^+ = n - d$. Since $d_k^+ = n$ (see Lemma 3.5), (3.21) implies (3.20) in the "+ case". Similarly,

$$\ell_k^- = k\ell + \left\lfloor \frac{\ell n^-}{n} \right\rfloor = k\ell + \frac{\ell n^-}{n} - \left(\frac{\ell n^-}{n} \bmod 1 \right) = \frac{\ell n_k^-}{n} - \left(\frac{\ell d}{n} \bmod 1 \right) , \tag{3.22}$$

which with $-d_k^- \bmod n_k^- = n$, leads to (3.20) in the "− case". □

The next result provides us with an alternative interpretation of ℓ^+ and ℓ^-. Here we state the result, present an example, then give a proof.

Lemma 3.7. *For any $\mathcal{F}[\ell,m,n]$, ℓ^+ is equal to the number of L's in $\hat{\mathcal{X}}$, and ℓ^- is equal to the number of L's in $\hat{\mathcal{Y}}$. Moreover, $\ell^+ + \ell^- = \ell$.*

Example 3.3. Consider $\mathcal{F}[3,5,7] = LRRLRRL$. Here $\frac{m}{n} = \frac{5}{7}$, thus $\frac{m^+}{n^+} = \frac{3}{4}$ and $\frac{m^-}{n^-} = \frac{2}{3}$. Therefore $\ell^+ = \left\lceil \frac{\ell n^+}{n} \right\rceil = \left\lceil \frac{12}{7} \right\rceil = 2$, and $\ell^- = \left\lfloor \frac{\ell n^-}{n} \right\rfloor = \left\lfloor \frac{9}{7} \right\rfloor = 1$.

Also $d = 3$, so by (3.8), $\hat{\mathcal{X}} = LRRL$ and $\hat{\mathcal{Y}} = RRL$. Thus the number of L's in $\hat{\mathcal{X}}$ is 2 and the number of L's in $\hat{\mathcal{Y}}$ is 1, in agreement with Lemma 3.7.

Proof of Lemma 3.7. Let $\hat{\ell}^+$ denote the number of L's in $\hat{\mathcal{X}}$. By (2.7),

$$\hat{\ell}^+ = \left| \left\{ i = 0, \ldots, n^+ - 1 \;\middle|\; im \bmod n < \ell \right\} \right| . \tag{3.23}$$

For each $i = 0, \ldots, n^+ - 1$,

$$im \bmod n = \left(im + \frac{i}{n^+} \right) \bmod n = \frac{im^+ n}{n^+} \bmod n , \tag{3.24}$$

where we have used $m^+ n - m n^+ = 1$ in the last equality. Using (3.24) we can rewrite (3.23) as

$$\hat{\ell}^+ = \left| \left\{ i = 0, \ldots, n^+ - 1 \;\middle|\; im^+ \bmod n^+ < \frac{\ell n^+}{n} \right\} \right| . \tag{3.25}$$

Since $\gcd(m^+, n^+) = 1$, (3.25) is the same as $\hat{\ell}^+ = \left| \left\{ j = 0, \ldots, n^+ - 1 \;\middle|\; j \bmod n^+ < \frac{\ell n^+}{n} \right\} \right|$. That is, $\hat{\ell}^+ = \left\lceil \frac{\ell n^+}{n} \right\rceil = \ell^+$, as required.

Also, $\ell^- = \left\lfloor \frac{\ell n^-}{n} \right\rfloor = \ell + \left\lfloor \frac{\ell n^-}{n} - \ell \right\rfloor = \ell - \left\lceil \ell - \frac{\ell n^-}{n} \right\rceil = \ell - \left\lceil \frac{\ell n^+}{n} \right\rceil = \ell - \ell^+$, where we have used $n^- + n^+ = n$. Therefore ℓ^- is equal to the number of L's in $\mathcal{F}[\ell,m,n]$ minus the number of L's in $\hat{\mathcal{X}}$. Since $\mathcal{F}[\ell,m,n] = \hat{\mathcal{X}}\hat{\mathcal{Y}}$, see (3.10), ℓ^- equals the number of L's in $\hat{\mathcal{Y}}$. □

The final result of this section provides explicit expressions for $\mathcal{G}^{\pm}[k,\chi]$ in terms of $\mathcal{S} = \mathcal{F}[\ell,m,n]$, $\hat{\mathcal{X}}$ and $\hat{\mathcal{Y}}$. Again we state the result, present an example, then give a proof.

Proposition 3.8. *For any $k \in \mathbb{Z}^+$, $|\chi| < k$, and $\mathcal{F}[\ell,m,n]$,*

$$\mathcal{G}^+[k,\chi] = \begin{cases} \mathcal{S}^{k+\chi}\hat{\mathcal{X}}\left(\mathcal{S}^{\overline{0}}\right)^{-\chi}, & \chi = -k+1,\ldots,-1 \\ \left(\mathcal{S}^{\overline{\ell d}}\right)^{\chi}\mathcal{S}^{k-\chi}\hat{\mathcal{X}}, & \chi = 0,\ldots,k-1 \end{cases}, \tag{3.26}$$

$$\mathcal{G}^-[k,\chi] = \begin{cases} \mathcal{S}\left(\mathcal{S}^{\overline{0}}\right)^{-\chi}\hat{\mathcal{Y}}\mathcal{S}^{k+\chi-1}, & \chi = -k+1,\ldots,0 \\ \mathcal{S}^{\overline{\ell d}}\hat{\mathcal{Y}}\mathcal{S}^{k-\chi}\left(\mathcal{S}^{\overline{\ell d}}\right)^{\chi-1}, & \chi = 1,\ldots,k-1 \end{cases}. \tag{3.27}$$

Example 3.4. Consider again $\mathcal{F}[3,5,7] = LRRLRRL$. Here $\hat{\mathcal{X}} = LRRL$ and $\hat{\mathcal{Y}} = RRL$. With $k = 3$, for example,

$$\begin{aligned} \ell_3^+ &= 3\times 3+2 = 11\,, & \ell_3^- &= 3\times 3+1 = 10\,, \\ m_3^+ &= 3\times 5+3 = 18\,, & m_3^- &= 3\times 5+2 = 17\,, \\ n_3^+ &= 3\times 7+4 = 25\,, & n_3^- &= 3\times 7+3 = 24\,. \end{aligned}$$

Therefore with $\chi = 0$, for example,

$$\begin{aligned} \mathcal{G}^+[3,0] &= \mathcal{F}[11,18,25] = LRRLRRLLRRLRRLLRRLRRLLRRL = \mathcal{S}^3\hat{\mathcal{X}}\,, \\ \mathcal{G}^-[3,0] &= \mathcal{F}[10,17,24] = LRRLRRLRRLLRRLRRLLRRLRRL = \mathcal{S}\hat{\mathcal{Y}}\mathcal{S}^2\,, \end{aligned}$$

matching Proposition 3.8.

These sequences are illustrated in Fig. 15. Notice that for both $\mathcal{G}^+[3,0]$ and $\mathcal{G}^-[3,0]$, node 2 lies immediately to the right of the upper intersection of the circle and the line. This is because with $\chi = 0$, by (3.20), $\tilde{\ell}d_k^{\pm} = \ell d \bmod n = 3\times 3 \bmod 7 = 2$. Also $d_k^+ = n = 7$, thus node 7 of $\mathcal{G}^+[3,0]$ lies immediately to the left of node 0. Similarly $-d_k^- \bmod n_k^- = n = 7$, thus node 7 of $\mathcal{G}^-[3,0]$ lies immediately to the right of node 0.

Proof of Proposition 3.8. Here we prove the result for $\mathcal{G}^+[k,\chi]$. The result for $\mathcal{G}^-[k,\chi]$ can be obtained similarly.

By the definition of a rotational symbol sequence (2.7), $\mathcal{G}^+[k,\chi]_i = L$ if $\frac{im_k^+}{n_k^+} \bmod 1 < \frac{\tilde{\ell}}{n_k^+}$, and $\mathcal{G}^+[k,\chi]_i = R$ otherwise. To evaluate $\frac{im_k^+}{n_k^+} \bmod 1$, for each $i = 0,\ldots,n_k^{\pm}-1$, we write $i = jn+r$ with $j = 0,\ldots,k$ and $r = 0,\ldots,n-1$ (for $j = k$, $r = 0,\ldots,n^+-1$). Using $m_k^+n - mn_k^+ = 1$ we obtain

$$\frac{im_k^+}{n_k^+} \bmod 1 = \frac{(jn+r)(mn_k^+ + 1)}{nn_k^+} \bmod 1 = \left(\frac{rm}{n} + \frac{j}{n_k^+} + \frac{r}{nn_k^+}\right) \bmod 1\,. \tag{3.28}$$

Now let $s = rm \bmod n$. Then

$$\frac{im_k^+}{n_k^+} \bmod 1 = \frac{s}{n} + \frac{j}{n_k^+} + \frac{r}{nn_k^+}\,, \tag{3.29}$$

where the "mod 1" is omitted on the right hand side of (3.29) because the right hand side has a value between 0 and 1.

Next, by combining (3.21), (3.29) and $\tilde{\ell} = \ell_k^+ + \chi$, we obtain

$$\frac{im_k^+}{n_k^+} \bmod 1 - \frac{\tilde{\ell}}{n_k^+} = \frac{s-\ell}{n} + \frac{j-\chi}{n_k^+} + \frac{r-(\ell d \bmod n)}{nn_k^+} \,. \tag{3.30}$$

Notice that the sign of (3.30) determines the symbol $\mathcal{G}^+[k,\chi]_i$. In contrast, $\mathcal{S}_i$ is determined by the sign of

$$\frac{rm}{n} \bmod 1 - \frac{\ell}{n} = \frac{s-\ell}{n} \,. \tag{3.31}$$

In the case $\chi = 0$, it is straight-forward to see that for all j and r the right hand-sides of (3.30) and (3.31) have the same sign, and so $\mathcal{G}^+[k,0]_i = \mathcal{S}_i$ for all i. We therefore have (3.26) in the case $\chi = 0$.

With $s = \ell$, we have $r = \ell d \bmod n$. Substituting this into (3.30) produces $\frac{im_k^+}{n_k^+} \bmod 1 - \frac{\ell_k^+ + \chi}{n_k^+} = \frac{j-\chi}{n_k^+}$, which is negative if and only if $j < \chi$, and this implies (3.26) in the case $\chi > 0$.

Similarly with $s = \ell - 1$, we have $r = (\ell - 1)d \bmod n$. Since we can rewrite $i = jn + (\ell-1)d \bmod n$ as $i = ((j-k-1)n + \ell d \bmod n) \bmod n_k^+$, into (3.30) we can substitute $r = \ell d \bmod n$, $s = \ell$ and $j \mapsto j-k-1$ to obtain $\frac{im_k^+}{n_k^+} \bmod 1 - \frac{\ell_k^+ + \chi}{n_k^+} = \frac{j-k+1-\chi}{n_k^+}$. This is negative if and only if $j < k+1+\chi$, which implies (3.26) in the case $\chi < 0$. □

4 Periodic solutions

In this section we provide some essential algebraic results for periodic solutions of (1.1). Much of this theory is also developed in [6, 14, 15]. We begin in §4.1 by briefly reviewing some specific

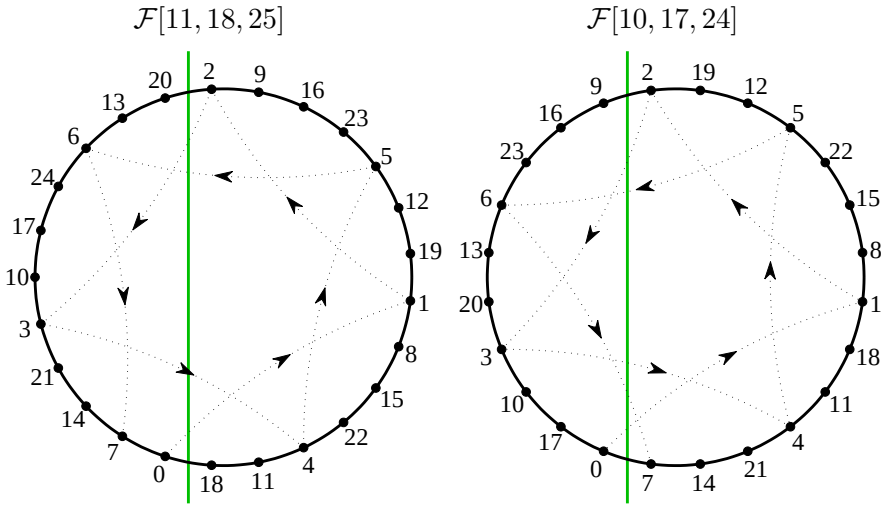

Figure 15: Pictorial interpretations of $\mathcal{G}^+[3,0]$ and $\mathcal{G}^-[3,0]$, using $\mathcal{F}[3,5,7] = LRRLRRL$, given in Example 3.4.

linear algebra concepts. Then in §4.2 we characterise periodic solutions of (1.1) as $\mathcal{S}$-cycles and describe their properties. Lastly in §4.3 we provide additional results relating to $\mathcal{S}$-cycles when it is known that the matrix $M_{\mathcal{S}^{\overline{0}}}$ is non-singular (as is the case at an $\mathcal{S}$-shrinking point).

4.1 Linear algebra tools

Given an $N \times N$ matrix A, let m_{ij} denote the determinant of the $(N-1)\times(N-1)$ matrix formed by removing the i^{th} row and j^{th} column from A (the m_{ij} are the *minors* of A). The *adjugate* of A is then defined by $\text{adj}(A)_{ij} = (-1)^{i+j} m_{ji}$. For any A,

$$\text{adj}(A)A = A\,\text{adj}(A) = \det(A) I \;, \tag{4.1}$$

and if A is nonsingular, $A^{-1} = \frac{\text{adj}(A)}{\det(A)}$, see [25, 26, 27] for further details.

The following result is known as the matrix determinant lemma. For a proof using partitioned matrices, see [28].

Lemma 4.1. *Let A be an $N \times N$ matrix, and $u, v \in \mathbb{R}^N$. Then*

$$\det\left(A + vu^{\mathsf{T}}\right) = \det(A) + u^{\mathsf{T}}\text{adj}(A)v \;. \tag{4.2}$$

The next result is useful to us in view of the relationship between A_L and A_R, (1.3). Indeed in later sections we only require (4.3) with $u = e_1$, and in this case (4.3) follows immediately from the above definition of an adjugate matrix [6, 29]. For completeness we provide a proof of Lemma 4.2 in Appendix A.

Lemma 4.2. *Let A be an $N \times N$ matrix, and $u, v \in \mathbb{R}^N$. Then*

$$u^{\mathsf{T}}\text{adj}\left(A + vu^{\mathsf{T}}\right) = u^{\mathsf{T}}\text{adj}(A) \;. \tag{4.3}$$

The next result provides an explicit formula for the adjugate of a singular matrix. A proof is given in Appendix A. Related properties of adjugate matrices are discussed in [30, 31].

Lemma 4.3. *Let A be an $N \times N$ matrix. If* $\text{rank}(A) = N-1$*, then*

$$\text{adj}(A) = cvu^{\mathsf{T}} \;, \tag{4.4}$$

where $u^{\mathsf{T}}A = 0$, $Av = 0$, $u^{\mathsf{T}}v = 1$, and c is the product of all nonzero eigenvalues of A, counting multiplicity. If $\text{rank}(A) < N-1$*, then* $\text{adj}(A)$ *is the zero matrix.*

4.2 Basic properties of periodic solutions

An $\mathcal{S}$-cycle is a periodic solution $\{x_i^{\mathcal{S}}\}$ of the half maps of (1.1) in the order determined by $\mathcal{S}$, refer to Definition 2.1 for a formal statement. If $s_i^{\mathcal{S}} \le 0$ whenever $\mathcal{S}_i = L$, and $s_i^{\mathcal{S}} \ge 0$ whenever $\mathcal{S}_i = R$, then the $\mathcal{S}$-cycle is a periodic solution of (1.1) and said to be *admissible*, otherwise it is said to be *virtual*. The following result relates to border-collision bifurcations of $\mathcal{S}$-cycles (at which $s_j^{\mathcal{S}} = 0$, for some j) and is an immediate consequence of the continuity of (1.1).

Lemma 4.4. *Let $\{x_i^{\mathcal{S}}\}$ be an $\mathcal{S}$-cycle. If $s_j^{\mathcal{S}} = 0$, for some j, then $\{x_i^{\mathcal{S}}\}$ is also an $\mathcal{S}^{\overline{j}}$-cycle.*

Each $x_i^{\mathcal{S}}$ is a fixed point of

$$f^{\mathcal{S}^{(i)}}(x) = M_{\mathcal{S}^{(i)}} x + P_{\mathcal{S}^{(i)}} B\mu \ , \tag{4.5}$$

see (2.3), where $\mathcal{S}^{(i)}$ denotes the i^{th} left shift permutation of $\mathcal{S}$. By (2.4), changing i only changes the cyclic order in which A_L and A_R are multiplied to produce $M_{\mathcal{S}^{(i)}}$. This is the basis for the following result which is a minor generalisation of a result proved in [14, 15], and so we omit a proof.

Lemma 4.5. *The determinant of $M_{\mathcal{S}^{(i)}}$, and its eigenvalues and the multiplicities of the eigenvalues, are independent of i.*

In view of (4.5), the stability of an $\mathcal{S}$-cycle is governed by the eigenvalues of $M_{\mathcal{S}^{(i)}}$, and by Lemma 4.5 it suffices to consider $i = 0$. These observations provide us with the following result.

Proposition 4.6. *An admissible $\mathcal{S}$-cycle, with $s_i^{\mathcal{S}} \neq 0$ for all i, is attracting if and only if all eigenvalues of $M_{\mathcal{S}}$ have modulus less than* 1*.*

Equation (4.5) provides us with an explicit expression for each $x_i^{\mathcal{S}}$, as stated in the next result.

Proposition 4.7. *The $\mathcal{S}$-cycle is unique if and only if $I - M_{\mathcal{S}}$ is nonsingular, and if $I - M_{\mathcal{S}}$ is nonsingular then*

$$x_i^{\mathcal{S}} = (I - M_{\mathcal{S}^{(i)}})^{-1} P_{\mathcal{S}^{(i)}} B\mu \ . \tag{4.6}$$

Lastly, to obtain a useful explicit expression for each $s_i^{\mathcal{S}}$ (the first component of $x_i^{\mathcal{S}}$), we use the row vector

$$\varrho^{\mathsf{T}} := e_1^{\mathsf{T}} \mathrm{adj}\,(I - A_L) = e_1^{\mathsf{T}} \mathrm{adj}\,(I - A_R) \ , \tag{4.7}$$

where the second equality is a consequence of (1.3) and (4.3). The following identity,

$$e_1^{\mathsf{T}} \mathrm{adj}\,(I - M_{\mathcal{S}^{(i)}})\, P_{\mathcal{S}^{(i)}} = \det\,(P_{\mathcal{S}^{(i)}})\, \varrho^{\mathsf{T}} \ , \tag{4.8}$$

is a consequence of (1.3), see [15, 16] for a derivation. By combining (4.6) and (4.8) we obtain

$$\det(I - M_{\mathcal{S}}) s_i^{\mathcal{S}} = \det\,(P_{\mathcal{S}^{(i)}})\, \varrho^{\mathsf{T}} B\mu \ , \tag{4.9}$$

from which the next result follows immediately.

Proposition 4.8.

i) If $I - M_{\mathcal{S}}$ is nonsingular, then

$$s_i^{\mathcal{S}} = \frac{\det\,(P_{\mathcal{S}^{(i)}})\, \varrho^{\mathsf{T}} B\mu}{\det\,(I - M_{\mathcal{S}})} \ . \tag{4.10}$$

ii) If $I - M_{\mathcal{S}}$ is singular, $f^{\mathcal{S}}$ has a fixed point, $\mu \neq 0$, and $\varrho^{\mathsf{T}} B \neq 0$, then $P_{\mathcal{S}^{(i)}}$ is singular for all i.

4.3 Consequences of $\det(I - M_{\mathcal{S}^{\overline{0}}}) \neq 0$

Our definition of a shrinking point (Definition 2.3) includes the assumption $\det(I - M_{\mathcal{S}^{\overline{0}}}) \neq 0$. By Proposition 4.7, this ensures that the $\mathcal{S}^{\overline{0}}$-cycle is unique. In this section we provide two important results requiring the assumption $\det(I - M_{\mathcal{S}^{\overline{0}}}) \neq 0$.

Lemma 4.9. *Suppose $I - M_{\mathcal{S}^{\overline{0}}}$ is nonsingular and $I - M_{\mathcal{S}}$ is singular. Then the eigenvalue 1 of $M_{\mathcal{S}}$ has algebraic multiplicity 1, and the corresponding right eigenspace of $M_{\mathcal{S}}$ is not orthogonal to e_1.*

Proof. By (1.3) and (2.4), we can write

$$M_{\mathcal{S}^{\overline{0}}} = M_{\mathcal{S}} + C_{\mathcal{S}} e_1^{\mathsf{T}} , \tag{4.11}$$

for some $C_{\mathcal{S}} \in \mathbb{R}^N$. By Lemma 4.1,

$$\det(I - M_{\mathcal{S}^{\overline{0}}}) = \det\left(I - M_{\mathcal{S}} - C_{\mathcal{S}} e_1^{\mathsf{T}}\right) = e_1^{\mathsf{T}} \mathrm{adj}(I - M_{\mathcal{S}})\, C_{\mathcal{S}} , \tag{4.12}$$

because $\det(I - M_{\mathcal{S}}) = 0$. Since $\det(I - M_{\mathcal{S}^{\overline{0}}}) \neq 0$, by assumption, $\mathrm{adj}(I - M_{\mathcal{S}})$ cannot be the zero matrix. Thus by Lemma 4.3, the eigenvalue 1 of $M_{\mathcal{S}}$ has algebraic multiplicity 1.

Let $v \in \mathbb{R}^N$ be an eigenvector of $M_{\mathcal{S}}$ corresponding to the eigenvalue 1. That is $v \neq 0$ and

$$0 = (I - M_{\mathcal{S}})\, v = (I - M_{\mathcal{S}^{\overline{0}}})\, v + C_{\mathcal{S}} e_1^{\mathsf{T}} v . \tag{4.13}$$

But $(I - M_{\mathcal{S}^{\overline{0}}})\, v \neq 0$, because $I - M_{\mathcal{S}^{\overline{0}}}$ is nonsingular, therefore $e_1^{\mathsf{T}} v \neq 0$ as required. □

Lemma 4.10. *Suppose $I - M_{\mathcal{S}^{\overline{0}}}$ is nonsingular, $I - M_{\mathcal{S}}$ and $P_{\mathcal{S}}$ are singular, $\mu \neq 0$, and $\varrho^{\mathsf{T}} B \neq 0$. Then $P_{\mathcal{S}^{(i)}}$ is singular for all i.*

Proof. Since $I - M_{\mathcal{S}^{\overline{0}}}$ is nonsingular, there exists a unique $\mathcal{S}^{\overline{0}}$-cycle, $\left\{x_i^{\mathcal{S}^{\overline{0}}}\right\}$. The matrix $P_{\mathcal{S}^{\overline{0}}}$ is singular because $P_{\mathcal{S}^{\overline{0}}} = P_{\mathcal{S}}$, (2.5). Therefore $s_0^{\mathcal{S}^{\overline{0}}} = 0$, (4.10). By Lemma 4.4, $\left\{x_i^{\mathcal{S}^{\overline{0}}}\right\}$ is also an $\mathcal{S}$-cycle, and so $x_0^{\mathcal{S}^{\overline{0}}}$ is a fixed point of $f^{\mathcal{S}}$. Therefore, by Proposition 4.8(ii), $P_{\mathcal{S}^{(i)}}$ is singular for all i. □

5 Shrinking points

Our definition of a shrinking point, Definition 2.3, is based on the conditions $s_0^{\mathcal{S}^{\overline{0}}} = 0$ and $s_{\ell d}^{\mathcal{S}^{\overline{0}}} = 0$, where the $s_i^{\mathcal{S}^{\overline{0}}}$ are the first coordinates of the points of the $\mathcal{S}^{\overline{0}}$-cycle, and $\mathcal{S} = \mathcal{F}[\ell, m, n]$ is a rotational symbol sequence. Here we begin by providing additional motivation for our restriction to rotational symbol sequences, and the choice of the indices $i = 0$ and $i = \ell d$ in Definition 2.3.

5.1 Motivation for Definition 2.3

Conceptually, a shrinking point is a point in parameter space where (1.1) has an $\mathcal{S}$-cycle, $\{x_i^{\mathcal{S}}\}$, with two points on the switching manifold. Without loss of generality we can suppose that one of these points is $x_0^{\mathcal{S}}$, and that $\mathcal{S}_0 = L$. Let $x_\alpha^{\mathcal{S}}$, where $1 \leq \alpha \leq n - 1$ and n is the period, be

the other point of the $\mathcal{S}$-cycle on the switching manifold. By a double application of Lemma 4.4, this $\mathcal{S}$-cycle is also an $\mathcal{S}^{\overline{0}\,\overline{\alpha}}$-cycle. If $\mathcal{S}_\alpha = R$, then $\mathcal{S}^{\overline{0}\,\overline{\alpha}}$ has the same number of L's as $\mathcal{S}$. In this case it is possible for there to exist an integer d such that

$$\mathcal{S}^{\overline{0}\,\overline{\alpha}(d)} = \mathcal{S} \, . \tag{5.1}$$

That is, if we flip the 0^{th} and α^{th} symbols of $\mathcal{S}$, then apply the d^{th} left shift permutation, we recover the original symbol sequence.

The next result tells us that if (5.1) holds, then $\mathcal{S}$ must equal $\mathcal{F}[\ell, m, n]$ for some integers ℓ and m, and $\alpha = \ell d \bmod n$. In other words, our restriction to rotational symbol sequences and the choice of the indices $i = 0$ and $i = \ell d$ in Definition 2.3 can be viewed as a consequence of supposing that the symbol sequence associated with a shrinking point satisfies (5.1) for some values of α and d.

Proposition 5.1. *Let $\mathcal{S}$ be a periodic symbol sequence of period n with $\mathcal{S}_0 = L$, and suppose $\mathcal{S}^{\overline{0}\,\overline{\alpha}(d)} = \mathcal{S}$, for some $1 \le \alpha \le n-1$ and $1 \le d \le n-1$ with $\gcd(d, n) = 1$. Let m denote the multiplicative inverse of d modulo n, and $\ell = m\alpha \bmod n$. Then $\mathcal{S} = \mathcal{F}[\ell, m, n]$, and $\alpha = \ell d \bmod n$.*

Proof. The formula $\alpha = \ell d \bmod n$ is a trivial consequence of our definitions of ℓ and m in the statement of the theorem. It remains to show that $\mathcal{S} = \mathcal{F}[\ell, m, n]$, which we achieve by verifying (3.1).

For any $j = 1, \ldots, \ell - 1$,

$$\mathcal{S}_{jd \bmod n} = \mathcal{S}^{\overline{0}\,\overline{\alpha}}_{jd \bmod n} = \mathcal{S}^{\overline{0}\,\overline{\alpha}(d)}_{(j-1)d \bmod n} \, , \tag{5.2}$$

because $j \neq 0, \ell$, and where the second equality follows from the definition of a shift permutation. Then

$$\mathcal{S}^{\overline{0}\,\overline{\alpha}(d)}_{(j-1)d \bmod n} = \mathcal{S}_{(j-1)d \bmod n} \, , \tag{5.3}$$

because $\mathcal{S}^{\overline{0}\,\overline{\alpha}(d)} = \mathcal{S}$, by assumption. By then starting with $\mathcal{S}_0 = L$, and recursively applying (5.2)-(5.3), we obtain $\mathcal{S}_0 = \mathcal{S}_d = \cdots = \mathcal{S}_{(\ell-1)d \bmod n}$, matching (3.1).

Equation (5.3) is true for all $j \in \mathbb{Z}$, whereas (5.2) is false for $j = \ell$ (because $\ell d \bmod n = \alpha$). This implies $\mathcal{S}_{\ell d \bmod n} \neq \mathcal{S}_{(\ell-1)d \bmod n}$, and thus $\mathcal{S}_{\ell d \bmod n} = R$. Finally, (5.2) is true for all $j = \ell + 1, \ldots, n-1$ and so a similar recursive argument gives us $\mathcal{S}_{\ell d \bmod n} = \mathcal{S}_{(\ell d+1) \bmod n} = \cdots = \mathcal{S}_{-d \bmod n} = R$, which verifies (3.1), and hence $\mathcal{S} = \mathcal{F}[\ell, m, n]$. □

5.2 Basic properties of shrinking points

Recall, at an $\mathcal{S}$-shrinking point, y_i denotes the i^{th} point of the $\mathcal{S}^{\overline{0}}$-cycle and t_i denotes the first coordinate of y_i, see §2.1. By assumption

$$t_0 = 0 \, , \qquad t_{\ell d} = 0 \, , \tag{5.4}$$

and $t_i \neq 0$, for all $i \neq 0, \ell d$. The $\mathcal{S}^{\overline{0}}$-cycle is assumed to be admissible, and this fixes the signs of the t_i. In particular,

$$t_d < 0 \, , \qquad t_{(\ell-1)d} < 0 \, , \qquad t_{(\ell+1)d} > 0 \, , \qquad t_{-d} > 0 \, , \tag{5.5}$$

see Fig. 16.

The next three results provide key properties of shrinking points.

Proposition 5.2. *At an $\mathcal{S}$-shrinking point, $\{y_i\}$ has period n.*

This is proved in [15] and is a consequence of the rotational nature of $\mathcal{F}[\ell, m, n]$.

Proposition 5.3. *At an $\mathcal{S}$-shrinking point,*

i) $\{y_i\}$ is both an $\mathcal{S}$-cycle and an $\mathcal{S}^{(-d)}$-cycle,

ii) $I - M_{\mathcal{S}}$ is singular,

iii) $P_{\mathcal{S}^{(i)}}$ is singular for all i.

Proof. By definition, $\{y_i\}$ is an $\mathcal{S}^{\overline{0}}$-cycle. Since $t_0 = 0$, by Lemma 4.4, $\{y_i\}$ is also an $\mathcal{S}$-cycle. Since $t_{\ell d} = 0$, $\{y_i\}$ is similarly also an $\mathcal{S}^{\overline{0}\,\overline{\ell d}}$-cycle, and so by (3.6), $\{y_i\}$ is also an $\mathcal{S}^{(-d)}$-cycle, which proves part (i).

By part (i), y_0 and y_d are both fixed points of $f^{\mathcal{S}}$. By (5.4) and (5.5) these points are distinct, hence by Proposition 4.7, $I - M_{\mathcal{S}}$ is singular. Finally, $P_{\mathcal{S}^{(i)}}$ is singular for all i by Proposition 4.8(ii). □

Proposition 5.4. *For any $\mathcal{S}$-shrinking point in the phase space of (1.1), let $\mathcal{P}$ denote the non-planar polygon formed by joining each y_i to $y_{(i+d)}$ by a line segment. Then each point on $\mathcal{P}$ belongs to an admissible $\mathcal{S}$-cycle of (1.1), and the restriction of (1.1) to $\mathcal{P}$ is homeomorphic to rigid rotation with rotation number $\frac{m}{n}$.*

Refer to [14, 15] for a proof.

5.3 Eigenvectors associated with shrinking points

By Proposition 5.3(ii), $M_{\mathcal{S}}$ has a unit eigenvalue. Since $\det(I - M_{\mathcal{S}^{\overline{0}}}) \neq 0$, by Lemma 4.9 the unit eigenvalue is of algebraic multiplicity one. Furthermore, by Lemma 4.5 each $M_{\mathcal{S}^{(i)}}$ has a unit eigenvalue of algebraic multiplicity one.

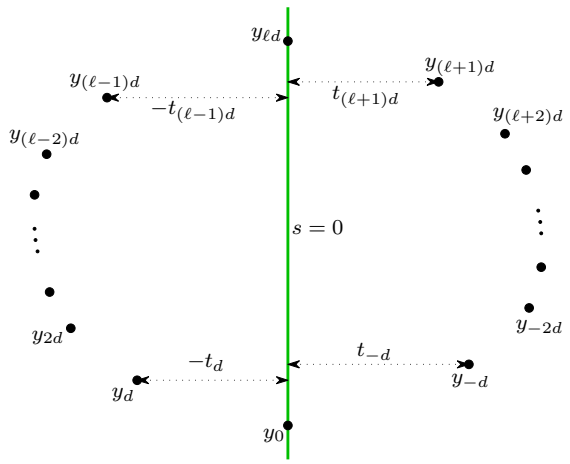

Figure 16: A schematic diagram showing the $\mathcal{S}^{\overline{0}}$-cycle at an $\mathcal{S}$-shrinking point.

Recall, in §2.1 we let u_j^T and v_j denote the left and right eigenvectors of $M_{\mathcal{S}^{(j)}}$ corresponding to the unit eigenvalue normalised by $u_j^\mathsf{T} v_j = 1$ and $e_1^\mathsf{T} v_j = 1$, for $j = 0, (\ell-1)d, \ell d, -d$. The following result provides explicit expressions for u_j^T and v_j.

Lemma 5.5. *At an $\mathcal{S}$-shrinking point, for each $j \in \{0, (\ell-1)d, \ell d, -d\}$,*

$$u_j^\mathsf{T} = \frac{e_1^\mathsf{T} \mathrm{adj}\,(I - M_{\mathcal{S}^{(j)}})}{c}\,, \qquad v_j = \frac{y_{j+d} - y_j}{t_{j+d} - t_j}\,, \tag{5.6}$$

where c is given by (2.11).

Proof. By applying Lemma 4.3 to the matrix $A = I - M_{\mathcal{S}^{(j)}}$, we obtain $\mathrm{adj}\,(I - M_{\mathcal{S}^{(j)}}) = c v_j u_j^\mathsf{T}$. Since also $e_1^\mathsf{T} v_j = 1$, this implies $\frac{e_1^\mathsf{T} \mathrm{adj}\left(I - M_{\mathcal{S}^{(j)}}\right)}{c} = u_j^\mathsf{T}$.

Next let $\hat{v}_j = \frac{y_{j+d} - y_j}{t_{j+d} - t_j}$. It remains to show that $\hat{v}_j = v_j$. Trivially $e_1^\mathsf{T} \hat{v}_j = 1$. By Proposition 5.3, y_j and y_{j+d} are both fixed points of $f^{\mathcal{S}^{(j)}}$, and thus

$$y_{j+d} - y_j = f^{\mathcal{S}^{(j)}}(y_{j+d}) - f^{\mathcal{S}^{(j)}}(y_j) = M_{\mathcal{S}^{(j)}}(y_{j+d} - y_j)\ . \tag{5.7}$$

Therefore $M_{\mathcal{S}^{(j)}} \hat{v}_j = \hat{v}_j$. That is, each $\hat{v}_j$ satisfies the same properties as v_j. But v_j is unique, hence $\hat{v}_j = v_j$, as required. □

The eigenvectors u_j^T and v_j are sketched in Fig. 17. By Lemma 5.5, the eigenvector v_0, for example, has the same direction as the line segment connecting y_0 to y_d, and $e_1^\mathsf{T} v_j = 1$. Let z be any point on this line segment other than y_0 and y_d. By Proposition 5.4, z is a fixed point of $f^{\mathcal{S}}$. Moreover, there exists a neighbourhood of z that follows the sequence $\mathcal{S}$ under the next n iterations of (1.1). Within this neighbourhood, the hyperplane that intersects z and is orthogonal to u_0^T is invariant. If all the eigenvalues of $M_{\mathcal{S}}$, other than the unit eigenvalue, have modulus less than 1 (i.e. $\sigma < 1$, see (2.14)), then within this neighbourhood the hyperplane is the stable manifold of z for the map $f^{\mathcal{S}}$. In summary, iterates of $f^{\mathcal{S}}$ approach the line segment connecting y_0 to y_d (which has direction v_0) on a hyperplane orthogonal to u_0^T. The remaining eigenvectors u_j^T and v_j can be interpreted similarly.

The next result indicates how the eigenvectors are related to one another algebraically.

Lemma 5.6. *We have*

$$v_{\ell d} = \frac{t_d}{t_{(\ell+1)d}} M_{\mathcal{X}} v_0\,, \qquad u_{\ell d}^\mathsf{T} = \frac{t_{(\ell+1)d}}{t_d} u_0^\mathsf{T} M_{\mathcal{Y}}\,, \tag{5.8}$$

$$v_0 = \frac{t_{(\ell+1)d}}{t_d} M_{\mathcal{Y}} v_{\ell d}\,, \qquad u_0^\mathsf{T} = \frac{t_d}{t_{(\ell+1)d}} u_{\ell d}^\mathsf{T} M_{\mathcal{X}}\,, \tag{5.9}$$

$$v_{(\ell-1)d} = \frac{t_{-d}}{t_{(\ell-1)d}} M_{\mathcal{X}^{\overline{0}}} v_{-d}\,, \qquad u_{(\ell-1)d}^\mathsf{T} = \frac{t_{(\ell-1)d}}{t_{-d}} u_{-d}^\mathsf{T} M_{\mathcal{Y}^{\overline{0}}}\,, \tag{5.10}$$

$$v_{-d} = \frac{t_{(\ell-1)d}}{t_{-d}} M_{\mathcal{Y}^{\overline{0}}} v_{(\ell-1)d}\,, \qquad u_{-d}^\mathsf{T} = \frac{t_{-d}}{t_{(\ell-1)d}} u_{(\ell-1)d}^\mathsf{T} M_{\mathcal{X}^{\overline{0}}}\,. \tag{5.11}$$

Furthermore,

$$v_{-d} = -\frac{t_d}{t_{-d}} M_{\hat{\mathcal{X}}} v_0 \ , \qquad u_{-d}^{\mathsf{T}} = -\frac{t_{-d}}{t_d} u_0^{\mathsf{T}} M_{\hat{\mathcal{Y}}} \ , \tag{5.12}$$

$$v_0 = -\frac{t_{-d}}{t_d} M_{\hat{\mathcal{Y}}} v_{-d} \ , \qquad u_0^{\mathsf{T}} = -\frac{t_d}{t_{-d}} u_{-d}^{\mathsf{T}} M_{\hat{\mathcal{X}}} \ , \tag{5.13}$$

$$v_{(\ell-1)d} = -\frac{t_{(\ell+1)d}}{t_{(\ell-1)d}} M_{\check{\mathcal{X}}} v_{\ell d} \ , \qquad u_{(\ell-1)d}^{\mathsf{T}} = -\frac{t_{(\ell-1)d}}{t_{(\ell+1)d}} u_{\ell d}^{\mathsf{T}} M_{\check{\mathcal{Y}}} \ , \tag{5.14}$$

$$v_{\ell d} = -\frac{t_{(\ell-1)d}}{t_{(\ell+1)d}} M_{\check{\mathcal{Y}}} v_{(\ell-1)d} \ , \qquad u_{\ell d}^{\mathsf{T}} = -\frac{t_{(\ell+1)d}}{t_{(\ell-1)d}} u_{(\ell-1)d}^{\mathsf{T}} M_{\check{\mathcal{X}}} \ . \tag{5.15}$$

Proof. By Proposition 5.3, $f^{\mathcal{X}}(y_0) = y_{\ell d}$ and $f^{\mathcal{X}}(y_d) = y_{(\ell+1)d}$. Therefore

$$M_{\mathcal{X}} v_0 = \frac{1}{t_d} M_{\mathcal{X}} \left(y_d - y_0 \right) = \frac{1}{t_d} \left(y_{(\ell+1)d} - y_{\ell d} \right) = \frac{t_{(\ell+1)d}}{t_d} v_{\ell d} \ , \tag{5.16}$$

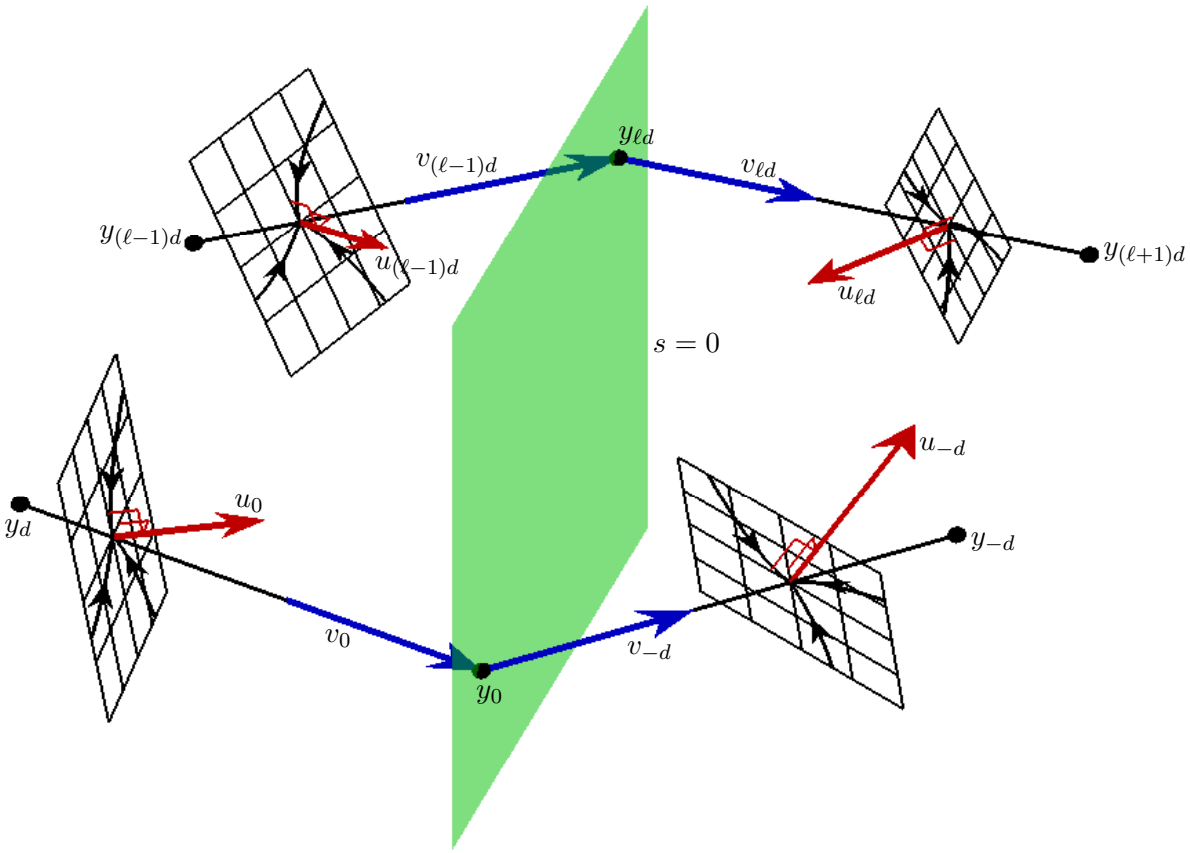

Figure 17: A schematic diagram illustrating the periodic solution $\{y_i\}$ and the eigenvectors u_j^{T} and v_j.

which verifies the first part of (5.8). The first parts of the remaining equations can be derived in the same fashion.

By (3.10) and (3.11),

$$M_{\mathcal{Y}} M_{\mathcal{S}^{(\ell d)}} = M_{\mathcal{Y}} M_{\mathcal{X}} M_{\mathcal{Y}} = M_{\mathcal{S}} M_{\mathcal{Y}} \ . \tag{5.17}$$

Therefore

$$u_0^{\mathsf{T}} M_{\mathcal{Y}} M_{\mathcal{S}^{(\ell d)}} = u_0^{\mathsf{T}} M_{\mathcal{S}} M_{\mathcal{Y}} = u_0^{\mathsf{T}} M_{\mathcal{Y}} \ , \tag{5.18}$$

i.e. $u_0^{\mathsf{T}} M_{\mathcal{Y}}$ is a left eigenvector of $M_{\mathcal{S}^{(\ell d)}}$ corresponding to the eigenvalue 1, and therefore is a multiple of $u_{\ell d}$. Also, by using the first part of (5.9) we obtain

$$\frac{t_{(\ell+1)d}}{t_d} u_0^{\mathsf{T}} M_{\mathcal{Y}} v_{\ell d} = u_0^{\mathsf{T}} v_0 = 1 \ . \tag{5.19}$$

Therefore $\frac{t_{(\ell+1)d}}{t_d} u_0^{\mathsf{T}} M_{\mathcal{Y}}$ has the same magnitude and direction as $u_{\ell d}$. This verifies the second part of (5.8), and second parts of the remaining equations can be demonstrated similarly. □

5.4 A basic unfolding of shrinking points

The behaviour of $\mathcal{F}[\ell, m, n]$-cycles and $\mathcal{F}[\ell \pm 1, m, n]$-cycles near an $\mathcal{S}$-shrinking point, where $\mathcal{S} = \mathcal{F}[\ell, m, n]$, was summarised in §2.1. In this section we review this behaviour more carefully.

We assume $\xi = (\xi_1, \xi_2) \in \mathbb{R}^2$, for simplicity, let ξ^* be an $\mathcal{S}$-shrinking point, and introduce local (η, ν)-coordinates (2.12). The condition $\det(J) \neq 0$, where J is given by (2.13), ensures that the coordinate change $(\xi_1, \xi_2) \leftrightarrow (\eta, \nu)$ is invertible.

The following result specifies curves of border-collision bifurcations, $\eta = \psi_1(\nu)$ and $\nu = \psi_2(\eta)$, along which $\mathcal{F}[\ell, m, n]$ and $\mathcal{F}[\ell+1, m, n]$-cycles coincide. The subsequent result provides a useful expression for $\det(I - M_{\mathcal{S}})$. Both results are proved in [14, 15], except that expressions for the coefficients in terms of the t_i are derived in [16].

Lemma 5.7. *Suppose (1.1) with $K \geq 2$ has an $\mathcal{S}$-shrinking point at $\xi = \xi^*$ and $\det(J) \neq 0$. Then, in a neighbourhood of $\xi = \xi^*$,*

i) there exists a unique C^K function $\psi_1 : \mathbb{R} \to \mathbb{R}$, with

$$\psi_1(\nu) = -\frac{t_d}{t_{(\ell-1)d} t_{(\ell+1)d}} \nu^2 + o\big(\nu^2\big) \ , \tag{5.20}$$

such that $s_{\ell d}^{\overline{\mathcal{S}^{\ell d}}} = 0$ on the locus $\eta = \psi_1(\nu)$,

ii) there exists a unique C^K function $\psi_2 : \mathbb{R} \to \mathbb{R}$, with

$$\psi_2(\eta) = -\frac{t_{(\ell-1)d}}{t_d t_{-d}} \eta^2 + o\big(\eta^2\big) \ , \tag{5.21}$$

such that $s_0^{\overline{\mathcal{S}^{\ell d}}} = 0$ on the locus $\nu = \psi_2(\eta)$.

Lemma 5.8. *Suppose (1.1) with $K \geq 2$ has an $\mathcal{S}$-shrinking point at $\xi = \xi^*$ and $\det(J) \neq 0$. Then*

$$\det(I - M_{\mathcal{S}}) = \frac{a}{t_d}\eta + \frac{a}{t_{(\ell-1)d}}\nu + \mathcal{O}\left((\eta,\nu)^2\right) \ , \tag{5.22}$$

where $a = \det\left(I - M_{\mathcal{S}^{\overline{0}}}\right)\big|_{\xi=\xi^*}$.

The next result identifies regions, Ψ_1 and Ψ_2, within which $\mathcal{F}[\ell-1,m,n]$, $\mathcal{F}[\ell,m,n]$ and $\mathcal{F}[\ell+1,m,n]$-cycles reside, and represents the basic unfolding of a shrinking point. The reader is referred to [14, 15] for a proof. Fig. 18 summarises the unfolding. If $\sigma < 1$, then some of the periodic solutions are stable, see Table 1, but note that Theorem 5.9 does not concern stability and holds for any value of σ.

Theorem 5.9. *Suppose (1.1) with $K \geq 2$ has an $\mathcal{S}$-shrinking point at $\xi = \xi^*$ and $\det(J) \neq 0$. Let $\Psi_1 = \left\{(\eta,\nu) \;\middle|\; \eta,\nu \geq 0\right\}$ and $\Psi_2 = \left\{(\eta,\nu) \;\middle|\; \eta \leq \psi_1(\nu),\, \nu \leq \psi_2(\eta)\right\}$, where ψ_1 and ψ_2 are specified by Lemma 5.7. Then there exists a neighbourhood $\mathcal{N}$ of $(\eta,\nu) = (0,0)$, such that (1.1) has unique admissible $\mathcal{F}[\ell,m,n]$ and $\mathcal{F}[\ell-1,m,n]$ cycles in $\Psi_1 \cap \mathcal{N} \setminus \{(0,0)\}$ and (1.1) has admissible $\mathcal{F}[\ell,m,n]$ and $\mathcal{F}[\ell+1,m,n]$ cycles in $\Psi_2 \cap \mathcal{N} \setminus \{(0,0)\}$.*

5.5 Further identities relating to shrinking points

We conclude this section by deriving additional algebraic expressions regarding shrinking points that are used in later sections.

As implied by (5.22), $I - M_{\mathcal{S}}$ is singular along a curve passing through the $\mathcal{S}$-shrinking point. At points where $I - M_{\mathcal{S}}$ is non-singular, the $\mathcal{S}$-cycle is unique, and the following result provides us with an asymptotic expression for the location of the points of the $\mathcal{S}$-cycle.

Lemma 5.10. *Suppose (1.1) with $K \geq 2$ has an $\mathcal{S}$-shrinking point at $\xi = \xi^*$ and $\det(J) \neq 0$. Then for all (η,ν) for which $\det(I - M_{\mathcal{S}}) \neq 0$, for all i,*

$$x_i^{\mathcal{S}} = \frac{\frac{y_{i+d}}{t_d}\eta + \frac{y_i}{t_{(\ell-1)d}}\nu + \mathcal{O}\left((\eta,\nu)^2\right)}{\frac{1}{t_d}\eta + \frac{1}{t_{(\ell-1)d}}\nu + \mathcal{O}\left((\eta,\nu)^2\right)} \ . \tag{5.23}$$

Proof. By (4.6), $x_i^{\mathcal{S}} = \frac{\mathrm{adj}\left(I - M_{\mathcal{S}^{(i)}}\right) P_{\mathcal{S}^{(i)}} B\mu}{\det(I - M_{\mathcal{S}})}$. Therefore we can write

$$x_i^{\mathcal{S}}(\eta,\nu) = \frac{C_0 + C_1\eta + C_2\nu + \mathcal{O}\left((\eta,\nu)^2\right)}{\frac{a}{t_d}\eta + \frac{a}{t_{(\ell-1)d}}\nu + \mathcal{O}\left((\eta,\nu)^2\right)} \ , \tag{5.24}$$

for some $C_0, C_1, C_2 \in \mathbb{R}^N$. When $\eta = 0$, $x_i^{\mathcal{S}} = x_i^{\mathcal{S}^{\overline{0}}}$, thus $x_i^{\mathcal{S}}(0,\nu) = y_i + \mathcal{O}(\eta,\nu)$, hence $C_0 = 0$ and $C_2 = \frac{a}{t_{(\ell-1)d}} y_i$. Similarly when $\nu = 0$, $x_i^{\mathcal{S}} = x_{i+d}^{\mathcal{S}^{\overline{0}}}$, thus $x_i^{\mathcal{S}}(\eta,0) = y_{i+d} + \mathcal{O}(\eta,\nu)$, hence $C_1 = \frac{a}{t_d} y_{i+d}$. By substituting these expressions for C_1 and C_2 into (5.24) and cancelling instances of a, we obtain (5.23) as required. ∎

At the shrinking point, $M_{\mathcal{S}}$ has a unit eigenvalue and so near the shrinking point $M_{\mathcal{S}}$ has an eigenvalue near 1. Throughout this paper this eigenvalue is denoted by λ. Locally λ is C^K function of η and ν because the algebraic multiplicity of the unit eigenvalue at the shrinking point is one, Lemma 4.9.

Lemma 5.11. *Suppose (1.1) with $K \geq 2$ has an $\mathcal{S}$-shrinking point at $\xi = \xi^*$ and* $\det(J) \neq 0$. *Then*

$$\lambda = 1 - \frac{a}{ct_d}\eta - \frac{a}{ct_{(\ell-1)d}}\nu + \mathcal{O}\left((\eta,\nu)^2\right) \ , \tag{5.25}$$

where c is the product of the nonzero eigenvalues of $I - M_{\mathcal{S}}$ at $\xi = \xi^*$, (2.11).

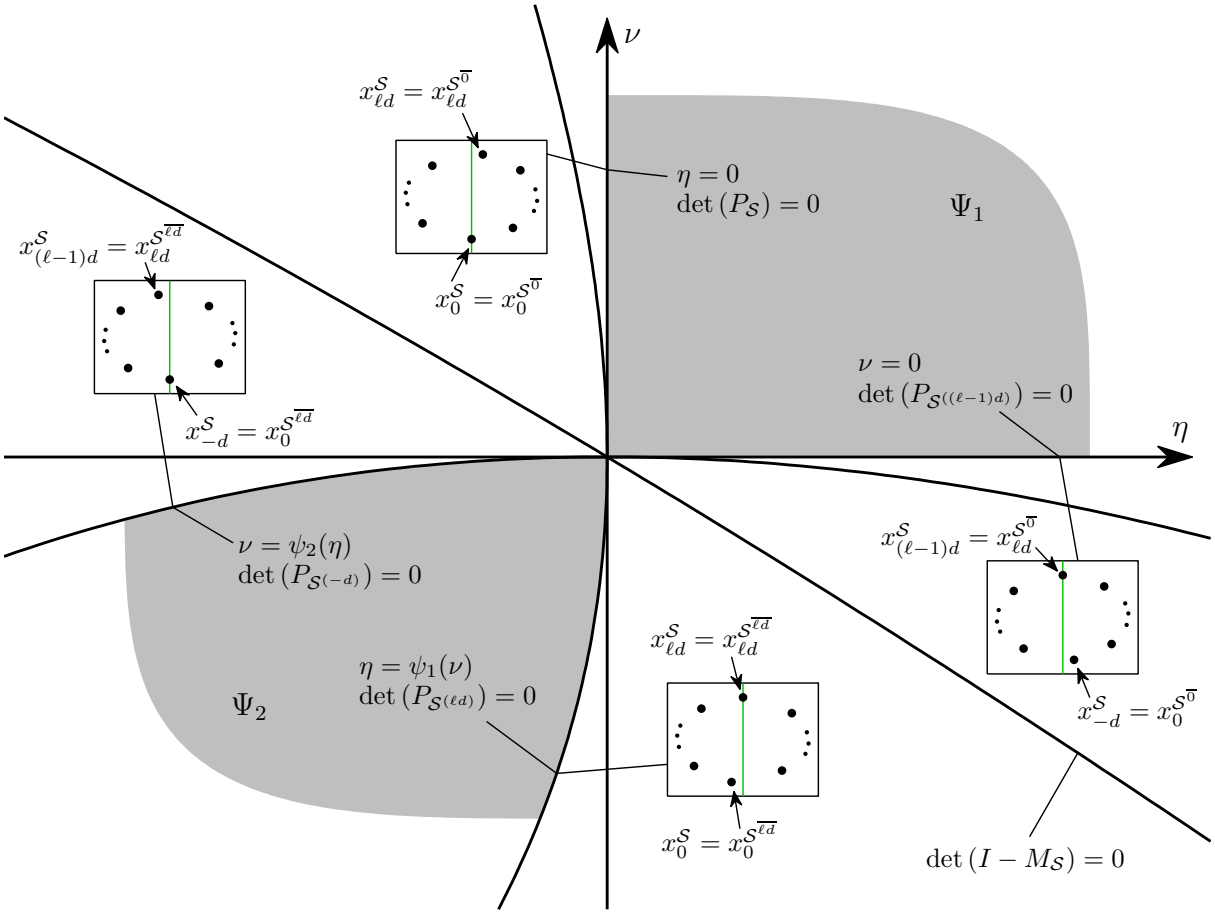

Figure 18: The basic unfolding of a shrinking point as specified by Theorem 5.9. In (η, ν)-coordinates, the shrinking point is located at the origin, the positive axes are border-collision bifurcation curves that bound the region Ψ_1, and $\eta = \psi_1(\nu)$ and $\nu = \psi_2(\eta)$ are border-collision bifurcation curves that bound Ψ_2. We have also included sketches of the $\mathcal{S}$-cycle in relation to the switching manifold at a typical point on each of the four boundaries.

Proof. Write $\lambda = 1 + k_1\eta + k_2\nu + \mathcal{O}(2)$, for some $k_1, k_2 \in \mathbb{R}$. Then

$$\begin{aligned}\det(I - M_{\mathcal{S}}) &= (1-\lambda)\left(c + \mathcal{O}(\eta,\nu)\right)\\ &= \left(-k_1\eta - k_2\nu + \mathcal{O}\left((\eta,\nu)^2\right)\right)\left(c + \mathcal{O}(\eta,\nu)\right)\\ &= -k_1 c\eta - k_2 c\nu + \mathcal{O}\left((\eta,\nu)^2\right)\ . \end{aligned} \tag{5.26}$$

By matching (5.22) and (5.26) we obtain (5.25) as required. □

The last two results provide identities that connect various quantities associated with a shrinking point. For a proof of Lemma 5.12, refer to [16]. The proof involves expanding $s_i^{\mathcal{S}^{\overline{0}}}$ and $s_i^{\mathcal{S}^{\overline{\ell d}}}$ in terms of η and ν (for certain values of i) and matching coefficients. This assumes $\det(J) \neq 0$, but we expect that Lemmas 5.12 and 5.13 hold regardless of how (1.1) varies with ξ as the results concern properties of the shrinking point itself.

Lemma 5.12. *Suppose (1.1) with $K \geq 2$ has an $\mathcal{S}$-shrinking point at $\xi = \xi^*$ and $\det(J) \neq 0$. Then*

$$\frac{a}{b} = -\frac{t_d t_{(\ell-1)d}}{t_{-d} t_{(\ell+1)d}}\ . \tag{5.27}$$

Lemma 5.13. *Suppose (1.1) with $K \geq 2$ has an $\mathcal{S}$-shrinking point at $\xi = \xi^*$ and $\det(J) \neq 0$. Then, repeating (2.10),*

$$\frac{u_0^{\mathsf{T}} v_{-d}}{a} + \frac{u_{\ell d}^{\mathsf{T}} v_{(\ell-1)d}}{b} = \frac{1}{c}\ , \tag{5.28}$$

$$\frac{u_{(\ell-1)d}^{\mathsf{T}} v_{\ell d}}{a} + \frac{u_{-d}^{\mathsf{T}} v_0}{b} = \frac{1}{c}\ . \tag{5.29}$$

Proof. Here we derive only (5.28). Equation (5.29) may be derived similarly.

By (5.9), (5.11) and (5.27),

$$u_0^{\mathsf{T}} v_{-d} = \left(\frac{t_d}{t_{(\ell+1)d}} u_{\ell d}^{\mathsf{T}} M_{\mathcal{X}}\right)\left(\frac{t_{(\ell-1)d}}{t_{-d}} M_{\mathcal{Y}^{\overline{0}}} v_{(\ell-1)d}\right) = -\frac{a u_{\ell d} M_{\mathcal{X}} M_{\mathcal{Y}^{\overline{0}}} v_{(\ell-1)d}}{b}\ . \tag{5.30}$$

Therefore

$$\frac{u_0^{\mathsf{T}} v_{-d}}{a} + \frac{u_{\ell d}^{\mathsf{T}} v_{(\ell-1)d}}{b} = \frac{u_{\ell d}^{\mathsf{T}}\left(I - M_{\mathcal{X}} M_{\mathcal{Y}^{\overline{0}}}\right) v_{(\ell-1)d}}{b}\ . \tag{5.31}$$

By (5.6), $u_{\ell d}^{\mathsf{T}} = \frac{e_1^{\mathsf{T}} \mathrm{adj}\left(I - M_{\mathcal{S}^{(\ell d)}}\right)}{c}$, and by (3.11), $M_{\mathcal{S}^{(\ell d)}} = M_{\mathcal{X}} M_{\mathcal{Y}}$. By (2.4) and Lemma 4.2, $e_1^{\mathsf{T}} \mathrm{adj}\left(I - M_{\mathcal{X}} M_{\mathcal{Y}}\right) = e_1^{\mathsf{T}} \mathrm{adj}\left(I - M_{\mathcal{X}} M_{\mathcal{Y}^{\overline{0}}}\right)$, thus

$$u_{\ell d}^{\mathsf{T}} = \frac{e_1^{\mathsf{T}} \mathrm{adj}\left(I - M_{\mathcal{X}} M_{\mathcal{Y}^{\overline{0}}}\right)}{c}\ . \tag{5.32}$$

By substituting (5.32) into (5.31) and using (4.1) we obtain

$$\frac{u_0^{\mathsf{T}} v_{-d}}{a} + \frac{u_{\ell d}^{\mathsf{T}} v_{(\ell-1)d}}{b} = \frac{e_1^{\mathsf{T}} v_{(\ell-1)d} \det\left(I - M_{\mathcal{X}} M_{\mathcal{Y}^{\overline{0}}}\right)}{bc}\ . \tag{5.33}$$

Finally, $\det\left(I - M_{\mathcal{X}} M_{\mathcal{Y}^{\overline{0}}}\right) = b$, because $M_{\mathcal{X}} M_{\mathcal{Y}^{\overline{0}}} = M_{\mathcal{S}^{(\ell d)\overline{0}}} = M_{\mathcal{S}^{\overline{\ell d}(\ell d)}} = M_{\mathcal{F}[\ell+1,m,n]^{(\ell d)}}$, by (3.4). Thus (5.33) reduces to (5.28), because also $e_1^{\mathsf{T}} v_{(\ell-1)d} = 1$, by definition. □

6 Locating nearby shrinking points

At an $\mathcal{S}$-shrinking point, for each j, the line segment connecting y_j to y_{j+d} consists of fixed points of $f^{\mathcal{S}^{(j)}}$, see Fig. 17. For parameter values near the shrinking point, the line segments persist as one-dimensional slow manifolds. These are described in §6.1. In §6.2 we then use these results to determine the location of nearby $\mathcal{G}^{\pm}[k,\chi]$-shrinking points to leading order.

6.1 Slow manifolds

In a neighbourhood of an $\mathcal{S}$-shrinking point, for each $j = 0, (\ell-1)d, \ell d, -d$, we let ω_j^{T} and ζ_j denote the left and right eigenvectors of $M_{\mathcal{S}^{(j)}}$ corresponding to λ. More specifically,

$$M_{\mathcal{S}^{(j)}}\zeta_j = \lambda\zeta_j \ , \qquad e_1^{\mathsf{T}}\zeta_j = 1 \ , \tag{6.1}$$

$$\omega_j^{\mathsf{T}} M_{\mathcal{S}^{(j)}} = \lambda\omega_j^{\mathsf{T}} \ , \qquad \omega_j^{\mathsf{T}}\zeta_j = 1 \ . \tag{6.2}$$

Each ω_j^{T} and ζ_j is a C^K function, of η and ν. Recall, u_j^{T} and v_j denote the eigenvectors at the shrinking point, see §2.1, thus

$$\zeta_j(0,0) = v_j \ , \qquad \omega_j^{\mathsf{T}}(0,0) = u_j^{\mathsf{T}} \ . \tag{6.3}$$

The following result relates the eigenvectors to one another based on the partitions of $\mathcal{S}$ introduced in Definition 3.2.

Lemma 6.1. *For any matrix Q,*

$$\omega_0^{\mathsf{T}} Q M_{\hat{\mathcal{X}}}\zeta_0 = \omega_{-d}^{\mathsf{T}} M_{\hat{\mathcal{X}}} Q\zeta_{-d} \ , \tag{6.4}$$

$$\omega_0^{\mathsf{T}} M_{\hat{\mathcal{Y}}} Q\zeta_0 = \omega_{-d}^{\mathsf{T}} Q M_{\hat{\mathcal{Y}}}\zeta_{-d} \ , \tag{6.5}$$

$$\omega_{\ell d}^{\mathsf{T}} Q M_{\check{\mathcal{X}}}\zeta_{\ell d} = \omega_{(\ell-1)d}^{\mathsf{T}} M_{\check{\mathcal{X}}} Q\zeta_{(\ell-1)d} \ , \tag{6.6}$$

$$\omega_{\ell d}^{\mathsf{T}} M_{\check{\mathcal{Y}}} Q\zeta_{\ell d} = \omega_{(\ell-1)d}^{\mathsf{T}} Q M_{\check{\mathcal{Y}}}\zeta_{(\ell-1)d} \ . \tag{6.7}$$

Proof. Here we derive (6.4). The remaining identities can be derived in the same fashion.

Since $M_{\mathcal{S}} = M_{\hat{\mathcal{Y}}} M_{\hat{\mathcal{X}}}$ and $M_{\mathcal{S}^{(-d)}} = M_{\hat{\mathcal{X}}} M_{\hat{\mathcal{Y}}}$, refer to (2.4), (3.10) and (3.12), by (6.1) we have

$$\zeta_0 = k_1 M_{\hat{\mathcal{Y}}}\zeta_{-d} \ , \tag{6.8}$$

for some $k_1 \in \mathbb{R}$. Similarly

$$\omega_0^{\mathsf{T}} = k_2 \omega_{-d}^{\mathsf{T}} M_{\hat{\mathcal{X}}} \ , \tag{6.9}$$

for some $k_2 \in \mathbb{R}$. By using (6.1)-(6.2), we then deduce

$$1 = \omega_0^{\mathsf{T}}\zeta_0 = k_1 k_2 \omega_{-d}^{\mathsf{T}} M_{\hat{\mathcal{X}}} M_{\hat{\mathcal{Y}}}\zeta_{-d} = k_1 k_2 \omega_{-d}^{\mathsf{T}}\lambda\zeta_{-d} = \lambda k_1 k_2 \ . \tag{6.10}$$

Finally, by combining (6.8)-(6.10) we obtain

$$\omega_0^{\mathsf{T}} Q M_{\hat{\mathcal{X}}}\zeta_0 = k_1 k_2 \omega_{-d}^{\mathsf{T}} M_{\hat{\mathcal{X}}} Q M_{\hat{\mathcal{X}}} M_{\hat{\mathcal{Y}}}\zeta_{-d} = k_1 k_2 \omega_{-d}^{\mathsf{T}} M_{\hat{\mathcal{X}}} Q\lambda\zeta_{-d} = \omega_{-d}^{\mathsf{T}} M_{\hat{\mathcal{X}}} Q\zeta_{-d} \ , \tag{6.11}$$

as required. □

Let us now consider the dynamics of $f^{\mathcal{S}^{(j)}}$ (for any $j = 0, (\ell-1)d, \ell d, -d$). If $\det(I - M_{\mathcal{S}}) \neq 0$, then $f^{\mathcal{S}^{(j)}}$ has a unique fixed point, $x_j^{\mathcal{S}}$. The line intersecting $x_j^{\mathcal{S}}$ and of direction ζ_j is a slow manifold on which the dynamics of $f^{\mathcal{S}^{(j)}}$ is dictated by the value of λ.

Since $x_j^{\mathcal{S}}$ is sensitive to changes in η and ν, see (5.23), instead of $x_j^{\mathcal{S}}$ it more helpful to use the intersection of the slow manifold with the switching manifold, call it φ_j, as a reference point about which we can perform calculations. If $\det(I - M_{\mathcal{S}}) \neq 0$, then this intersection point is given by

$$\varphi_j = \left(I - \zeta_j e_1^{\mathsf{T}}\right) x_j^{\mathcal{S}} \ . \tag{6.12}$$

The utility of φ_j lies in the fact that it is well-defined even when $\det(I - M_{\mathcal{S}}) = 0$, see Lemma 6.2.

Any point on the slow manifold can be written as $\varphi_j + h\zeta_j$, where $h \in \mathbb{R}$ is the first component of this point (since $e_1^{\mathsf{T}}\varphi_j = 0$ and $e_1^{\mathsf{T}}\zeta_j = 1$). If $\det(I - M_{\mathcal{S}}) \neq 0$, then, since $x_j^{\mathcal{S}}$ is a fixed point of $f^{\mathcal{S}^{(j)}}$ and $M_{\mathcal{S}^{(j)}}\zeta_j = \lambda\zeta_j$, we have

$$f^{\mathcal{S}^{(j)}}(\varphi_j + h\zeta_j) = \varphi_j + (h\lambda + \gamma_j)\,\zeta_j \ , \tag{6.13}$$

where,

$$\gamma_j = (1 - \lambda) e_1^{\mathsf{T}} x_j^{\mathcal{S}} \ . \tag{6.14}$$

Equation (6.13) describes the dynamics on the slow manifold, see Fig. 19. The next result justifies our use of φ_j and γ_j when $\det(I - M_{\mathcal{S}}) = 0$.

Lemma 6.2. *Suppose (1.1) with $K \geq 2$ has an $\mathcal{S}$-shrinking point at $\xi = \xi^*$ and $\det(J) \neq 0$. Then there exists a neighbourhood $\mathcal{N}$ of $(\eta, \nu) = (0, 0)$, such that for all $j \in \{0, (\ell-1)d, \ell d, -d\}$, there exists unique C^K functions $\varphi_j : \mathcal{N} \to \mathbb{R}^N$ and $\gamma_j : \mathcal{N} \to \mathbb{R}$ with $e_1^{\mathsf{T}}\varphi_j = 0$, $\gamma_j(0,0) = 0$, and*

$$\varphi_0(0,0) = \varphi_{-d}(0,0) = y_0 \ , \qquad \varphi_{(\ell-1)d}(0,0) = \varphi_{\ell d}(0,0) = y_{\ell d} \ , \tag{6.15}$$

such that (6.13) is satisfied for all $h \in \mathbb{R}$ and all $(\eta, \nu) \in \mathcal{N}$. Moreover, (6.12) and (6.14) are satisfied for all $(\eta, \nu) \in \mathcal{N}$ for which $\det(I - M_{\mathcal{S}}) \neq 0$.

Proof. Consider the matrix equation

$$\left((I - M_{\mathcal{S}^{(j)}})\left(I - e_1 e_1^{\mathsf{T}}\right) + \zeta_j e_1^{\mathsf{T}}\right)\phi_j = P_{\mathcal{S}^{(j)}} B\mu \ , \tag{6.16}$$

where we wish to solve for the unknown vector ϕ_j. Here we show that (6.16) defines ϕ_j uniquely, and that the desired quantities φ_j and γ_j are given by

$$\varphi_j = \left(I - e_1 e_1^{\mathsf{T}}\right)\phi_j \ , \qquad \gamma_j = e_1^{\mathsf{T}}\phi_j \ . \tag{6.17}$$

To show that (6.16) has a unique solution, we apply Lemma 4.1 to write

$$\begin{aligned}\det\left((I - M_{\mathcal{S}^{(j)}})\left(I - e_1 e_1^{\mathsf{T}}\right) + \zeta_j e_1^{\mathsf{T}}\right) &= \det(I - M_{\mathcal{S}^{(j)}})\det\left(I - e_1 e_1^{\mathsf{T}}\right) \\ &\quad + e_1^{\mathsf{T}}\mathrm{adj}\left(I - e_1 e_1^{\mathsf{T}}\right)\mathrm{adj}\,(I - M_{\mathcal{S}^{(j)}})\,\zeta_j \ .\end{aligned} \tag{6.18}$$

Since $\det\left(I - e_1 e_1^{\mathsf{T}}\right) = 0$ and $\mathrm{adj}\left(I - e_1 e_1^{\mathsf{T}}\right) = e_1 e_1^{\mathsf{T}}$, (6.18) reduces to

$$\det\left((I - M_{\mathcal{S}^{(j)}})\left(I - e_1 e_1^{\mathsf{T}}\right) + \zeta_j e_1^{\mathsf{T}}\right) = e_1^{\mathsf{T}}\mathrm{adj}\,(I - M_{\mathcal{S}^{(j)}})\,\zeta_j \ . \tag{6.19}$$

At $(\eta,\nu)=(0,0)$, $e_1^{\mathsf{T}}\mathrm{adj}\,(I-M_{\mathcal{S}^{(j)}})=cu_j^{\mathsf{T}}$ and $\zeta_j=v_j$, see (5.6) and (6.3). Using also $u_j^{\mathsf{T}}v_j=1$ we obtain

$$\det\left((I-M_{\mathcal{S}^{(j)}})\left(I-e_1e_1^{\mathsf{T}}\right)+\zeta_je_1^{\mathsf{T}}\right)=c+\mathcal{O}(\eta,\nu)\,, \tag{6.20}$$

which is nonzero in a neighbourhood of $(0,0)$. Thus (6.16) has a unique solution ϕ_j in this neighbourhood.

Next we define φ_j and γ_j by (6.17). These are C^K functions of η and ν because the components of (6.16) are C^K. By (6.17), $e_1^{\mathsf{T}}\varphi_j=0$. Also $\phi_j=\varphi_j+\gamma_je_1$, and by substituting this into (6.16) and simplifying we obtain

$$(I-M_{\mathcal{S}^{(j)}})\,\varphi_j+\gamma_j\zeta_j=P_{\mathcal{S}^{(j)}}B\mu\,. \tag{6.21}$$

Thus for any $h\in\mathbb{R}$

$$M_{\mathcal{S}^{(j)}}\left(\varphi_j+h\zeta_j\right)+P_{\mathcal{S}^{(j)}}B\mu=\varphi_j+(h\lambda+\gamma_j)\,\zeta_j\,, \tag{6.22}$$

where we have used $M_{\mathcal{S}^{(j)}}\zeta_j=\lambda_j\zeta_j$. and therefore (6.13). This shows that (6.13) is satisfied.

When $(\eta,\nu)=(0,0)$, (6.21) is satisfied by $\gamma_j=0$ and either $\varphi_j=y_0$ or $\varphi_j=y_{\ell d}$, as given in (6.15). This verifies (6.15) and $\gamma_j(0,0)=0$ because ϕ_j is unique. Similarly, when $\det(I-M_{\mathcal{S}})\neq 0$, (6.21) is satisfied by (6.12) and (6.14) because

$$(I-M_{\mathcal{S}^{(j)}})\left(I-\zeta_je_1^{\mathsf{T}}\right)x_j^{\mathcal{S}}+(1-\lambda)\zeta_je_1^{\mathsf{T}}x_j^{\mathcal{S}}=(I-M_{\mathcal{S}^{(j)}})\,x_j^{\mathcal{S}}\,, \tag{6.23}$$

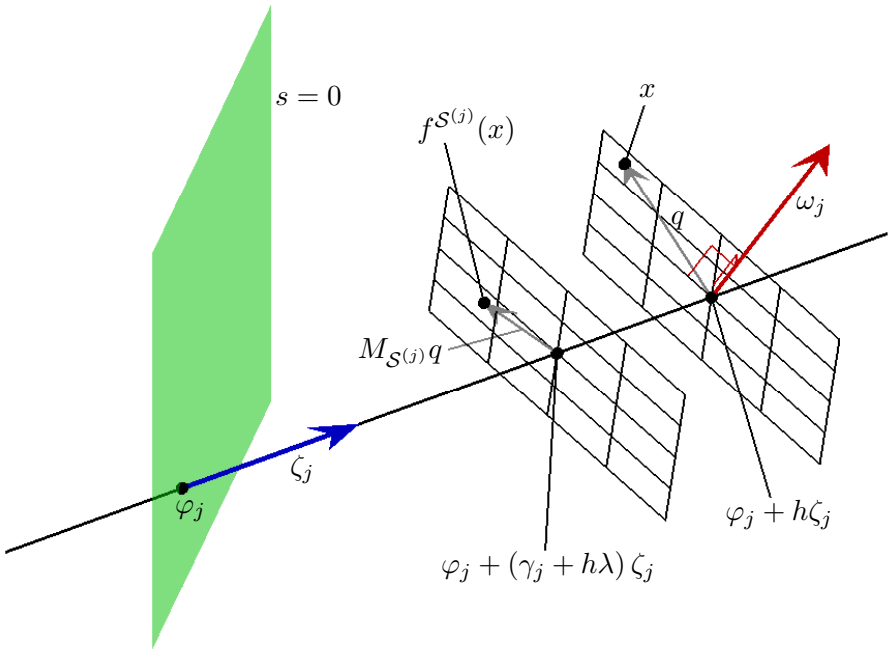

Figure 19: An illustration of dynamics near the slow manifold of $f^{\mathcal{S}^{(j)}}$, for any $j=0,(\ell-1)d,\ell d,-d$, for parameter values near an $\mathcal{S}$-shrinking point. The slow manifold is a line of direction ζ_j (the slow eigenvector (6.1)) that intersects the switching manifold at φ_j In order to study images of x under $f^{\mathcal{S}^{(j)}}$, it is helpful to decompose x using the eigenspaces of $M_{\mathcal{S}^{(j)}}$, specifically (6.24).

and therefore $(I - M_{\mathcal{S}^{(j)}})\, x_j^{\mathcal{S}} = P_{\mathcal{S}} B\mu$. Again, because of the uniqueness of ϕ_j, (6.12) and (6.14) hold in a neighbourhood of $(\eta, \nu) = (0, 0)$. □

For any j, and any $x \in \mathbb{R}^N$, it is helpful to write

$$x = \varphi_j + h\zeta_j + q \;, \tag{6.24}$$

where $h \in \mathbb{R}$ and $q \in \mathbb{R}^N$ with $\omega_j^{\mathsf{T}} q = 0$. The vector $h\zeta_j$ represents the component of $x - \varphi_j$ in the ζ_j direction. The vector q represents the component of $x - \varphi_j$ in the remaining eigendirections of $M_{\mathcal{S}^{(j)}}$. The decomposition (6.24) is unique and enables us to express iterates of x under $f^{\mathcal{S}^{(j)}}$ succinctly, Lemma 6.3. This is illustrated in Fig. 19 and formalised by the following result. We omit a proof as it is a straight-forward application of eigenspace decomposition.

Lemma 6.3. *For all $j \in \{0, (\ell-1)d, \ell d, -d\}$, and for all $x \in \mathbb{R}^N$, there exists unique $h \in \mathbb{R}$ and $q \in \mathbb{R}^N$ with $\omega_j^{\mathsf{T}} q = 0$ such that $x = \varphi_j + h\zeta_j + q$. Moreover*

$$h = \omega_j^{\mathsf{T}} (x - \varphi_j) \;, \qquad q = \left(I - \zeta_j \omega_j^{\mathsf{T}}\right)(x - \varphi_j) \;, \tag{6.25}$$

and for any $k \in \mathbb{Z}^+$,

$$f^{\left(\mathcal{S}^{(j)}\right)^k}(x) = \varphi_j + \left(\gamma_j \sum_{j=0}^{k-1} \lambda^j + h\lambda^k\right)\zeta_j + M_{\mathcal{S}^{(j)}}^k q \;. \tag{6.26}$$

The remaining results of this paper assume $\sigma < 1$, where σ denotes the maximum modulus of the eigenvalues of $M_{\mathcal{S}}$, excluding the unit eigenvalue, at the $\mathcal{S}$-shrinking point, (2.14). This assumption ensures iterates under $f^{\mathcal{S}(j)}$ converge to the slow manifold, which is central to the validity of our main results.

Lemma 6.4. *If $\sigma < 1$, then $c > 0$.*

Proof. As in (2.14), let $\rho_1, \ldots, \rho_N$ be the eigenvalues of $M_{\mathcal{S}}$, counting multiplicity, and $\rho_1 = 1$. By the definition of c (2.11), $c = \prod_{i=2}^{N}(1 - \rho_i)$. The assumption $\sigma < 1$ implies $|\rho_i| < 1$, for each $i \neq 1$. If $\rho_i \in \mathbb{R}$, then $1 - \rho_i > 0$. Any $\rho_i \notin \mathbb{R}$ appear in complex conjugate pairs with $(1 - \rho_i)(1 - \overline{\rho}_i) > 0$. Thus $\prod_{i=2}^{N}(1 - \rho_i)$ can be expressed as a product of positive numbers, and so $c > 0$ as required. □

As described above, q is a linear combination of the eigendirections of $M_{\mathcal{S}}$ other than ζ_j. If $\sigma < 1$, then the corresponding eigenvalues all have modulus less than 1, in which case $\left\|M_{\mathcal{S}^{(j)}}^k q\right\| \to 0$, as $k \to \infty$. Moreover, we can write $M_{\mathcal{S}^{(j)}}^k q = \mathcal{O}\left(\sigma^k\right)$. This is true for any q of the form (6.25), thus we have the following result.

Lemma 6.5. *If $\sigma < 1$, then for each $j \in \{0, (\ell-1)d, \ell d, -d\}$,*

$$M_{\mathcal{S}^{(j)}}^k \left(I - \zeta_j \omega_j^{\mathsf{T}}\right) = \mathcal{O}\left(\sigma^k\right) \;. \tag{6.27}$$

6.2 Calculations for nearby shrinking points

In this section we derive formulas for the border-collision bifurcation curves of $\mathcal{G}^{\pm}[k,\chi]$-cycles. The first result provides us with expressions for $\det\left(\rho I - M_{\mathcal{G}^{\pm}[k,\chi]}\right)$, useful for large values of $k \in \mathbb{Z}^+$.

Lemma 6.6. *Suppose (1.1) with $K \geq 2$ has an $\mathcal{S}$-shrinking point at $\xi = \xi^*$ and $\det(J) \neq 0$ and $\sigma < 1$. Choose any $\chi_{\max} \in \mathbb{Z}^+$, $k \in \mathbb{Z}^+$, and $\rho \in \mathbb{C}$. Then, in a neighbourhood of $(\eta,\nu) = (0,0)$,*

$$\det\left(\rho I - M_{\mathcal{G}^+[k,\chi]}\right) = \begin{cases} \rho^N\left(1 - \frac{\lambda^{k+\chi+1}}{\rho}\omega_{\ell d}^{\mathsf{T}}\left(M_{\mathcal{X}\overline{0}}M_{\mathcal{Y}}\right)^{-\chi-1}M_{\check{\mathcal{X}}}\zeta_{\ell d}\right) + \mathcal{O}\left(\sigma^k\right), & -\chi_{\max} \leq \chi \leq -1 \\ \rho^N\left(1 - \frac{\lambda^{k-\chi}}{\rho}\omega_0^{\mathsf{T}}\left(M_{\mathcal{Y}\overline{0}}M_{\mathcal{X}}\right)^{\chi}M_{\hat{\mathcal{X}}}\zeta_0\right) + \mathcal{O}\left(\sigma^k\right), & 0 \leq \chi \leq \chi_{\max} \end{cases}, \tag{6.28}$$

$$\det\left(\rho I - M_{\mathcal{G}^-[k,\chi]}\right) = \begin{cases} \rho^N\left(1 - \frac{\lambda^{k+\chi}}{\rho}\omega_{-d}^{\mathsf{T}}\left(M_{\mathcal{Y}}M_{\mathcal{X}\overline{0}}\right)^{-\chi}M_{\hat{\mathcal{Y}}}\zeta_{-d}\right) + \mathcal{O}\left(\sigma^k\right), & -\chi_{\max} \leq \chi \leq 0 \\ \rho^N\left(1 - \frac{\lambda^{k-\chi+1}}{\rho}\omega_{(\ell-1)d}^{\mathsf{T}}\left(M_{\mathcal{X}}M_{\mathcal{Y}\overline{0}}\right)^{\chi-1}M_{\check{\mathcal{Y}}}\zeta_{(\ell-1)d}\right) + \mathcal{O}\left(\sigma^k\right), & 1 \leq \chi \leq \chi_{\max} \end{cases}. \tag{6.29}$$

Proof. Here we derive (6.28) for $0 \leq \chi \leq \chi_{\max}$. The remaining formulas can be derived similarly.

By Lemma 4.5, $M_{\mathcal{G}^+[k,\chi]}$ and $M_{\mathcal{G}^+[k,\chi]^{(i)}}$ share the same eigenvalues and multiplicities, for any i. The same is true for $\rho I - M_{\mathcal{G}^+[k,\chi]}$ and $\rho I - M_{\mathcal{G}^+[k,\chi]^{(i)}}$, thus, for any i,

$$\det\left(\rho I - M_{\mathcal{G}^+[k,\chi]}\right) = \det\left(\rho I - M_{\mathcal{G}^+[k,\chi]^{(i)}}\right). \tag{6.30}$$

For any $0 \leq \chi \leq \chi_{\max}$, $\mathcal{G}^+[k,\chi] = \left(\mathcal{S}^{\overline{\ell d}}\right)^{\chi}\mathcal{S}^{k-\chi}\hat{\mathcal{X}}$, (3.26). The word $\hat{\mathcal{X}}$ has $n-d$ symbols (3.2), thus

$$\mathcal{G}^+[k,\chi]^{(d-n)} = \hat{\mathcal{X}}\left(\mathcal{S}^{\overline{\ell d}}\right)^{\chi}\mathcal{S}^{k-\chi}. \tag{6.31}$$

$\mathcal{G}^+[k,\chi]^{(d-n)}$ is a particularly useful permutation of $\mathcal{G}^+[k,\chi]$ for the purposes of this proof because, by (6.31), it ends in a power involving k. By (6.31),

$$M_{\mathcal{G}^+[k,\chi]^{(d-n)}} = M_{\mathcal{S}}^{k-\chi}M_{\mathcal{S}^{\overline{\ell d}}}^{\chi}M_{\hat{\mathcal{X}}}. \tag{6.32}$$

Since $M_{\mathcal{S}}\zeta_0 = \lambda\zeta_0$, by Lemma 6.5 with $j = 0$ we can write

$$M_{\mathcal{S}}^{k-\chi} = M_{\mathcal{S}}^{k-\chi}\zeta_0\omega_0^{\mathsf{T}} + M_{\mathcal{S}}^{k-\chi}\left(I - \zeta_0\omega_0^{\mathsf{T}}\right) = \lambda^{k-\chi}\zeta_0\omega_0^{\mathsf{T}} + \mathcal{O}\left(\sigma^k\right), \tag{6.33}$$

with which (6.32) becomes

$$M_{\mathcal{G}^+[k,\chi]^{(d-n)}} = \lambda^{k-\chi}\zeta_0\omega_0^{\mathsf{T}}\left(M_{\mathcal{Y}\overline{0}}M_{\mathcal{X}}\right)^{\chi}M_{\hat{\mathcal{X}}} + \mathcal{O}\left(\sigma^k\right), \tag{6.34}$$

where we have also substituted $M_{\mathcal{S}^{\overline{\ell d}}} = M_{\mathcal{Y}\overline{0}}M_{\mathcal{X}}$. Finally, by using Lemma 4.1, (6.30) with $i = n-d$, and (6.34), we arrive at (6.28) for $0 \leq \chi \leq \chi_{\max}$ as required. ∎

To motivate the next result, recall that boundaries of $\mathcal{G}_k^{\pm}$-mode-locking regions are points where $s_i^{\mathcal{G}^{\pm}[k,\chi]} = 0$, for certain values of i. Each $s_i^{\mathcal{G}^{\pm}[k,\chi]}$ can be evaluated using (2.6). The following result provides asymptotic expressions for the numerator of (2.6), applied to $s_i^{\mathcal{G}^{\pm}[k,\chi]}$. In view of Proposition 3.1 and Lemma 4.4, different values of χ and i can give the same boundary $s_i^{\mathcal{G}^{\pm}[k,\chi]} = 0$. This gives us some choice as to the values of χ and i that we can use to describe a given boundary. In Lemma 6.7 we choose the index i that provides the simplest algebraic expression, leading to four different cases, as indicated.

Lemma 6.7. *Suppose (1.1) with $K \geq 2$ has an $\mathcal{S}$-shrinking point at $\xi = \xi^*$ and $\det(J) \neq 0$ and $\sigma < 1$. Choose any $\chi_{\max} \in \mathbb{Z}^+$ and $k \in \mathbb{Z}^+$. Then, in a neighbourhood of $(\eta, \nu) = (0,0)$,*

$$\det\left(P_{\mathcal{G}^+[k,\chi]\left(\tilde{\ell}d_k^+\right)}\right)\varrho^{\mathsf{T}}B\mu = \gamma_{(\ell-1)d}\sum_{j=0}^{k+\chi}\lambda^j + \omega_{(\ell-1)d}^{\mathsf{T}}\left(f^{\left(\mathcal{Y}\mathcal{X}^{\overline{0}}\right)^{-\chi-1}\check{\mathcal{X}}}\left(\varphi_{(\ell-1)d}\right) - \varphi_{(\ell-1)d}\right)\lambda^{k+\chi+1} + \mathcal{O}\left(\sigma^k\right)\ , \text{ for all } -\chi_{\max} \leq \chi \leq -1\ , \tag{6.35}$$

$$\det\left(P_{\mathcal{G}^+[k,\chi]}\right)\varrho^{\mathsf{T}}B\mu = \gamma_{-d}\sum_{j=0}^{k-\chi-1}\lambda^j + \omega_{-d}^{\mathsf{T}}\left(f^{\left(\mathcal{X}\mathcal{Y}^{\overline{0}}\right)^{\chi}\hat{\mathcal{X}}}\left(\varphi_{-d}\right) - \varphi_{-d}\right)\lambda^{k-\chi} + \mathcal{O}\left(\sigma^k\right)\ , \quad \text{for all } 0 \leq \chi \leq \chi_{\max}\ , \tag{6.36}$$

$$\det\left(P_{\mathcal{G}^-[k,\chi]\left(-d_k^-\right)}\right)\varrho^{\mathsf{T}}B\mu = \gamma_0\sum_{j=0}^{k-\chi-1}\lambda^j + \omega_0^{\mathsf{T}}\left(f^{\left(\mathcal{X}^{\overline{0}}\mathcal{Y}\right)^{-\chi}\hat{\mathcal{Y}}}\left(\varphi_0\right) - \varphi_0\right)\lambda^{k+\chi} + \mathcal{O}\left(\sigma^k\right)\ , \quad \text{for all } -\chi_{\max} \leq \chi \leq 0\ , \tag{6.37}$$

$$\det\left(P_{\mathcal{G}^-[k,\chi]\left((\tilde{\ell}-1)d_k^-\right)}\right)\varrho^{\mathsf{T}}B\mu = \gamma_{\ell d}\sum_{j=0}^{k-\chi}\lambda^j + \omega_{\ell d}^{\mathsf{T}}\left(f^{\left(\mathcal{Y}^{\overline{0}}\mathcal{X}\right)^{\chi-1}\check{\mathcal{Y}}}\left(\varphi_{\ell d}\right) - \varphi_{\ell d}\right)\lambda^{k-\chi+1} + \mathcal{O}\left(\sigma^k\right)\ , \quad \text{for all } 1 \leq \chi \leq \chi_{\max}\ . \tag{6.38}$$

Proof. Here we derive (6.36). The remaining expressions can be derived in the same fashion.

By (3.10), (3.12), (3.14) and (3.15),

$$\mathcal{S}\hat{\mathcal{X}} = \mathcal{X}\mathcal{Y}\hat{\mathcal{X}} = \mathcal{X}\check{\mathcal{Y}}\mathcal{Y}^{\overline{0}} = \hat{\mathcal{X}}\mathcal{X}^{\overline{0}}\mathcal{Y}^{\overline{0}} = \hat{\mathcal{X}}\mathcal{S}^{(-d)}\ . \tag{6.39}$$

Thus, for $0 \leq \chi \leq \chi_{\max}$, (3.26) can be rewritten as

$$\mathcal{G}^+[k,\chi] = \left(\mathcal{S}^{\overline{\ell d}}\right)^{\chi}\hat{\mathcal{X}}\left(\mathcal{S}^{(-d)}\right)^{k-\chi}\ . \tag{6.40}$$

Then, by Lemma 6.3 with $j=-d$, for any $x\in\mathbb{R}^N$,

$$\begin{aligned}
f^{\mathcal{G}^+[k,\chi]}(x) &= f^{\left(\mathcal{S}^{(-d)}\right)^{k-\chi}}\left(f^{\left(\mathcal{S}^{\overline{\ell d}}\right)^{\chi}\hat{\mathcal{X}}}(x)\right)\\
&= f^{\left(\mathcal{S}^{(-d)}\right)^{k-\chi}}\left(M_{\left(\mathcal{S}^{\overline{\ell d}}\right)^{\chi}\hat{\mathcal{X}}}x + P_{\left(\mathcal{S}^{\overline{\ell d}}\right)^{\chi}\hat{\mathcal{X}}}B\mu\right)\\
&= \varphi_{-d} + \left(\gamma_{-d}\sum_{j=0}^{k-\chi-1}\lambda^j + \omega_{-d}^{\mathsf{T}}\left(M_{\left(\mathcal{S}^{\overline{\ell d}}\right)^{\chi}\hat{\mathcal{X}}}x + P_{\left(\mathcal{S}^{\overline{\ell d}}\right)^{\chi}\hat{\mathcal{X}}}B\mu - \varphi_{-d}\right)\lambda^{k-\chi}\right)\zeta_{-d}\\
&\quad + M_{\mathcal{S}^{(-d)}}^{k-\chi}\left(I-\zeta_{-d}\omega_{-d}^{\mathsf{T}}\right)\left(M_{\left(\mathcal{S}^{\overline{\ell d}}\right)^{\chi}\hat{\mathcal{X}}}x + P_{\left(\mathcal{S}^{\overline{\ell d}}\right)^{\chi}\hat{\mathcal{X}}}B\mu - \varphi_{-d}\right)\ . \qquad (6.41)
\end{aligned}$$

Now suppose $\det\left(I-M_{\mathcal{G}^+[k,\chi]}\right)\neq 0$. Then $x_0^{\mathcal{G}^+[k,\chi]}$ is well-defined and is the unique fixed point of $f^{\mathcal{G}^+[k,\chi]}$. By Lemma 6.3 we can uniquely write

$$x_0^{\mathcal{G}^+[k,\chi]} = \varphi_{-d} + h\zeta_{-d} + q\ , \qquad (6.42)$$

where $h\in\mathbb{R}$ and $\omega_{-d}^{\mathsf{T}}q=0$. By substituting (6.42) for x and $f^{\mathcal{G}^+[k,\chi]}(x)$ in (6.41), multiplying both sides of (6.41) by e_1^{T} on the left, and applying Lemma 6.5, we obtain

$$h = \gamma_{-d}\sum_{j=0}^{k-\chi-1}\lambda^j + \omega_{-d}^{\mathsf{T}}\left(M_{\left(\mathcal{S}^{\overline{\ell d}}\right)^{\chi}\hat{\mathcal{X}}}\left(\varphi_{-d}+h\zeta_{-d}\right) + P_{\left(\mathcal{S}^{\overline{\ell d}}\right)^{\chi}\hat{\mathcal{X}}}B\mu - \varphi_{-d}\right)\lambda^{k-\chi} + \mathcal{O}\left(\sigma^k\right)\ , \qquad (6.43)$$

and

$$q = \mathcal{O}\left(\sigma^k\right)\ . \qquad (6.44)$$

By (6.42) and (6.44), $s_0^{\mathcal{G}^+[k,\chi]} = h + \mathcal{O}\left(\sigma^k\right)$, and by solving for h in (6.43), we arrive at

$$s_0^{\mathcal{G}^+[k,\chi]} = \frac{\gamma_{-d}\sum_{j=0}^{k-\chi-1}\lambda^j + \omega_{-d}^{\mathsf{T}}\left(f^{\left(\mathcal{S}^{\overline{\ell d}}\right)^{\chi}\hat{\mathcal{X}}}\left(\varphi_{-d}\right)-\varphi_{-d}\right)\lambda^{k-\chi}}{1-\lambda^{k-\chi}\omega_{-d}^{\mathsf{T}}M_{\hat{\mathcal{X}}}\left(M_{\mathcal{S}^{\overline{\ell d}}}\right)^{\chi}\zeta_{-d}} + \mathcal{O}\left(\sigma^k\right)\ , \qquad (6.45)$$

Finally, by (6.4) with $Q = M_{\mathcal{S}^{\overline{\ell d}}} = M_{\mathcal{Y}^{\overline{0}}}M_{\mathcal{X}}$, and (6.28) with $0\leq\chi\leq\chi_{\max}$ and $\rho=1$, we obtain

$$\det\left(I-M_{\mathcal{G}^+[k,\chi]}\right) = 1-\lambda^{k-\chi}\omega_{-d}^{\mathsf{T}}M_{\hat{\mathcal{X}}}\left(M_{\mathcal{S}^{\overline{\ell d}}}\right)^{\chi}\zeta_{-d} + \mathcal{O}\left(\sigma^k\right)\ . \qquad (6.46)$$

Therefore, by (2.6), (6.45) and (6.46), we produce (6.36), as required. Above we assumed $\det\left(I-M_{\mathcal{G}^+[k,\chi]}\right)\neq 0$. By continuity, (6.36) also holds at points near $(\eta,\nu)=(0,0)$ for which $\det\left(I-M_{\mathcal{G}^+[k,\chi]}\right)=0$. □

We have now developed the tools necessary to prove Theorem 2.1. The proof is given Appendix A. In this proof we obtain additional asymptotic expressions for the boundary curves that are useful below. Specifically, on the curves $\det\left(P_{\mathcal{G}^+[k,\chi]}\right)=0$ and $\det\left(P_{\mathcal{G}^+[k,\chi]^{\left((\tilde{\ell}-1)d_k^+\right)}}\right)=0$, we have

$$\frac{\lambda^k}{t_d}\eta + \frac{1}{t_{(\ell-1)d}}\nu + \mathcal{O}\left((\eta,\nu)^2\right) = 0\ , \qquad (6.47)$$

and on the curves $\det\left(P_{\mathcal{G}^-[k,\chi]}\right)=0$ and $\det\left(P_{\mathcal{G}^-[k,\chi]\left((\tilde{\ell}-1)d_k^+\right)}\right)=0$, we have

$$\frac{1}{t_d}\eta+\frac{\lambda^k}{t_{(\ell-1)d}}\nu+\mathcal{O}\left((\eta,\nu)^2\right)=0\,. \tag{6.48}$$

The next result concerns the eigenvalues of $M_{\mathcal{G}^\pm[k,\chi]}$ and is used below to prove Theorem 2.2. Theorem 2.3 follows from this and is proved in Appendix A.

Lemma 6.8. *Suppose (1.1) with $K\geq 2$ has an $\mathcal{S}$-shrinking point at $\xi=\xi^*$ and $\det(J)\neq 0$ and $\sigma<1$. Choose any $\chi_{\max}\in\mathbb{Z}^+$ and $k\in\mathbb{Z}^+$. Then, in a neighbourhood of $(\eta,\nu)=(0,0)$, for any $|\chi|\leq\chi_{\max}$, $M_{\mathcal{G}^\pm[k,\chi]}$ has an eigenvalue $\rho_{\mathcal{G}^+[k,\chi]}$ satisfying*

$$\rho_{\mathcal{G}^+[k,\chi]}=\begin{cases}\lambda^{k+\chi+1}\omega_{\ell d}^{\mathsf{T}}\left(M_{\mathcal{X}^{\overline{0}}}M_{\mathcal{Y}}\right)^{-\chi-1}M_{\check{\mathcal{X}}}\zeta_{\ell d}+\mathcal{O}\left(\sigma^k\right)\,, & -\chi_{\max}\leq\chi\leq -1\\ \lambda^{k-\chi}\omega_0^{\mathsf{T}}\left(M_{\mathcal{Y}^{\overline{0}}}M_{\mathcal{X}}\right)^{\chi}M_{\hat{\mathcal{X}}}\zeta_0+\mathcal{O}\left(\sigma^k\right)\,, & 0\leq\chi\leq\chi_{\max}\end{cases}\,, \tag{6.49}$$

$$\rho_{\mathcal{G}^-[k,\chi]}=\begin{cases}\lambda^{k+\chi}\omega_{-d}^{\mathsf{T}}\left(M_{\mathcal{Y}}M_{\mathcal{X}^{\overline{0}}}\right)^{-\chi}M_{\hat{\mathcal{Y}}}\zeta_{-d}+\mathcal{O}\left(\sigma^k\right)\,, & -\chi_{\max}\leq\chi\leq 0\\ \lambda^{k-\chi+1}\omega_{(\ell-1)d}^{\mathsf{T}}\left(M_{\mathcal{X}}M_{\mathcal{Y}^{\overline{0}}}\right)^{\chi-1}M_{\check{\mathcal{Y}}}\zeta_{(\ell-1)d}+\mathcal{O}\left(\sigma^k\right)\,, & 1\leq\chi\leq\chi_{\max}\end{cases}\,, \tag{6.50}$$

and all other eigenvalues of $M_{\mathcal{G}^\pm[k,\chi]}$ are $\mathcal{O}\left(\sigma^k\right)$.

Proof. Here we prove the result for $\mathcal{G}^+[k,\chi]$ with $0\leq\chi\leq\chi_{\max}$. The remaining parts can be proved similarly.

By Lemma 4.5, the eigenvalues of $M_{\mathcal{G}^+[k,\chi]}$ are the same as those of $M_{\mathcal{G}^+[k,\chi]^{(d-n)}}$, where the latter matrix is given by (6.34). Therefore the eigenvalues of $M_{\mathcal{G}^+[k,\chi]}$ differ from those of the rank-one matrix $\lambda^{k-\chi}\zeta_0\omega_0^{\mathsf{T}}\left(M_{\mathcal{Y}^{\overline{0}}}M_{\mathcal{X}}\right)^{\chi}M_{\hat{\mathcal{X}}}$, by $\mathcal{O}\left(\sigma^k\right)$, and the only non-zero eigenvalue of this matrix is $\lambda^{k-\chi}\omega_0^{\mathsf{T}}\left(M_{\mathcal{Y}^{\overline{0}}}M_{\mathcal{X}}\right)^{\chi}M_{\hat{\mathcal{X}}}\zeta_0$. □

Proof of Theorem 2.2. Here we prove the result for $\mathcal{G}^+[k,\chi]$, with $0\leq\chi\leq\chi_{\max}$. The remaining parts of Theorem 2.2 can be proved in a similar fashion.

We look for intersections of $\det\left(P_{\mathcal{G}^+[k,\chi]}\right)=0$, with $\det\left(\rho I-M_{\mathcal{G}^+[k,\chi]}\right)=0$, for $\rho=\pm 1$. Along $\det\left(P_{\mathcal{G}^+[k,\chi]}\right)=0$, the parameters η and ν are $\mathcal{O}\left(\frac{1}{k}\right)$, and satisfy (6.47). In polar coordinates (2.18), $\tan(\theta)=-\frac{t_d\nu}{t_{(\ell-1)d}\eta}$. Thus by (6.47), if $\det\left(P_{\mathcal{G}^+[k,\chi]}\right)=0$, then

$$\tan(\theta)=-\lambda^k+\mathcal{O}\left(\frac{1}{k}\right)\,. \tag{6.51}$$

Notice $\det\left(\rho I-M_{\mathcal{G}^+[k,\chi]}\right)=0$ when $\rho=\rho_{\mathcal{G}^+[k,\chi]}$, as given by (6.49). Thus by rearranging (6.49) with $0\leq\chi\leq\chi_{\max}$ and putting $\rho_{\mathcal{G}^+[k,\chi]}=\pm 1$, we see that $\det\left(\rho I-M_{\mathcal{G}^+[k,\chi]}\right)=0$ when

$$\lambda^k=\left.\frac{\pm 1}{u_0^{\mathsf{T}}\left(M_{\mathcal{Y}^{\overline{0}}}M_{\mathcal{X}}\right)^{\chi}M_{\hat{\mathcal{X}}}v_0}\right|_{(0,0)}+\mathcal{O}\left(\frac{1}{k}\right)\,, \tag{6.52}$$

where we have used the fact that ω_0^{T} and ζ_0 are equal to u_0^{T} and v_0, to leading order (6.3). Since $M_{\mathcal{S}^{\overline{\ell d}}}=M_{\mathcal{Y}^{\overline{0}}}M_{\mathcal{X}}$ and $v_{-d}=-\frac{t_d}{t_{-d}}M_{\hat{\mathcal{X}}}v_0$ (5.12), by (2.23), (6.52) reduces to

$$\lambda^k=\frac{\mp t_d}{t_{-d}\kappa_\chi^+}+\mathcal{O}\left(\frac{1}{k}\right)\,, \tag{6.53}$$

where κ_χ^+ is given by (2.23), and we assume $\kappa_\chi^+ \neq 0$.

Therefore, by (6.51) and (6.53), any intersection of $\det\left(P_{\mathcal{G}^+[k,\chi]}\right) = 0$ and $\det\left(I - M_{\mathcal{G}^+[k,\chi]}\right) = 0$ must satisfy $\tan(\theta) = \frac{t_d}{t_{-d}\kappa_\chi^+} + \mathcal{O}\left(\frac{1}{k}\right)$. Since $\tan(\theta) < 0$, $t_d < 0$ and $t_{-d} > 0$, the intersection point exists if and only if $\kappa_\chi^+ > 0$.

Similarly any intersection of $\det\left(P_{\mathcal{G}^+[k,\chi]}\right) = 0$ and $\det\left(-I - M_{\mathcal{G}^+[k,\chi]}\right) = 0$ must satisfy $\tan(\theta) = \frac{-t_d}{t_{-d}\kappa_\chi^+} + \mathcal{O}\left(\frac{1}{k}\right)$. In this case the intersection point exists if and only if $\kappa_\chi^+ < 0$. □

7 Properties of nearby shrinking points

In this section we work towards a proof of Theorem 2.4.

Recall, $\eta = s_0^{\mathcal{S}^{\overline{0}}}$ and $\nu = s_{\ell d}^{\mathcal{S}^{\overline{0}}}$ (2.12) provide a convenient local coordinate system in which to study the dynamics of (1.1) near an $\mathcal{S}$-shrinking point. As in §2.1, let $\tilde{\eta} = s_0^{\mathcal{T}^{\overline{0}}}$ and $\tilde{\nu} = s_{\ell d_k^\pm}^{\mathcal{T}^{\overline{0}}}$ denote the analogous coordinates for a nearby $\mathcal{T} = \mathcal{G}^\pm[k,\chi]$-shrinking point, where the $\mathcal{T}$-shrinking point is located at $(\eta,\nu) = (\eta_\mathcal{T}, \nu_\mathcal{T})$, Theorem 2.2.

In order to relate $\tilde{\eta}$ and $\tilde{\nu}$ to η and ν, we first represent points (η,ν) as perturbations from $(\eta_\mathcal{T}, \nu_\mathcal{T})$, by writing

$$(\eta,\nu) = (\eta_\mathcal{T} + \Delta\eta, \nu_\mathcal{T} + \Delta\nu) \ . \tag{7.1}$$

At the $\mathcal{T}$-shrinking point, $\Delta\eta = \Delta\nu = 0$ and $\tilde{\eta} = \tilde{\nu} = 0$. From Lemmas 6.6 and 6.7 and (2.6), it can be seen that $\frac{\partial s_0^{\mathcal{T}^{\overline{0}}}}{\partial\eta}$ and $\frac{\partial s_0^{\mathcal{T}^{\overline{0}}}}{\partial\nu}$ are $\mathcal{O}(k)$, as are the first derivatives of $s_{\ell d_k^\pm}^{\mathcal{T}^{\overline{0}}}$. It follows that $\tilde{\eta}$ and $\tilde{\nu}$ admit the following expansion:

$$\tilde{\eta} = \left(p_1 k + p_3 + \mathcal{O}\left(\frac{1}{k}\right)\right)\Delta\eta + \left(p_2 k + p_4 + \mathcal{O}\left(\frac{1}{k}\right)\right)\Delta\nu + \mathcal{O}\left((\Delta\eta,\Delta\nu)^2\right) \ , \tag{7.2}$$

$$\tilde{\nu} = \left(q_1 k + q_3 + \mathcal{O}\left(\frac{1}{k}\right)\right)\Delta\eta + \left(q_2 k + q_4 + \mathcal{O}\left(\frac{1}{k}\right)\right)\Delta\nu + \mathcal{O}\left((\Delta\eta,\Delta\nu)^2\right) \ , \tag{7.3}$$

for some constants $p_i, q_i \in \mathbb{R}$.

The condition $\det(J) \neq 0$ ensures that the change of coordinates from $(\xi_1,\xi_2) \leftrightarrow (\eta,\nu)$ is locally invertible. Similarly, the condition $\det(\tilde{J}) \neq 0$, where $\tilde{J}$ is given by (2.28), ensures that the change of coordinates $(\eta,\nu) \leftrightarrow (\tilde{\eta},\tilde{\nu})$ is locally invertible. In view of (7.2) and (7.3), we can write

$$\tilde{J} := \left.\begin{bmatrix} \frac{\partial\tilde{\eta}}{\partial\eta} & \frac{\partial\tilde{\eta}}{\partial\nu} \\ \frac{\partial\tilde{\nu}}{\partial\eta} & \frac{\partial\tilde{\nu}}{\partial\nu} \end{bmatrix}\right|_{(\eta_\mathcal{T},\nu_\mathcal{T})} = \begin{bmatrix} p_1 k + p_3 & p_2 k + p_4 \\ q_1 k + q_3 & q_2 k + q_4 \end{bmatrix} + \mathcal{O}\left(\frac{1}{k}\right) \ . \tag{7.4}$$

Below in Lemma 7.2 we derive identities involving the constants $p_i, q_i \in \mathbb{R}$. First we show that in the analogous expansion for $\det(I - M_\mathcal{T})$ the leading order coefficients take a simple form and are independent to the choice of $\mathcal{T}$.

Lemma 7.1. *Suppose (1.1) with $K \geq 2$ has an $\mathcal{S}$-shrinking point at $\xi = \xi^*$ and $\det(J) \neq 0$ and $\sigma < 1$. Then for any $\mathcal{T} = \mathcal{G}^\pm[k,\chi]$,*

$$\det(I - M_\mathcal{T}) = \left(\frac{a}{ct_d}k + \mathcal{O}(1)\right)\Delta\eta + \left(\frac{a}{ct_{(\ell-1)d}}k + \mathcal{O}(1)\right)\Delta\nu + \mathcal{O}\left((\Delta\eta,\Delta\nu)^2\right) \ . \tag{7.5}$$

Proof. By (5.25),

$$\lambda^k = \left(1 - \frac{a}{ct_d}\eta - \frac{a}{ct_{(\ell-1)d}}\nu + \mathcal{O}\left((\eta,\nu)^2\right)\right)^k . \tag{7.6}$$

By (5.25), $\frac{\partial\lambda}{\partial\eta}(\eta_{\mathcal{T}},\nu_{\mathcal{T}}) = \frac{-a}{ct_d} + \mathcal{O}\left(\frac{1}{k}\right)$, and $\frac{\partial\lambda}{\partial\nu}(\eta_{\mathcal{T}},\nu_{\mathcal{T}}) = \frac{-a}{ct_{(\ell-1)d}} + \mathcal{O}\left(\frac{1}{k}\right)$. Therefore by expanding (7.6) about $(\eta,\nu) = (\eta_{\mathcal{T}},\nu_{\mathcal{T}})$, we obtain

$$\lambda^k(\eta,\nu) = \lambda^k(\eta_{\mathcal{T}},\nu_{\mathcal{T}})\left(1 - \left(\frac{a}{ct_d}k + \mathcal{O}(1)\right)\Delta\eta - \left(\frac{a}{ct_{(\ell-1)d}}k + \mathcal{O}(1)\right)\Delta\nu + \mathcal{O}\left((\Delta\eta,\Delta\nu)^2\right)\right) , \tag{7.7}$$

where we have also substituted $\lambda^{k-1}(\eta_{\mathcal{T}},\nu_{\mathcal{T}}) = \lambda^k(\eta_{\mathcal{T}},\nu_{\mathcal{T}}) + \mathcal{O}\left(\frac{1}{k}\right)$.

By Lemma 6.6 we can write

$$\det(I - M_{\mathcal{T}}) = 1 - c_1\lambda^k + \mathcal{O}\left(\frac{1}{k}\right) , \tag{7.8}$$

where $c_1 \in \mathbb{R}$ depends on $\mathcal{T}$ but is independent of k. We have $\det(I - M_{\mathcal{T}}) = 0$ at $(\eta,\nu) = (\eta_{\mathcal{T}},\nu_{\mathcal{T}})$, thus

$$\lambda^k(\eta_{\mathcal{T}},\nu_{\mathcal{T}}) = \frac{1}{c_1(\eta_{\mathcal{T}},\nu_{\mathcal{T}})} + \mathcal{O}\left(\frac{1}{k}\right) . \tag{7.9}$$

With (7.7) and (7.9), (7.8) reduces to (7.5) as required. □

Lemma 7.2. *For any $\mathcal{T} = \mathcal{G}^{\pm}[k,\chi]$, the coefficients of (7.2) and (7.3) satisfy*

$$\frac{1}{t_{(\ell-1)d}}\left(1 \mp \frac{\operatorname{sgn}(a)}{\Gamma\left(\theta_\chi^+\right)\sin\left(\theta_\chi^+\right)}\right)p_1 - \frac{1}{t_d}\left(1 \pm \frac{\operatorname{sgn}(a)}{\Gamma\left(\theta_\chi^+\right)\cos\left(\theta_\chi^+\right)}\right)p_2 = 0 , \tag{7.10}$$

$$\frac{1}{t_{(\ell-1)d}}\left(1 \mp \frac{\operatorname{sgn}(a)}{\Gamma\left(\theta_\chi^+\right)\sin\left(\theta_\chi^+\right)}\right)q_1 - \frac{1}{t_d}\left(1 \pm \frac{\operatorname{sgn}(a)}{\Gamma\left(\theta_\chi^+\right)\cos\left(\theta_\chi^+\right)}\right)q_2 = 0 , \tag{7.11}$$

where Γ is given by (2.19)-(2.20) and the $\theta_\chi^\pm$ are given by (2.25)-(2.26).

Proof. Here we prove the result for $\mathcal{T} = \mathcal{G}^+[k,\chi]$. The result for $\mathcal{T} = \mathcal{G}^-[k,\chi]$ can be proved in the same fashion.

The curve $\tilde{\eta} = 0$ is a boundary of the $\mathcal{G}_k^+$-mode-locking region emanating from the $\mathcal{T} = G^+[k,\chi]$-shrinking point. Note that $\det\left(P_{\mathcal{G}^+[k,\chi]}\right) = 0$, which is approximated by (6.47), defines the same curve. By evaluating (6.47) at the $\mathcal{T}$-shrinking point, we obtain

$$\lambda^k(\eta_{\mathcal{T}},\nu_{\mathcal{T}}) = \frac{-t_d\nu_{\mathcal{T}}}{t_{(\ell-1)d}\eta_{\mathcal{T}}} + \mathcal{O}\left(\frac{1}{k}\right) . \tag{7.12}$$

By further expanding (6.47) about the $\mathcal{T}$-shrinking point with (7.1), we determine that $\tilde{\eta} = 0$ is described by

$$\frac{1}{t_d}\left(1 - \frac{ak\eta_{\mathcal{T}}}{ct_d} + \mathcal{O}\left(\frac{1}{k}\right)\right)\Delta\eta + \frac{1}{t_{(\ell-1)d}}\left(\frac{1}{\lambda^k(\eta_{\mathcal{T}},\nu_{\mathcal{T}})} - \frac{ak\eta_{\mathcal{T}}}{ct_d} + \mathcal{O}\left(\frac{1}{k}\right)\right)\Delta\nu + \mathcal{O}\left((\Delta\eta,\Delta\nu)^2\right) = 0 . \tag{7.13}$$

By multiplying both sides of (7.13) by $\frac{-ct_d}{a\eta_{\mathcal{T}}k}$ and substituting (7.12), we obtain

$$\left(\frac{1}{t_d}-\frac{c}{a\eta_{\mathcal{T}}k}+\mathcal{O}\left(\frac{1}{k}\right)\right)\Delta\eta+\left(\frac{1}{t_{(\ell-1)d}}+\frac{c}{a\nu_{\mathcal{T}}k}+\mathcal{O}\left(\frac{1}{k}\right)\right)\Delta\nu+\mathcal{O}\left((\Delta\eta,\Delta\nu)^2\right)\ . \tag{7.14}$$

By then evaluating $\eta_{\mathcal{T}}$ and $\nu_{\mathcal{T}}$ with (2.18) and (2.21), and taking care to accommodate different cases depending on the sign of a, we determine that $\tilde{\eta}=0$ is described by

$$\begin{aligned}&\frac{1}{t_d}\left(1+\frac{\operatorname{sgn}(a)}{\Gamma\left(\theta_\chi^+\right)\cos\left(\theta_\chi^+\right)}+\mathcal{O}\left(\frac{1}{k}\right)\right)\Delta\eta\\&+\frac{1}{t_{(\ell-1)d}}\left(1-\frac{\operatorname{sgn}(a)}{\Gamma\left(\theta_\chi^+\right)\sin\left(\theta_\chi^+\right)}+\mathcal{O}\left(\frac{1}{k}\right)\right)\Delta\nu+\mathcal{O}\left((\Delta\eta,\Delta\nu)^2\right)\ .\end{aligned} \tag{7.15}$$

By matching (7.2) and (7.15) we obtain (7.10) for $\mathcal{T}=\mathcal{G}^+[k,\chi]$. The curve $\tilde{\nu}=0$ is also given by (6.47), hence the same result holds for q_1 and q_2, i.e. (7.11). □

We complete this section by deriving a novel identity for the leading order term of $\det\left(\tilde{J}\right)$. This is used to prove Theorem 2.4 in Appendix A. First note that by (5.22) we can write

$$\det\left(I-M_{\mathcal{T}}\right)=\frac{\tilde{a}}{\tilde{t}_{d_k^\pm}}\tilde{\eta}+\frac{\tilde{a}}{\tilde{t}_{\left(\tilde{\ell}-1\right)d_k^\pm}}\tilde{\nu}+\mathcal{O}\left((\tilde{\eta},\tilde{\nu})^2\right)\ . \tag{7.16}$$

Moreover, from Lemmas 6.6 and 6.7 it can be seen that $\tilde{t}_{d_k^\pm}$ and $\tilde{t}_{\left(\tilde{\ell}-1\right)d_k^\pm}$ are $\mathcal{O}\left(\frac{1}{k}\right)$, and $\tilde{a}$ is $\mathcal{O}(1)$, and therefore we can write

$$\det\left(I-M_{\mathcal{T}}\right)=\left(r_1k+r_3+\mathcal{O}\left(\frac{1}{k}\right)\right)\tilde{\eta}+\left(r_2k+r_4+\mathcal{O}\left(\frac{1}{k}\right)\right)\tilde{\nu}+\mathcal{O}\left((\tilde{\eta},\tilde{\nu})^2\right)\ , \tag{7.17}$$

for some constants $r_i\in\mathbb{R}$.

Lemma 7.3. *For any $\mathcal{T}=\mathcal{G}^\pm[k,\chi]$, the coefficients of (7.17) satisfy*

$$p_1r_1+q_1r_2=0\ , \tag{7.18}$$

and $\tilde{J}$ (7.4) satisfies

$$\det\left(\tilde{J}\right)=\frac{a}{cr_1}\left(\frac{q_2}{t_d}-\frac{q_1}{t_{(\ell-1)d}}\right)k+\mathcal{O}(1)\ . \tag{7.19}$$

Proof. By (7.4),

$$\det\left(\tilde{J}\right)=\left(p_1q_4+p_3q_2-p_2q_3-p_4q_1\right)k+\mathcal{O}(1)\ , \tag{7.20}$$

where the k^2-term has vanished because (7.10) and (7.11) imply

$$p_1q_2-p_2q_1=0\ . \tag{7.21}$$

By substituting (7.2) and (7.3) into (7.17) we obtain

$$\begin{aligned}\det\left(I-M_{\mathcal{S}}\right) = &\left(\left(p_1r_1+q_1r_2\right)k^2+\left(p_1r_3+p_3r_1+q_1r_4+q_3r_2\right)k+\mathcal{O}(1)\right)\Delta\eta\\ &+\left(\left(p_2r_1+q_2r_2\right)k^2+\left(p_2r_3+p_4r_1+q_2r_4+q_4r_2\right)k+\mathcal{O}(1)\right)\Delta\nu+\mathcal{O}\left(\left(\Delta\eta,\Delta\nu\right)^2\right)\ .\end{aligned} \tag{7.22}$$

By matching the k^2-terms of (7.5) and (7.22), we deduce that $p_1r_1+q_1r_2=0$ (verifying (7.18)) and $p_2r_1+q_2r_2=0$. Note that these equations are equivalent in view of (7.21). By then matching the k-terms of (7.5) and (7.22), we obtain

$$p_1r_3+p_3r_1+q_1r_4+q_3r_2=\frac{a}{ct_d}\ ,\qquad p_2r_3+p_4r_1+q_2r_4+q_4r_2=\frac{a}{ct_{(\ell-1)d}}\ . \tag{7.23}$$

By combining (7.18), (7.21) and (7.23), we obtain

$$\frac{a}{c}\left(\frac{q_2}{t_d}-\frac{q_1}{t_{(\ell-1)d}}\right)=r_1\left(p_1q_4+p_3q_2-p_2q_3-p_4q_1\right)\ , \tag{7.24}$$

which by (7.20) yields (7.19), as required. □

8 Summary

Shrinking points are codimension-two points in the parameter space of piecewise-linear continuous maps at which mode-locking regions have zero width. In this paper we have studied the N-dimensional map (1.1), which has a single switching manifold, $s=0$. We have considered mode-locking regions that, in a symbolic sense, can be assigned a rotation number, $\frac{m}{n}$. At any shrinking point in such a mode-locking region there exists an invariant polygon in the phase space of (1.1). All orbits on the polygon have period n, rotation number $\frac{m}{n}$, and, say, ℓ points to the left of the switching manifold per period (except a special periodic orbit, labelled $\{y_i\}$, that has two points on the switching manifold).

This paper provides the first rigorous study into the dynamics near an arbitrary shrinking point, other than the period-n dynamics within the mode-locking region itself which was examined in [14]. We refer to the shrinking point as an $\mathcal{S}$-shrinking point, where $\mathcal{S}=\mathcal{F}[\ell,m,n]$ is the symbol sequence associated with orbits on the invariant polygon. On each side of the mode-locking region connected to an $\mathcal{S}$-shrinking point, there is a sequence of mode-locking regions. On one side the mode-locking regions have associated rotation numbers $\frac{km+m^-}{kn+n^-}$, and on the other side the mode-locking regions have associated rotation numbers $\frac{km+m^+}{kn+n^+}$, where $k\in\mathbb{Z}^+$ and $\frac{m^-}{n^-}$ and $\frac{m^+}{n^+}$ are the left and right Farey roots of $\frac{m}{n}$. The local curvature and relative spacing of these mode-locking regions was described using polar coordinates and the nonlinear function Γ (2.19)-(2.20), as indicated in Theorem 2.1.

The two sequences of mode-locking regions themselves have shrinking points. Thus sequences of shrinking points converge to the $\mathcal{S}$-shrinking point. We have characterised these shrinking points with symbol sequences, $\mathcal{G}^{\pm}[k,\chi]$. But the $\mathcal{G}^{\pm}[k,\chi]$-shrinking points only exist for particular values of $\chi\in\mathbb{Z}$. We proved, subject to certain non-degeneracy conditions, see Theorem 2.2, that there exists a sequence of potential $\mathcal{G}^{\pm}[k,\chi]$-shrinking points, that converge to the $\mathcal{S}$-shrinking

point as $k \to \infty$, if and only if $\kappa_\chi^\pm > 0$, where $\kappa_\chi^\pm$ are scalar constants associated with the $\mathcal{S}$-shrinking point. The angular coordinates of the potential $\mathcal{G}^\pm[k,\chi]$-shrinking points are given, to leading order, by $\theta_\chi^\pm$. Numerical investigations reveal that these points are commonly valid shrinking points, but may not be due a lack of admissibility of the orbits on the associated invariant polygon. Theorem 2.3 and equation (2.10) show that there are some restrictions on the combinations of signs possible for the $\kappa_\chi^\pm$. Theorem 2.4 tells us that nearby $\mathcal{G}^\pm[k,\chi]$-shrinking points are non-degenerate and have the same orientation as the $\mathcal{S}$-shrinking point.

It remains to describe other dynamics near shrinking points, such as periodic, quasiperiodic and chaotic dynamics at points in parameter space between the nearby mode-locking regions that we have identified, and consider more general classes of piecewise-smooth maps. Such maps arise in diverse applications, and if there is only weak nonlinearity in the smooth pieces of the map (or if the relevant orbits are only traversing parts of phase space that involve weak nonlinearity), then the mode-locking regions can exhibit a sausage-string structure involving points of near-zero width [11, 12, 32]. Border-collision bifurcations are described by piecewise-smooth continuous maps, and the influence of the nonlinearity in the pieces of the map increases with the distance in parameter space from the border-collision bifurcation. This influence on mode-locking region boundaries emanating from shrinking points was explained in [16], but it remains to understand the effect of such nonlinearities on other local dynamics.

A Additional proofs

Proof of Lemma 4.2. First, suppose that A and $A + vu^\mathsf{T}$ are nonsingular. The identity

$$\left(A + vu^\mathsf{T}\right)^{-1} = A^{-1} - \frac{A^{-1}vu^\mathsf{T}A^{-1}}{1 + u^\mathsf{T}A^{-1}v}\,, \tag{A.1}$$

is known as the Sherman-Morrison formula and be can verified directly. We use (4.1) to rewrite (A.1) as

$$\frac{\mathrm{adj}\left(A + vu^\mathsf{T}\right)}{\det\left(A + vu^\mathsf{T}\right)} = \frac{\mathrm{adj}(A)}{\det(A)} - \frac{\mathrm{adj}(A)vu^\mathsf{T}\mathrm{adj}(A)}{\det(A)\det\left(A + vu^\mathsf{T}\right)}\,, \tag{A.2}$$

and therefore

$$\mathrm{adj}\left(A + vu^\mathsf{T}\right) = \mathrm{adj}(A) + \mathrm{adj}(A)u^\mathsf{T}\mathrm{adj}(A)v - \mathrm{adj}(A)vu^\mathsf{T}\mathrm{adj}(A)\,. \tag{A.3}$$

Upon multiplying (A.3) by u^T on the left, the last two terms cancel leaving us with (4.3).

The subset of triples (A,u,v) for which both A and $A + vu^\mathsf{T}$ are nonsingular is dense in the set of all triples (A,u,v). Therefore since both sides of (4.3) are continuous functions of A, u and v, (4.3) holds in general. □

Proof of Lemma 4.3. First, suppose $\mathrm{rank}(A) = N-1$. Then 0 is an eigenvalue of A, and so there exist $u, v \in \mathbb{R}^N$ such that $u^\mathsf{T}A = 0$, $Av = 0$, and $u^\mathsf{T}v = 1$. By (4.1), $\mathrm{adj}(A)$ must be of the form

$$\mathrm{adj}(A) = \hat{c}vu^\mathsf{T}\,, \tag{A.4}$$

for some $\hat{c} \in \mathbb{R}$. To demonstrate (4.4) it remains to show that $\hat{c} = c$.

Let $\varepsilon \in \mathbb{R}$. Then by (4.1) and $Av = 0$, we have

$$\det(A+\varepsilon I)v = \operatorname{adj}(A+\varepsilon I)(A+\varepsilon I)v = \operatorname{adj}(A+\varepsilon I)v\varepsilon = \operatorname{adj}(A)v\varepsilon + \mathcal{O}\left(\varepsilon^2\right) . \tag{A.5}$$

By substituting (A.4) into (A.5) and using $u^{\mathsf{T}}v = 1$, we obtain

$$\det(A+\varepsilon I)v = \hat{c}v\varepsilon + \mathcal{O}\left(\varepsilon^2\right) . \tag{A.6}$$

Notice, ε is an eigenvalue of $A+\varepsilon I$. Let $\lambda_j(\varepsilon)$, for $j = 2, \ldots, N$, denote the remaining eigenvalues of $A+\varepsilon I$, counting multiplicity. By definition, $c = \prod_{j=2}^{N} \lambda_j(0)$, and $\det(A+\varepsilon I)$ is the product of all eigenvalues of $A+\varepsilon I$, thus

$$\det(A+\varepsilon I) = \varepsilon \prod_{j=2}^{N} \lambda_j(\varepsilon) = c\varepsilon + \mathcal{O}\left(\varepsilon^2\right) . \tag{A.7}$$

By matching (A.6) and (A.7), we deduce that $\hat{c} = c$, and therefore (4.4) as required.

Second, if $\operatorname{rank}(A) < N-1$ then for any i and j, the $(N-1)\times(N-1)$ matrix formed by removing the i^{th} row and j^{th} column from A also has rank less than $N-1$. Thus $m_{ij} = 0$ for all i and j and so $\operatorname{adj}(A)$ is the zero matrix. □

Proof of Theorem 2.1. Here we construct C^K curves along which $\det\left(P_{\mathcal{G}^+[k,\chi]}\right) = 0$, for $0 \le \chi \le \chi_{\max}$, and $\det\left(P_{\mathcal{G}^+[k,\chi]\left((\tilde{\ell}-1)d_k^+\right)}\right) = 0$, for $1 \le \chi \le \chi_{\max}$, and verify (2.21)-(2.22) for these curves. The result for the remaining curves can be obtained in the same fashion.

To solve $\det\left(P_{\mathcal{G}^+[k,\chi]}\right) = 0$ we use (6.36). In (6.36) we substitute $\varphi_{-d} = y_0 + \mathcal{O}(\eta,\nu)$, $f^{\mathcal{S}^{\overline{\ell d}}}(y_0) = y_0 + \mathcal{O}(\eta,\nu)$, and $f^{\hat{\mathcal{X}}}(y_0) = y_{-d} + \mathcal{O}(\eta,\nu)$, to obtain

$$\begin{aligned}\omega_{-d}^{\mathsf{T}}\left(f^{\left(\mathcal{S}^{\overline{\ell d}}\right)^{\chi}\hat{\mathcal{X}}}(\varphi_{-d}) - \varphi_{-d}\right) &= u_{-d}^{\mathsf{T}}(y_{-d} - y_0) + \mathcal{O}(\eta,\nu) \\ &= t_{-d} + \mathcal{O}(\eta,\nu) .\end{aligned} \tag{A.8}$$

Thus by (6.36), if $\det(I - M_{\mathcal{S}}) \neq 0$ (in which case $\lambda \neq 1$), we can write

$$\det\left(P_{\mathcal{G}^+[k,\chi]}\right)\varrho^{\mathsf{T}}B\mu = \frac{\gamma_{-d}\left(1-\lambda^{k-\chi}\right)}{1-\lambda} + \lambda^{k-\chi}\left(t_{-d} + \mathcal{O}(\eta,\nu)\right) + \mathcal{O}\left(\sigma^k\right) . \tag{A.9}$$

By (5.25),

$$1 - \lambda = \frac{a}{ct_d}\eta + \frac{a}{ct_{(\ell-1)d}}\nu + \mathcal{O}\left((\eta,\nu)^2\right) . \tag{A.10}$$

To evaluate γ_{-d}, we substitute (5.23) and (A.10) into (6.14) to obtain, after simplification,

$$\gamma_{-d} = \frac{at_{-d}}{ct_{(\ell-1)d}}\nu + \mathcal{O}\left((\eta,\nu)^2\right) . \tag{A.11}$$

Also, since $\lambda = 1 + \mathcal{O}(\eta,\nu)$ and χ is a constant (independent of k), we can write $\lambda^{k-\chi} = \lambda^k\left(1 + \mathcal{O}(\eta,\nu)\right)$. By substituting these expressions into (A.9) we arrive at

$$\det\left(P_{\mathcal{G}^+[k,\chi]}\right)\varrho^{\mathsf{T}}B\mu = \frac{at_{-d}}{c(1-\lambda)}\left(\frac{\lambda^k}{t_d}\eta + \frac{1}{t_{(\ell-1)d}}\nu + \mathcal{O}\left((\eta,\nu)^2\right)\right) . \tag{A.12}$$

Note, the apparent singularity $\lambda = 1$ in (A.12) is spurious because $\det\left(P_{\mathcal{G}^+[k,\chi]}\right) \varrho^{\mathsf{T}} B\mu$ is C^K in a neighbourhood of $(\eta, \nu) = (0, 0)$.

The only instance of k in the leading order term of (A.12) occurs in the quantity λ^k, where by (A.10)

$$\lambda^k = \left(1 - \frac{a}{ct_d}\eta - \frac{a}{ct_{(\ell-1)d}}\nu + \mathcal{O}\left((\eta,\nu)^2\right)\right)^k . \tag{A.13}$$

Therefore, in the limit $k \to \infty$, λ^k only can take $\mathcal{O}(1)$ values other than 0 and 1 if $\eta, \nu = \mathcal{O}\left(\frac{1}{k}\right)$, as the limit is taken. For this reason it is appropriate to write

$$\eta = \frac{\hat{\eta}}{k} , \qquad \nu = \frac{\hat{\nu}}{k} . \tag{A.14}$$

and treat $\hat{\eta}$ and $\hat{\nu}$ as $\mathcal{O}(1)$ constants. By substituting (A.14) into (A.13) we obtain

$$\lambda^k = \mathrm{e}^{-\frac{a}{c}\left(\frac{\hat{\eta}}{t_d} + \frac{\hat{\nu}}{t_{(\ell-1)d}}\right)} + \mathcal{O}\left(\frac{1}{k}\right) . \tag{A.15}$$

Then by substituting (A.10) and (A.15) into (A.12) we obtain

$$\det\left(P_{\mathcal{G}^+[k,\chi]}\right) \varrho^{\mathsf{T}} B\mu = \frac{t_{-d}}{\mathrm{e}^{\frac{a\hat{\nu}}{ct_{(\ell-1)d}}}} \frac{\frac{\hat{\eta}}{t_d}\mathrm{e}^{-\frac{a\hat{\eta}}{ct_d}} + \frac{\hat{\nu}}{t_{(\ell-1)d}}\mathrm{e}^{\frac{a\hat{\nu}}{ct_{(\ell-1)d}}}}{\frac{\hat{\eta}}{t_d} + \frac{\hat{\nu}}{t_{(\ell-1)d}}} + \mathcal{O}\left(\frac{1}{k}\right) . \tag{A.16}$$

Next we work in polar coordinates (2.18). For clarity, we consider only the case $a < 0$. The result for $a > 0$ can be obtained by switching signs in the expressions that follow appropriately.

Since $t_d < 0$, $t_{(\ell-1)d} < 0$, see (5.5), and $c > 0$ (Lemma 6.4), with $a < 0$,

$$\hat{\eta} = \frac{ct_d}{a}\hat{r}\cos(\theta) , \qquad \hat{\nu} = \frac{ct_{(\ell-1)d}}{a}\hat{r}\sin(\theta) , \tag{A.17}$$

where we let

$$\hat{r} = \frac{r}{k} . \tag{A.18}$$

Then by (A.17) and (A.16) we can write

$$\det\left(P_{\mathcal{G}^+[k,\chi]}\right) \varrho^{\mathsf{T}} B\mu = \frac{t_{-d}}{\mathrm{e}^{\hat{r}\sin(\theta)}} H_1(\hat{r},\theta) , \tag{A.19}$$

where H_1 is a C^K function and

$$H_1(\hat{r},\theta) = H_2(\hat{r},\theta) + \mathcal{O}\left(\frac{1}{k}\right) , \tag{A.20}$$

where

$$H_2(\hat{r},\theta) = \frac{\cos(\theta)\,\mathrm{e}^{-\hat{r}\cos(\theta)} + \sin(\theta)\,\mathrm{e}^{\hat{r}\sin(\theta)}}{\cos(\theta) - \sin(\theta)} . \tag{A.21}$$

It is a straight-forward exercise to show that $H_2\left(\Gamma(\theta),\theta\right) = 0$, where Γ is given by (2.19) and $\theta \in \left(\frac{3\pi}{2}, 2\pi\right)$.

Next we employ the implicit function theorem to find where the right hand-side of (A.19) is zero. We define,

$$H_3(\hat{r},\theta,\varepsilon) = k\varepsilon H_1(\hat{r},\theta) + (1-k\varepsilon)H_2(\hat{r},\theta)\ , \tag{A.22}$$

and we are interested in small values of $\varepsilon \in \mathbb{R}$. Notice H_3 is C^K, $H_3\left(\Gamma(\theta),\theta,0\right) = 0$, and $H_3(\hat{r},\theta,\varepsilon) = H_2(\hat{r},\theta) + \mathcal{O}(\varepsilon)$. Therefore, for any $\theta \in \left(\frac{3\pi}{2}, 2\pi\right)$, there exists a neighbourhood of $(\hat{r},\varepsilon) = (\Gamma(\theta),0)$ in which we can apply the implicit function theorem. That is, there exists a unique C^K function $\tilde{\Gamma}(\theta,\varepsilon)$, such that $H_3\left(\tilde{\Gamma}(\theta,\varepsilon),\theta,\varepsilon\right) = 0$, inside the neighbourhood, and $\tilde{\Gamma}(\theta,0) = \Gamma(\theta)$. Then, assuming k is sufficiently large, $H_1\left(\tilde{\Gamma}\left(\theta,\frac{1}{k}\right),\theta\right) \equiv 0$. By (A.19), this shows that $\det\left(P_{\mathcal{G}^+[k,\chi]}\right) = 0$ along a unique C^K curve satisfying (2.21) and (2.22).

To obtain the same result for $\det\left(P_{\mathcal{G}^+[k,\chi]^{\left((\tilde{\ell}-1)d_k^+\right)}}\right)$, we begin by using (3.20) to write

$$\left(\tilde{\ell}-1\right)d_k^+ \bmod n_k^+ = \ell d \bmod n + (\chi-1)n\ , \tag{A.23}$$

where "mod n_k^+" is not needed on the right hand-side by assuming $1 \le \chi \le \chi_{\max}$. Thus by (6.40), the first $\left(\tilde{\ell}-1\right)d_k^+ \bmod n_k^+$ symbols of $\mathcal{G}^+[k,\chi]$ are given by $\left(\mathcal{S}^{\overline{\ell d}}\right)^{\chi-1}\mathcal{X}$, and so we can write

$$x^{\mathcal{G}^+[k,\chi]}_{(\tilde{\ell}-1)d_k^+} = f^{\left(\mathcal{S}^{\overline{\ell d}}\right)^{\chi-1}\mathcal{X}}\left(x_0^{\mathcal{G}^+[k,\chi]}\right)\ . \tag{A.24}$$

Substituting $x_0^{\mathcal{G}^+[k,\chi]} = \varphi_{-d} + h\zeta_{-d} + q$ (6.42) into (A.24) gives

$$x^{\mathcal{G}^+[k,\chi]}_{(\tilde{\ell}-1)d_k^+} = f^{\left(\mathcal{S}^{\overline{\ell d}}\right)^{\chi-1}\mathcal{X}}\left(\varphi_{-d}\right) + M_{\mathcal{X}}M^{\chi-1}_{\mathcal{S}^{\overline{\ell d}}}\left(h\zeta_{-d}+q\right)\ . \tag{A.25}$$

By then substituting $h = s_0^{\mathcal{G}^+[k,\chi]} + \mathcal{O}\left(\sigma^k\right)$, and $q = \mathcal{O}\left(\sigma^k\right)$ (refer to the proof of Lemma 6.7) into (A.25), and multiplying both sides of (A.25) by $e_1^{\mathsf{T}}\det\left(I - \mathcal{G}^+[k,\chi]\right)$ on the left and using (2.6), we produce

$$\begin{aligned}\det\left(P_{\mathcal{G}^+[k,\chi]^{\left((\tilde{\ell}-1)d_k^+\right)}}\right)\varrho^{\mathsf{T}}B\mu = {}& e_1^{\mathsf{T}}f^{\left(\mathcal{S}^{\overline{\ell d}}\right)^{\chi-1}\mathcal{X}}\left(\varphi_{-d}\right)\det\left(I - M_{\mathcal{G}^+[k,\chi]}\right)\\ &+ e_1^{\mathsf{T}}M_{\mathcal{X}}M^{\chi-1}_{\mathcal{S}^{\overline{\ell d}}}\zeta_{-d}\det\left(P_{\mathcal{G}^+[k,\chi]}\right)\varrho^{\mathsf{T}}B\mu + \mathcal{O}\left(\sigma^k\right)\ .\end{aligned} \tag{A.26}$$

The solution to $\det\left(P_{\mathcal{G}^+[k,\chi]^{\left((\tilde{\ell}-1)d_k^+\right)}}\right) = 0$ is the same, to leading order, as the solution to $\det\left(P_{\mathcal{G}^+[k,\chi]}\right) = 0$, because $f^{\left(\mathcal{S}^{\overline{\ell d}}\right)^{\chi-1}\mathcal{X}}\left(\varphi_{-d}\right) = y_{\ell d} + \mathcal{O}\left(\frac{1}{k}\right)$ and so the first term in (A.26) is higher order than the term involving $\det\left(P_{\mathcal{G}^+[k,\chi]}\right)$. Therefore near $(\eta,\nu) = (0,0)$ there exists a unique C^K curve satisfying (2.21) and (2.22) along which $\det\left(P_{\mathcal{G}^+[k,\chi]^{\left((\tilde{\ell}-1)d_k^+\right)}}\right) = 0$. □

Proof of Theorem 2.3. For brevity we restrict our attention to $\mathcal{G}^+[k,\chi]$ with $0 \le \chi \le \chi_{\max}$.

By Proposition 5.3(i), $\{\tilde{y}_i\}$ is a $\mathcal{G}^+[k,\chi]$-cycle. Thus $\tilde{y}_0$ maps to $\tilde{y}_{\tilde{\ell}d_k^+}$ under f^L and f^R in the order specified by the first $\tilde{\ell}d_k^+ \bmod n_k^+$ symbols of $\mathcal{G}^+[k,\chi]$. Since $0 \le \chi \le \chi_{\max}$, by (3.20),

$\tilde{\ell}d_k^+ \bmod n_k^+ = \ell d \bmod n + \chi n$. Thus, by (3.26), the first $\tilde{\ell}d_k^+ \bmod n_k^+$ symbols of $\mathcal{G}^+[k,\chi]$ are $\left(\mathcal{S}^{\overline{\ell d}}\right)^{\chi}\mathcal{X}$, and therefore

$$\tilde{y}_{\tilde{\ell}d_k^+} = f^{\left(\mathcal{S}^{\overline{\ell d}}\right)^{\chi}\mathcal{X}}(\tilde{y}_0) \ . \tag{A.27}$$

Also, by Proposition 5.3(i), $\{\tilde{y}_i\}$ is a $\mathcal{G}^+[k,\chi]^{\left(-d_k^+\right)}$-cycle. Thus $\tilde{y}_{d_k^+}$ maps to $\tilde{y}_{\left(\tilde{\ell}+1\right)d_k^+}$ following the first $\tilde{\ell}d_k^+ \bmod n_k^+$ symbols of $\mathcal{G}^+[k,\chi]$. That is,

$$\tilde{y}_{\left(\tilde{\ell}+1\right)d_k^+} = f^{\left(\mathcal{S}^{\overline{\ell d}}\right)^{\chi}\mathcal{X}}\left(\tilde{y}_{d_k^+}\right) \ . \tag{A.28}$$

In addition

$$\tilde{y}_{d_k^+} = f^{\mathcal{S}^{(-d)}}(\tilde{y}_0) \ , \tag{A.29}$$

because $d_k^+ = n$ (see Lemma 3.5) and the first n symbols of $\mathcal{G}^+[k,\chi]^{\overline{0}}$ are $\mathcal{S}^{\overline{\ell d}\,\overline{0}} = \mathcal{X}^{\overline{0}}\mathcal{Y}^{\overline{0}} = \mathcal{S}^{(-d)}$, by (3.26) and (3.12).

In the form $\tilde{y}_0 = \varphi_{-d} + h\zeta_{-d} + q$ (6.24), we have $q = \mathcal{O}\left(\sigma^k\right)$ (for the same reasons as for $x_0^{\mathcal{G}^+[k,\chi]}$ in the proof of Lemma 6.7), thus

$$\tilde{y}_0 = \varphi_{-d} + \mathcal{O}\left(\sigma^k\right) \ , \tag{A.30}$$

because also $e_1^{\mathsf{T}}\tilde{y}_0 = 0$, $e_1^{\mathsf{T}}\varphi_{-d} = 0$, and $e_1^{\mathsf{T}}\zeta_{-d} = 1$. By (6.26) and (A.29),

$$\tilde{y}_{d_k^+} = \varphi_{-d} + \gamma_{-d}\zeta_{-d} + \mathcal{O}\left(\sigma^k\right) \ , \tag{A.31}$$

and by (A.28), (A.30) and (A.31),

$$\begin{aligned}\tilde{y}_{\left(\tilde{\ell}+1\right)d_k^+} &= f^{\left(\mathcal{S}^{\overline{\ell d}}\right)^{\chi}\mathcal{X}}\left(\tilde{y}_0 + \gamma_{-d}\zeta_{-d} + \mathcal{O}\left(\sigma^k\right)\right) \\ &= f^{\left(\mathcal{S}^{\overline{\ell d}}\right)^{\chi}\mathcal{X}}(\tilde{y}_0) + \gamma_{-d}M_{\mathcal{X}}M^{\chi}_{\mathcal{S}^{\overline{\ell d}}}\zeta_{-d} + \mathcal{O}\left(\sigma^k\right) \ .\end{aligned} \tag{A.32}$$

By then multiplying (A.32) by e_1^{T} on the left and using (A.27) and $e_1^{\mathsf{T}}\tilde{y}_{\tilde{\ell}d_k^+} = 0$, we obtain

$$\tilde{t}_{\left(\tilde{\ell}+1\right)d_k^+} = \gamma_{-d}e_1^{\mathsf{T}}M_{\mathcal{X}}(0,0)M^{\chi}_{\mathcal{S}^{\overline{\ell d}}}(0,0)v_{-d} + \mathcal{O}\left(\frac{1}{k^2}\right) \ , \tag{A.33}$$

where we have also used $\zeta_{-d}(0,0) = v_{-d}$.

Our next step is to derive the following identity

$$u_0^{\mathsf{T}}\left(I - M_{\mathcal{S}^{\overline{\ell d}}}(0,0)\right) = \frac{bt_d e_1^{\mathsf{T}}M_{\mathcal{X}}(0,0)}{ct_{(\ell+1)d}} \ . \tag{A.34}$$

By substituting (5.6) for $u_{\ell d}^{\mathsf{T}}$ into (5.9) we obtain

$$u_0^{\mathsf{T}} = \frac{t_d e_1^{\mathsf{T}}\mathrm{adj}\left(I - M_{\mathcal{S}^{(\ell d)}}(0,0)\right)M_{\mathcal{X}}(0,0)}{ct_{(\ell+1)d}} \ . \tag{A.35}$$

We have $M_{\mathcal{S}^{(\ell d)}} = M_{\mathcal{X}} M_{\mathcal{Y}}$ (3.10), and in view of (2.4) and (4.3) we can substitute $M_{\mathcal{Y}}$ for $M_{\mathcal{Y}^{\overline{0}}}$ to obtain

$$u_0^{\mathsf{T}} = \frac{t_d e_1^{\mathsf{T}} \mathrm{adj}\left(I - M_{\mathcal{X}}(0,0) M_{\mathcal{Y}^{\overline{0}}}(0,0)\right) M_{\mathcal{X}}(0,0)}{c t_{(\ell+1)d}} \,. \tag{A.36}$$

Note, $\det\left(I - M_{\mathcal{X}}(0,0) M_{\mathcal{Y}^{\overline{0}}}(0,0)\right) = b$, because $M_{\mathcal{X}} M_{\mathcal{Y}^{\overline{0}}} = M_{\mathcal{S}^{(\ell d)\overline{0}}} = M_{\mathcal{S}^{\overline{\ell d}(\ell d)}}$, refer to (2.9), (3.11) and Lemma (4.5). Thus by (4.1) and (A.36),

$$u_0^{\mathsf{T}} = \frac{b t_d e_1^{\mathsf{T}} \left(I - M_{\mathcal{X}}(0,0) M_{\mathcal{Y}^{\overline{0}}}(0,0)\right)^{-1} M_{\mathcal{X}}(0,0)}{c t_{(\ell+1)d}} \,. \tag{A.37}$$

By substituting $\left(I - M_{\mathcal{X}} M_{\mathcal{Y}^{\overline{0}}}\right)^{-1} M_{\mathcal{X}} = M_{\mathcal{X}} \left(I - M_{\mathcal{Y}^{\overline{0}}} M_{\mathcal{X}}\right)^{-1}$ and multiply both sides of (A.37) by $I - M_{\mathcal{Y}^{\overline{0}}} M_{\mathcal{X}}$ on the right we arrive at (A.34).

By substituting (A.34) into (A.33) we obtain

$$\tilde{t}_{\left(\tilde{\ell}+1\right)d_k^+} = \frac{\gamma_{-d} c t_{(\ell+1)d} u_0^{\mathsf{T}} \left(I - M_{\mathcal{S}^{\overline{\ell d}}}(0,0)\right) M_{\mathcal{S}^{\overline{\ell d}}}^{\chi}(0,0) v_{-d}}{b t_d} + \mathcal{O}\left(\frac{1}{k^2}\right) \,. \tag{A.38}$$

By using (5.27) and $\gamma_{-d} = \frac{a t_{-d} \nu_{\mathcal{G}^+[k,\chi]}}{c t_{(\ell-1)d}} + \mathcal{O}\left(\frac{1}{k^2}\right)$ (A.11), (A.38) simplifies to

$$\tilde{t}_{\left(\tilde{\ell}+1\right)d_k^+} = \nu_{\mathcal{G}^+[k,\chi]} \left(\kappa_{\chi+1}^+ - \kappa_{\chi}^+\right) + \mathcal{O}\left(\frac{1}{k^2}\right) \,, \tag{A.39}$$

where we have substituted (2.23).

If $a > 0$, then $\theta_\chi^+ \in \left(\frac{\pi}{2}, \pi\right)$ (see Table 2), thus $\sin\left(\theta_\chi^+\right) > 0$, and so by (2.18) $\nu_{\mathcal{G}^+[k,\chi]} > 0$ for arbitrarily large values of k. Since $\kappa_\chi^+ > 0$ and $\tilde{t}_{\left(\tilde{\ell}+1\right)d_k^+} > 0$ (by the assumption that $\left(\eta_{\mathcal{G}^+[k,\chi]}, \nu_{\mathcal{G}^+[k,\chi]}\right)$ is a $\mathcal{G}^+[k,\chi]$-shrinking point), by (A.39) we must have $\kappa_{\chi+1}^+ > 0$, as claimed.

If $\chi \geq 1$, we can similarly show that

$$\tilde{t}_{\left(\tilde{\ell}-1\right)d_k^+} = \nu_{\mathcal{G}^+[k,\chi]} \left(\kappa_{\chi-1}^+ - \kappa_{\chi}^+\right) + \mathcal{O}\left(\frac{1}{k^2}\right) \,, \tag{A.40}$$

based on the knowledge that $\tilde{y}_0$ and $\tilde{y}_{d_k^+}$ map to $\tilde{y}_{\left(\tilde{\ell}-1\right)d_k^+}$ and $\tilde{y}_{\tilde{\ell}d_k^+}$, respectively, under $f^{\left(\mathcal{S}^{\overline{\ell d}}\right)^{\chi-1}\mathcal{X}}$. Then if $a < 0$, $\nu_{\mathcal{G}^+[k,\chi]} < 0$, for arbitrarily large values of k, and thus since $\kappa_\chi^+ > 0$ and $\tilde{t}_{\left(\tilde{\ell}-1\right)d_k^+} < 0$, by (A.40) we must have $\kappa_{\chi-1}^+ > 0$, as claimed.

The remaining cases can be proved in the same fashion. □

Proof of Theorem 2.4. Part (ii) of the theorem is an immediate consequence of Lemma 6.8. We prove part (i) for $\mathcal{G}^+[k,\chi]$ with $0 \leq \chi \leq \chi_{\max}$. Other cases may be proved in a similar fashion.

We first show that $\mathrm{sgn}(\tilde{a}) = \mathrm{sgn}(a)$. At $(\eta,\nu) = (\eta_{\mathcal{T}}, \nu_{\mathcal{T}})$, $\det\left(I - M_{\mathcal{G}^+[k,\chi]}\right) = 0$ and $\det\left(I - M_{\mathcal{G}^+[k,\chi+1]}\right) = \tilde{b}$. Thus, by (6.28) with $\rho = 1$,

$$1 - \left(\lambda^{k-\chi} \omega_0^{\mathsf{T}} M_{\mathcal{S}^{\overline{\ell d}}}^{\chi} M_{\hat{\mathcal{X}}} \zeta_0\right)\Big|_{(\eta_{\mathcal{T}}, \nu_{\mathcal{T}})} + \mathcal{O}\left(\sigma^k\right) = 0 \,, \tag{A.41}$$

$$1 - \left(\lambda^{k-\chi-1} \omega_0^{\mathsf{T}} M_{\mathcal{S}^{\overline{\ell d}}}^{\chi+1} M_{\hat{\mathcal{X}}} \zeta_0\right)\Big|_{(\eta_{\mathcal{T}}, \nu_{\mathcal{T}})} + \mathcal{O}\left(\sigma^k\right) = \tilde{b} \,. \tag{A.42}$$

By combining (A.41) and (A.42) and using (5.12) we obtain

$$\tilde{b} = 1 - \frac{u_0^{\mathsf{T}} M_{\mathcal{S}^{\overline{\ell d}}}^{\chi+1}(0,0) v_{-d}}{u_0^{\mathsf{T}} M_{\mathcal{S}^{\overline{\ell d}}}^{\chi}(0,0) v_{-d}} + \mathcal{O}\left(\frac{1}{k}\right) \ . \tag{A.43}$$

Then by (2.23),

$$\tilde{b} = 1 - \frac{\kappa_{\chi+1}^+}{\kappa_\chi^+} + \mathcal{O}\left(\frac{1}{k}\right) \ , \tag{A.44}$$

and by (A.39),

$$\tilde{b} = \frac{-\tilde{t}_{(\tilde{\ell}+1)d_k^+}}{\kappa_\chi^+ \nu_{\mathcal{G}^+[k,\chi]}} + \mathcal{O}\left(\frac{1}{k}\right) \ . \tag{A.45}$$

Since $\kappa_\chi^+ > 0$ and $\tilde{t}_{(\tilde{\ell}+1)d_k^+} > 0$, (A.45) tells us that $\operatorname{sgn}(\tilde{b}) = -\operatorname{sgn}\left(\nu_{\mathcal{G}^+[k,\chi]}\right)$. Hence by (2.18) and Table 2, $\operatorname{sgn}(\tilde{b}) = -\operatorname{sgn}(a)$. Since $\operatorname{sgn}(a) = -\operatorname{sgn}(b)$, for any shrinking point (5.27), we have $\operatorname{sgn}(\tilde{a}) = -\operatorname{sgn}(\tilde{b})$, and therefore

$$\operatorname{sgn}(\tilde{a}) = \operatorname{sgn}(a) \ , \tag{A.46}$$

as required.

Next we derive an explicit expression for p_1 (a coefficient of a leading order term in (7.2)) from which we can ascertain the sign of p_1. The desired result ($\det\left(\tilde{J}\right) > 0$) then follows from Lemma 7.3 and some additional identities.

By (3.3), $\mathcal{G}^+[k,\chi]^{\overline{0}} = \mathcal{G}^+[k,\chi-1]^{(-d_k^+)}$. Therefore by (7.1) and (7.2) we can write

$$p_1 = \lim_{k\to\infty} \frac{1}{k} \frac{\partial s_{-d_k^+}^{\mathcal{G}^+[k,\chi-1]}}{\partial \eta}\bigg|_{\left(\eta_{\mathcal{G}^+[k,\chi]}, \nu_{\mathcal{G}^+[k,\chi]}\right)} \ . \tag{A.47}$$

Here we use Lemma 6.7 to evaluate $s_{-d_k^+}^{\mathcal{G}^+[k,\chi-1]}$. This requires separate calculations for the cases $\chi = 0$ and $\chi \geq 1$. If $\chi \geq 1$, we express $s_{-d_k^+}^{\mathcal{G}^+[k,\chi-1]}$ in terms of $s_0^{\mathcal{G}^+[k,\chi-1]}$ so that we can apply (6.36). If $\chi = 0$, we express $s_{-d_k^+}^{\mathcal{G}^+[k,-1]}$ in terms of $s_{\left(\ell_k^+-1\right)d_k^+}^{\mathcal{G}^+[k,-1]}$ so that we can apply (6.35). For brevity here we provide details only for the case $\chi \geq 1$.

In the proof of Lemma 6.7, it was shown that $x_0^{\mathcal{G}^+[k,\chi-1]}$ lies within $\mathcal{O}\left(\sigma^k\right)$ of the slow manifold with $j = -d$, see (6.42) and (6.44). The same is true for $x_{-d_k^+}^{\mathcal{G}^+[k,\chi-1]}$, because $x_0^{\mathcal{G}^+[k,\chi-1]} = f^{\mathcal{S}^{(-d)}}\left(x_{-d_k^+}^{\mathcal{G}^+[k,\chi-1]}\right)$. That is,

$$x_i^{\mathcal{G}^+[k,\chi-1]} = \varphi_{-d} + s_i^{\mathcal{G}^+[k,\chi-1]} \zeta_{-d} + \mathcal{O}\left(\sigma^k\right) \ , \tag{A.48}$$

for $i = 0$ and $i = -d_k^+$. By (6.26), we obtain

$$s_{-d_k^+}^{\mathcal{G}^+[k,\chi-1]} = \frac{s_0^{\mathcal{G}^+[k,\chi-1]} - \gamma_{-d}}{\lambda} + \mathcal{O}\left(\sigma^k\right) \ . \tag{A.49}$$

Since $\lambda = 1 + \mathcal{O}\left(\frac{1}{k}\right)$, and γ_{-d} is independent of k, by (A.47)

$$p_1 = \lim_{k\to\infty} \frac{1}{k} \frac{\partial s_0^{\mathcal{G}^+[k,\chi-1]}}{\partial \eta}\bigg|_{\left(\eta_{\mathcal{G}^+[k,\chi]}, \nu_{\mathcal{G}^+[k,\chi]}\right)} . \tag{A.50}$$

To evaluate (A.50) we use (4.10) to write

$$s_0^{\mathcal{G}^+[k,\chi-1]} = \frac{\det\left(P_{\mathcal{G}^+[k,\chi-1]}\right) \varrho^{\mathsf{T}} B\mu}{\det\left(I - M_{\mathcal{G}^+[k,\chi-1]}\right)} . \tag{A.51}$$

Here it is sufficient to write the denominator of (A.51) as

$$\det\left(I - M_{\mathcal{G}^+[k,\chi-1]}\right) = \tilde{a} + \mathcal{O}\left(\Delta\eta, \Delta\nu\right) . \tag{A.52}$$

Since we assuming $\chi \geq 1$, by (6.36) the numerator of (A.51) is

$$\det\left(P_{\mathcal{G}^+[k,\chi-1]}\right) \varrho^{\mathsf{T}} B\mu = \gamma_{-d} \sum_{j=0}^{k-\chi} \lambda^j + \omega_{-d}^{\mathsf{T}} \left(f^{\left(\mathcal{S}^{\overline{\ell d}}\right)^{\chi-1} \hat{\mathcal{X}}}\left(\varphi_{-d}\right) - \varphi_{-d} \right) \lambda^{k-\chi+1} + \mathcal{O}\left(\sigma^k\right) . \tag{A.53}$$

We now evaluate the components of (A.53). We have $\varphi_{-d} = y_0 + \mathcal{O}\left(\frac{1}{k}\right)$, and so $f^{\left(\mathcal{S}^{\overline{\ell d}}\right)^{\chi-1} \hat{\mathcal{X}}}\left(\varphi_{-d}\right) = f^{\left(\mathcal{S}^{\overline{\ell d}}\right)^{\chi-1} \hat{\mathcal{X}}}\left(y_0\right) + \mathcal{O}\left(\sigma^k\right) = f^{\hat{\mathcal{X}}}\left(y_0\right) + \mathcal{O}\left(\sigma^k\right) = y_{-d} + \mathcal{O}\left(\frac{1}{k}\right)$. Thus

$$\omega_{-d}^{\mathsf{T}} \left(f^{\left(\mathcal{S}^{\overline{\ell d}}\right)^{\chi-1} \hat{\mathcal{X}}}\left(\varphi_{-d}\right) - \varphi_{-d} \right) = t_{-d} + \mathcal{O}\left(\frac{1}{k}\right) . \tag{A.54}$$

By (6.14), and the formula for the sum of a truncated geometric series, when $\lambda \neq 1$,

$$\gamma_{-d} \sum_{j=0}^{k-\chi} \lambda^j = e_1^{\mathsf{T}} x_{-d}^{\mathcal{S}} \left(1 - \lambda^{k-\chi+1}\right) . \tag{A.55}$$

Since $\lambda = 1 + \mathcal{O}\left(\frac{1}{k}\right)$, and χ is independent of k, we can write $\lambda^{k-\chi+1} = \lambda^k + \mathcal{O}\left(\frac{1}{k}\right)$. By (7.7) and (7.12),

$$\lambda^k = \frac{-t_d \nu_{\mathcal{T}}}{t_{(\ell-1)d}\eta_{\mathcal{T}}} \left(1 - \left(\frac{a}{ct_d} k + \mathcal{O}(1) \right) \Delta\eta - \left(\frac{a}{ct_{(\ell-1)d}} k + \mathcal{O}(1) \right) \Delta\nu + \mathcal{O}\left((\Delta\eta, \Delta\nu)^2 \right) \right) , \tag{A.56}$$

Also by (5.23),

$$\begin{aligned} e_1^{\mathsf{T}} x_{-d}^{\mathcal{S}} &= \frac{\frac{t_{-d}}{t_{(\ell-1)d}}\nu + \mathcal{O}\left((\eta,\nu)^2\right)}{\frac{1}{t_d}\eta + \frac{1}{t_{(\ell-1)d}}\nu + \mathcal{O}\left((\eta,\nu)^2\right)} \\ &= \frac{t_{-d}\nu_{\mathcal{T}}}{t_{(\ell-1)d}\eta_{\mathcal{T}}\left(\frac{1}{t_d} + \frac{\nu_{\mathcal{T}}}{t_{(\ell-1)d}\eta_{\mathcal{T}}}\right)} + \mathcal{O}\left(\frac{1}{k}\right) + \left(-\frac{t_{-d}\nu_{\mathcal{T}}}{t_d t_{(\ell-1)d}\eta_{\mathcal{T}}^2 \left(\frac{1}{t_d} + \frac{\nu_{\mathcal{T}}}{t_{(\ell-1)d}\eta_{\mathcal{T}}}\right)^2} + \mathcal{O}(1) \right) \Delta\eta \\ &\quad + \left(\frac{t_{-d}}{t_d t_{(\ell-1)d}\eta_{\mathcal{T}} \left(\frac{1}{t_d} + \frac{\nu_{\mathcal{T}}}{t_{(\ell-1)d}\eta_{\mathcal{T}}}\right)^2} + \mathcal{O}(1) \right) \Delta\nu + \mathcal{O}\left((\Delta\eta, \Delta\nu)^2\right) . \end{aligned} \tag{A.57}$$

Finally by (2.18) and (2.25), since $\kappa_\chi^+ > 0$,

$$\frac{\nu_\mathcal{T}}{\eta_\mathcal{T}} = \frac{t_{(\ell-1)d}\tan\left(\theta_\chi^+\right)}{t_d} + \mathcal{O}\left(\frac{1}{k}\right) \ . \tag{A.58}$$

By substituting (A.54)-(A.58) into (A.53) we obtain

$$\begin{aligned}\det\left(P_{\mathcal{G}^+[k,\chi-1]}\right)\varrho^\mathsf{T}B\mu = &\left(\frac{\frac{at_{-d}k}{ct_d} - \frac{t_{-d}}{\eta_\mathcal{T}}}{1+\frac{1}{\tan\left(\theta_\chi^+\right)}} + \mathcal{O}(1)\right)\Delta\eta \\ + &\left(\frac{\frac{at_{-d}k}{ct_{(\ell-1)d}} + \frac{t_dt_{-d}}{t_{(\ell-1)d}\eta_\mathcal{T}\tan\left(\theta_\chi^+\right)}}{1+\frac{1}{\tan\left(\theta_\chi^+\right)}} + \mathcal{O}(1)\right)\Delta\nu + \mathcal{O}\left((\Delta\eta,\Delta\nu)^2\right) \ . \end{aligned} \tag{A.59}$$

By substituting (A.52) and (A.59) into (A.51), and then evaluating (A.50), we arrive at

$$p_1 = \frac{at_{-d}\left(1+\frac{\mathrm{sgn}(a)}{\Gamma\left(\theta_\chi^+\right)\cos\left(\theta_\chi^+\right)}\right)}{\tilde{a}ct_d\left(1+\frac{1}{\tan\left(\theta_\chi^+\right)}\right)} \ , \tag{A.60}$$

where we have used $\lim_{k\to\infty} k\eta_\mathcal{T} = \left|\frac{ct_d}{a}\right|\Gamma\left(\theta_\chi^+\right)\cos\left(\theta_\chi^+\right)$, which is due to (2.18) and (2.21).

We now use (A.60) to show that $p_1 > 0$. From the definition of Γ (2.19)-(2.20), and a bit of care with the different cases of the sign of a, see Table 2, we obtain

$$\frac{1+\frac{\mathrm{sgn}(a)}{\Gamma\left(\theta_\chi^+\right)\cos\left(\theta_\chi^+\right)}}{1+\frac{1}{\tan\left(\theta_\chi^+\right)}} = \frac{\tan\left(\theta_\chi^+\right)}{1+\tan\left(\theta_\chi^+\right)} + \frac{\tan\left(\theta_\chi^+\right)}{\ln\left(-\tan\left(\theta_\chi^+\right)\right)} \ , \tag{A.61}$$

which has a negative value. Since $c > 0$ (Lemma 6.4), $t_d < 0$, $t_{-d} > 0$ (5.5), and $\mathrm{sgn}(\tilde{a}) = \mathrm{sgn}(a)$ (A.46), from (A.60) and (A.61) we conclude that $p_1 > 0$.

Finally, since $\tilde{t}_{d_k} < 0$ and $\tilde{t}_{\left(\tilde{\ell}-1\right)d_k} < 0$, by (7.16) and (7.17),

$$\mathrm{sgn}(r_1) = \mathrm{sgn}(r_2) = -\mathrm{sgn}(\tilde{a}) = -\mathrm{sgn}(a) \ . \tag{A.62}$$

Since $p_1 > 0$, by (7.18) and (A.62), $q_1 < 0$. From (7.11) we obtain

$$q_2 = \frac{t_d}{t_{(\ell-1)d}}\frac{1-\frac{\tan\left(\theta_\chi^+\right)+1}{\tan\left(\theta_\chi^+\right)\ln\left(-\tan\left(\theta_\chi^+\right)\right)}}{1+\frac{\tan\left(\theta_\chi^+\right)+1}{\ln\left(-\tan\left(\theta_\chi^+\right)\right)}}q_1 \ . \tag{A.63}$$

Since $t_d < 0$, $t_{(\ell-1)d} < 0$ and $q_1 < 0$, by (A.63) we must have $q_2 > 0$. Therefore $\frac{q_2}{t_d} - \frac{q_1}{t_{(\ell-1)d}} < 0$, and so by (7.19) and (A.62), we have $\det\left(\tilde{J}\right) > 0$, as required. □

References

[1] R. Lozi. Un attracteur étrange(?) du type attracteur de Hénon. *J. Phys. (Paris)*, 39(C5):9–10, 1978. In French.

[2] M. Misiurewicz. Strange attractors for the Lozi mappings. In R.G. Helleman, editor, *Nonlinear dynamics, Annals of the New York Academy of Sciences*, pages 348–358, 1980.

[3] T. Puu and I. Sushko, editors. *Business Cycle Dynamics: Models and Tools.* Springer-Verlag, New York, 2006.

[4] H.E. Nusse and J.A. Yorke. Border-collision bifurcations including "period two to period three" for piecewise smooth systems. *Phys. D*, 57:39–57, 1992.

[5] M. di Bernardo, C.J. Budd, A.R. Champneys, and P. Kowalczyk. *Piecewise-smooth Dynamical Systems. Theory and Applications.* Springer-Verlag, New York, 2008.

[6] D.J.W. Simpson. Border-collision bifurcations in $\mathbb{R}^n$. To appear: *SIAM Rev.*, 2015.

[7] W.-M. Yang and B.-L. Hao. How the Arnol'd tongues become sausages in a piecewise linear circle map. *Comm. Theoret. Phys.*, 8:1–15, 1987.

[8] D.K. Campbell, R. Galeeva, C. Tresser, and D.J. Uherka. Piecewise linear models for the quasiperiodic transition to chaos. *Chaos*, 6(2):121–154, 1996.

[9] Z.T. Zhusubaliyev, E.A. Soukhoterin, and E. Mosekilde. Border-collision bifurcations on a two-dimensional torus. *Chaos Solitons Fractals*, 13(9):1889–1915, 2002.

[10] M. Gallegati, L. Gardini, T. Puu, and I. Sushko. Hicks' trade cycle revisited: Cycles and bifurcations. *Math. Comput. Simulation*, 63:505–527, 2003.

[11] P.H.E. Tiesinga. Precision and reliability of periodically and quasiperiodically driven integrate-and-fire neurons. *Phys. Rev. E*, 65(4):041913, 2002.

[12] R. Szalai and H.M. Osinga. Arnol'd tongues arising from a grazing-sliding bifurcation. *SIAM J. Appl. Dyn. Sys.*, 8(4):1434–1461, 2009.

[13] M. McGuinness, Y. Hong, D. Galletly, and P. Larsen. Arnold tongues in human cardiorespiratory systems. *Chaos*, 14(1):1–6, 2004.

[14] D.J.W. Simpson and J.D. Meiss. Shrinking point bifurcations of resonance tongues for piecewise-smooth, continuous maps. *Nonlinearity*, 22(5):1123–1144, 2009.

[15] D.J.W. Simpson. *Bifurcations in Piecewise-Smooth Continuous Systems.*, volume 70 of *Nonlinear Science*. World Scientific, Singapore, 2010.

[16] D.J.W. Simpson and J.D. Meiss. Resonance near border-collision bifurcations in piecewise-smooth, continuous maps. *Nonlinearity*, 23(12):3091–3118, 2010.

[17] Z.T. Zhusubaliyev, E. Mosekilde, S. Maity, S. Mohanan, and S. Banerjee. Border collision route to quasiperiodicity: Numerical investigation and experimental confirmation. *Chaos*, 16(2):023122, 2006.

[18] D.J.W. Simpson and J.D. Meiss. Neimark-Sacker bifurcations in planar, piecewise-smooth, continuous maps. *SIAM J. Appl. Dyn. Sys.*, 7(3):795–824, 2008.

[19] M. di Bernardo, P. Kowalczyk, and A. Nordmark. Bifurcations of dynamical systems with sliding: Derivation of normal-form mappings. *Phys. D*, 170:175–205, 2002.

[20] M.R. Jeffrey and S.J. Hogan. The geometry of generic sliding bifurcations. *SIAM Rev.*, 53(3):505–525, 2011.

[21] N.B. Slater. The distribution of the integers N for which $\{\theta N\} < \phi$. *Proc. Cambridge Philos. Soc.*, 46:525–534, 1950.

[22] N.B. Slater. Gaps and steps for the sequence $n\theta$ mod 1. *Proc. Cambridge Philos. Soc.*, 63:1115–1123, 1967.

[23] J.C. Lagarias and C. Tresser. A walk along the branches of the extended Farey tree. *IBM J. Res. Dev.*, 39(3):283–294, 1995.

[24] K. Brucks, J. Ringland, and C. Tresser. An embedding of the Farey web in the parameter space of simple families of circle maps. *Phys. D*, 161:142–162, 2002.

[25] S.K. Berberian. *Linear Algebra.* Oxford University Press, New York, 1992.

[26] B. Kolman. *Elementary Linear Algebra.* Prentice Hall, Upper Saddle River, NJ, 1996.

[27] R. Piziak and P.L. Odell. *Matrix Theory. From Generalized Inverses to Jordan Form.* CRC Press, Boca Raton, FL, 2007.

[28] D.S. Bernstein. *Matrix mathematics: Theory, facts, and formulas with application to linear systems theory.* Princeton University Press, Princeton, NJ, 2005.

[29] M. di Bernardo, M.I. Feigin, S.J. Hogan, and M.E. Homer. Local analysis of C-bifurcations in n-dimensional piecewise-smooth dynamical systems. *Chaos Solitons Fractals*, 10(11):1881–1908, 1999.

[30] R. Sinkhorn. The range of the adjugate map. *Math. Mag.*, 66(2):109–113, 1993.

[31] G.W. Stewart. On the adjugate matrix. *Linear Algebra Appl.*, 283:151–164, 1998.

[32] Z.T. Zhusubaliyev and E. Mosekilde. Equilibrium-torus bifurcation in nonsmooth systems. *Phys. D*, 237:930–936, 2008.